POLITECNICO DI MILANO

Faculty of Environmental and Civil Engineering

POLO TERRITORIALE DI COMO

Master of Science in Environmental and Geomatic Engineering

GIS-BASED ANALYSIS OF THE URBANIZATION EFFECT ON TERRITORIAL SETTINGS AND SURFACE RUNOFF: THE CASE OF THE BURIED TORRENTS OF COMO CITY

Supervisor: Prof.ssa Maria Antonia BROVELLI
Co-Supervisor: Eng. Priscila ESCOBAR ROJO

Master Graduation Thesis by:
Daniele OXOLI
Student Id. 804296

Accademic Year 2014/ 2015

Alla mia famiglia ed alla mia città.

TABLE OF CONTENTS

TABLE OF CONTENTS....iii

List of figures.... vi

List of tables....x

List of equations....xi

List of graphs.... xii

List of appendix tables xiii

Abstract xiv

Riassunto xv

INTRODUCTION....1

1. URBAN DEVELOPMENT OF COMO CITY....3

1.1 From Romans Till the XIX Century....3

1.2 The Last Century....6

1.3 Grading of the Study and Similar Cases....9

2. SOFTWARE INVOLVED 12

2.1 QGIS for Historical Map Processing.... 12

2.2 ArcGIS for Watersheds Characterization.... 14

2.3 Geopaparazzi for Field Data Collection 15

2.4 Hydrological Modelling Software 16

2.4.1 WinTR-55.... 17

2.4.2 URBIS2003v.2.... 17

2.5 HEC-RAS and HEC-GeoRAS for Hydraulic Modelling.... 18

2.6 WebGIS Technologies 19

3. GEOSPATIAL DATA 21

3.1 Historical Map Collection and Processing 21

3.1.1 The archives 21

3.1.2 Manipulation needed for GIS environment 23

3.2 Vector and Raster Dataset 28

3.2.1 Data collection 28

3.2.2 Editing and extraction of additional data 30

3.3 Qualitative Evidences of Changes 33

4. HYDROLOGICAL AND HYDRAULIC ASSESSMENT 36

4.1 Physiographical Characteristics of the Watersheds 37

4.1.1 Cosia Watershed 40

4.1.2 Valduce Watershed 43

4.2 Land Use and Soil Type Data 46

4.3 Project Storms 56

4.4 Time of Concentration 61

4.5 Peak Flood Discharges 63

4.5.1 WinTR-55 model 65

4.5.2 URBIS2003v.2 models 76

4.5.3 Disclosure of the results 81

4.6 Hydraulic Model 85

4.6.1 Pre-processing of input data with HEC-geoRAS 85

4.6.2 Hydraulic simulation with HEC-RAS 88

4.6.3 Results 96

5. WEBGIS 101

CONCLUSIONS AND FURTHER IMPROVEMENTS 106

References 108

Webliography 112

APPENDIX 113

Acknowledgments 115

LIST OF FIGURES

Figure 1: Novum Comum placed in the center of the valley (Caniggia 1963, Società Archeologica Comense). 4

Figure 2: View of Como City in the first half of the XIX century (A. Gueston). Lithographed by J. Jacotter and printed in Paris by Lemercier (Larius, IV, 41/1)....6

Figure 3: Map of Como City 1:2,000. Piano regolatore e di ampliamento della città 1919, (Archivio RAPu)....7

Figure 4: The flood of Bisagno River, Genoa 10/10/2014, (ANSA). 10

Figure 5: Screenshot of QGIS 2.4 user interface. 13

Figure 6: Screenshot of ArcMap 10.1 user interface.... 14

Figure 7: Geopaparazzi map panel. 16

Figure 8: Main window of URBIS2003v.2 (right) and WinTR-55 (left). 17

Figure 9: HEC-RAS geometry editor and 3D viewer panel. 18

Figure 10: Screenshot of the WebGIS client interface based on Leaflet. 20

Figure 11: RAPu Archive homepage.... 23

Figure 12: Homologous points collection with QGIS Georeferencer plugin.... 25

Figure 13: Map correctly placed in the geospace after georeferencing. 26

Figure 14: Lombardy Region geoportal homepage.... 29

Figure 15: Heli-DEM geoportal.... 30

Figure 16: Flow Direction process. a) Elevation grid. b) Flow Direction coding. c) Flow Direction grid. d) Graphical representation of the Flow Direction grid. 31

Figure 17: Flow Accumulation raster (computed from HeliDEM) clipped over Como Valley. The white lines represent the flow-paths for two different classification break values: 100(left) and 5,000(right) upstream flow cells. In the first case the catchment area of any visible stream is ≥ 0.04 km² while, in the second case, it is ≥ 2 km². 32

Figure 18: Comparison between Flow Accumulation rasters computed from TINITALY/01 DTM with SAGA GIS (left) and ArcGIS (Right). The calssification break value adopted is 100 (i.e catchment area ≥ 0.01 km²)..... 33

Figure 19: Valduce flow-path edited from Topographic map of Como, XVII century (red line) and real Valduce flow-path (blue line). 34

Figure 20: Valduce flow-path edited from Theresian Cadastre map, 1722 (purple line) and real Valduce flow-path (blue line)..... 34

Figure 21: Cosia flow-path within the city centre (red line) computed from a) HeliDEM 20m, b) TINITALY/01 10m, c) LIDAR 2m DTMs. The blue line represents the real flow-path. 35

Figure 22: Particular of Como south suburb in Theresian Cadastre, 1722 (left) and Como Master Plan, 1952 (right). Note how the watercourses in the oldest map are clearly visible while their path disappears, covered by roads, in the more recent map..... 35

Figure 23: Outlet point identification on the Flow Accumulation raster (left) and watershed area delineation (right) with ArcGIS. 38

Figure 24: Watersheds (area inside the red and purple divides) and main watercourses (light blue lines) under investigation..... 39

Figure 25: Cosia Torrent (blue line) principal tributaries (light blue lines). 1) Rondina Torrent, 2) Valloni Torrent, 3) Vallaccia Torrent, 4) Aperto Torrent. 40

Figure 26: Valduce Watershed (orange divide) and Valduce Torrent (blue line)..... 44

Figure 27: Land use DUSAF 4.0 clipped on Cosia Watershed (left) and Valduce Watershed (right). Different colours represent different land use classes..... 47

Figure 28: Pedological map clipped on Cosia Watershed (left) and Valduce Watershed (right). Different colours represent different soil type classes. 48

Figure 29: Intersection between land use and soil type shapefiles for Valduce Watershed. 51

Figure 30: Comparison between different land use scenarios (2012 and 1955, CN_max) for Cosia Watershed..... 55

Figure 31: Comparison between different land use sub-scenarios (CN_min and CN_max, 2012) for Cosia Watershed. 55

Figure 32: ARPA Lombardia WebGIS. 57

Figure 33: Reconstructed DDF parameter grid (6x9 cells) covering the study area. 58

Figure 34: OLS adjustment for DDF parameters estimation. a) DDF linearization, b) parameters estimation..... 61

Figure 35: NRCS Dimensionless Unit Hydrograph..... 65

Figure 36: WinTR-55 Valduce Watershed input data windows: a) Watershed characteristics, b) dimensionless DDF. WinTR-55 output windows: c) Hydrograph peak time table, d) Hydrographs. 67

Figure 37: Cosia Watershed divided in sub-watersheds (Ai). Oi represent the hydraulic junctions between Cosia Torrent and its main tributaries. 68

Figure 38: Fast field survey with Geopaparazzi..... 69

Figure 39: Examples of Geopaparazzi templates and tag positioning. 70

Figure 40: Exported KMZ tags displayed on Google Earth. 70

Figure 41: WinTR-55 Cosia Watershed input data windows. 71

Figure 42: Example of hyetograph (red) and net hyetograph (green) computed with URBIS2003v.2. 77

Figure 43: Example of hydrographs computed with URBIS2003v.2; Linear reservoir (blue), Kinematic (red) and Nash (green). 79

Figure 44: HEC-geoRAS data pre-processing. The visible features represent torrent flow-paths (blue lines), banks position (red lines), cross-section positions (green lines), obstruction areas (black stripes polygon), hydraulic roughness map (background pink polygons) and cross-section profiles (popup graph)..... 86

Figure 45: Cosia Torrent HEC-geoRAS layer dataset (up) and exported geometric model in HEC-RAS (down). 87

Figure 46: Valduce Torrent HEC-geoRAS layer dataset (up) and exported geometric model in HEC-RAS (down). 88

Figure 47: Examples of Cosia cross-section profiles obtained with HEC-geoRAS; a) Mountain course b) Medium-low course c) Buried path. 89

Figure 48: Example of modified cross-section profile for medium-low path of Aperto Torrent. Before (left) and after the modification (right). 90

Figure 49: Cosia buried channel cross-section (Cappelletti 2004). 90

Figure 50: Valduce buried channel cross-sections (Como Municipality Archive)..... 91

Figure 51: Cosia Torrent HEC-RAS geometric model. 92

Figure 52: Valduce Torrent HEC-RAS geometric model. 93

Figure 53: Buried channel profile showing a crawlspace between two consecutive bridge decks 94

Figure 54:Flow Energy balance equation parameters (U.S. Army Corps of Engineers 2010). 95

Figure 55: Example of simulated water profiles (light blue) with HEC-RAS. Cross-section view (up) and longitudinal profile view (down) 96

Figure 56: 11/10/2014, Valduce uplift manhole after intense rainfalls (QuiComo). 99

Figure 57: Landslide on Cosia Torrent, 1951 (Archivio Storico Istituto LUCE) 100

Figure 58: Layers preview with GeoServer. 102

Figure 59: WebGIS software architecture. 103

Figure 60: WebGIS features. 104

Figure 61: WebGIS displaying the buried channel paths. 104

Figure 62: WebGIS displaying different historical maps. 105

Figure 63: WebGIS displaying soil runoff capacity maps. 105

LIST OF TABLES

Table 1: Subset of Como Municipality shapefiles used for GCPs collection..... 24

Table 2: List of historical maps involved..... 27

Table 3: Physiographical characteristics of Cosia Watershed..... 43

Table 4: Physiographical characteristics of Valduce Watershed. 46

Table 5: Hydrologic Soil Group conductivity ranges. 48

Table 6: Pedological soil-classes translated to HSGs..... 49

Table 7: Translation table from DUSAF to NRCS land use classes. 51

Table 8: Curve Number table used in the study..... 53

Table 9: Antecedent Moisture Conditions. 54

Table 10: CN values for Cosia and Valduce watersheds. 56

Table 11: Test on rainfall depth variability among the cells of the reconstructed grid..... 59

Table 12: Average rainfall depth for Cosia and Valduce watersheds. 60

Table 13: Estimated DDF parameters..... 61

Table 14: Time of concentration for Cosia and Valduce watersheds..... 63

Table 15: $Qp[m3/s]$ at the watershed outlets, computed with WinTR-55. 73

Table 16: $Qp[m3/s]$ at the sub-watershed outlets (Ai) and junctions (Oi), computed with WinTR-55..... 76

Table 17: $Qp[m3/s]$ at the watershed outlets, computed with URBIS2003v.2. 80

LIST OF EQUATIONS

Equation 1: Polynomial system of equations..... 25

Equation 2: Gravelius's index..... 41

Equation 3: Watershed average altitude..... 42

Equation 4: Correction factors for AMC I (a) and AMC III (b). 54

Equation 5: Average CN..... 55

Equation 6: DDF curve. 56

Equation 7: DDF curve based on the GEV distribution..... 57

Equation 8: Average rainfall depth over the watershed. 58

Equation 9: Tournon's formula. 62

Equation 10: Kiprich's formula. 62

Equation 11: Pezzoli's formula. 62

Equation 12: Ferro's formula. 62

Equation 13: Mockus's formula. 63

Equation 14: NRCS-CN formula for ta. 63

Equation 15: NRCS-CN equations (Re, R and S are expressed in [mm]). 64

Equation 16: Peak discharge equation for standard NRCS DUH..... 66

Equation 17: Linear reservoir IUH. 78

Equation 18: Kinematic IUH. 78

Equation 19: Nash IUH. 78

Equation 20: Flow energy balance equation. 95

LIST OF GRAPHS

Graph 1: Hypsometric curve (a) and Hypsographic curve (b) of Cosia Watershed. 42

Graph 2: Cosia Torrent elevation profile; d represent the distance from the source. 43

Graph 3: Hypsometric curve (a) and Hypsographic curve (b) of Valduce Watershed..... 45

Graph 4: Valduce Torrent elevation profile, d represent the distance from the source..... 45

Graph 5: NRCS $R - Re$ relation plotted for λ=0.2 (Hawkins et al. 2009). 72

Graph 6: Cosia and Valduce peak discharges from the different land use scenarios. 81

Graph 7: Cosia and Valduce peak discharges from different land use sub-scenarios. 82

Graph 8: Valduce peak discharges from different models..... 83

Graph 9: Cosia peak discharges from different models. 84

Graph 10: Rating Curve representative for Cosia buried channel. 97

Graph 11: Rating Curve representative for Aperto buried channel. 98

Graph 12: Rating Curve representative for Valduce buried channel. 98

LIST OF APPENDIX TABLES

Appendix Table 1: Selected layers for the WebGIS, available as WMS layers at: http://geomobile.como.polimi.it:8080/geoserver 114

ABSTRACT

Studying territorial evolutions and investigating their underlying processes is essential to ensure continuity in well-done land management decisions. The case of Como City can be considered as a perfect small-scale example of how human influence acted on natural environment. Several watercourses buried under the road network of the city represent one of the meaningful consequences. GIS technologies and geospatial data, from different epochs of Como City historical development, allowed to trace the evolution of the territorial setting and the original position of the watercourses. We quantified the variations in their peak flood discharges, as a consequence of watersheds urbanization. The computed peak flood discharges were used for running water profile simulations, identifying the changes of the residual conveyance occurred in the buried channels. A WebGIS was created for an easy access to the outcomes of the study.

Keywords: *historical maps, watersheds urbanization, buried torrents, GIS, Como City*

RIASSUNTO

Lo studio dell'evoluzione territoriale e l'identificazione dei processi che la caratterizzano sono passaggi essenziali, per permettere ad ogni nuova azione di pianificazione ambientale di saldarsi armoniosamente e funzionalmente con il contesto preesistente. Il caso della città di Como può essere considerato un perfetto esempio, su piccola scala, di come l'azione dell'uomo abbia interferito sull'ambiente naturale. I numerosi corsi d'acqua, sepolti sotto la rete stradale cittadina, rappresentano una delle più significative conseguenze. Grazie all'utilizzo di tecnologie GIS e di dati geospaziali, relativi a differenti periodi dello sviluppo urbano di Como, è stato possibile ricostruire l'evoluzione dell'assetto territoriale della città ed identificare la probabile posizione naturale dei suoi corsi d'acqua. Per quest'ultimi sono stati stimati gli incrementi subiti dalle portate al colmo di piena, come conseguenza dell'urbanizzazione dei rispettivi bacini idrografici. Queste portate sono state utilizzate per ricostruire i profili di moto permanente, ad esse correlati, per la rete di drenaggio sotterranea. Così facendo è stato possibile valutare l'attuale efficienza idraulica dei canali tombati. Un apposito WebGIS è stato creato per permettere un facile accesso ai risultati dello studio.

Parole chiave: *mappe storiche, urbanizzazione dei bacini idrografici, torrenti sepolti, GIS, Como*

INTRODUCTION

The built environment, which constantly interferes with the natural one, can produce countless benefits for resident communities but also unpleasant consequences.

As a relevant example, we present here the temporal and spatial study of the watercourses – partially buried – of Como City. The origin of Como City dates back up to the old Roman times. As a result, the valley, in which the city is placed, has witnessed many transformations that have profoundly changed its natural landscape, especially regarding its watercourses. During different epochs, the watercourses were first diverted from their natural position, and finally were buried under roads in order to facilitate the city expansion.

Historical cartography is a valuable source of information for a wide range of applications. The temporal and spatial analysis of the human effects on the environment is among them. Historical large-scale mapping of Como City allows a detailed investigation of the territorial changes that occurred. In order to analyse and process geospatial data, the best available solution is represented by the GIS technologies. These tools need to be involved to ensure fairness, repeatability as well as customization for the analysis.

Actually, the urbanization process brought alterations also for the land use within the watersheds causing the increase of soil imperviousness. Consequently, the surface runoff affecting the watersheds is expected to increase; thus, the burial channels have to convey higher flowrates, with respect to the ones for which they were originally designed. Several flood cases in Italy can be reconducted to the inadequacy of hydraulic works as well as to the extensive land exploitation to the detriment of the watercourses. Upgraded hydrological and hydraulic studies are strongly advisable, in order to assess the actual efficiency of such hydraulic works in safety conveying increased flowrates.

The purpose of this thesis work was to reconstruct the urbanization process for Como City as well as to quantify its influences on the watercourses and the related watersheds, in terms of alteration of land use and peak discharges.

Moreover, the access to the meaningful geospatial data and results has been addressed through the implementation of a specific WebGIS.

To sum up, this thesis consists of five chapters:

Chapter 1 containing the investigation on Como City historical development. A literature review regarding similar case studies was also included.

Chapter 2 containing a description of the software, which were exploited in order to carry out this study.

Chapter 3 describing all the geospatial data involved in the study as well as their sources and the processing to which they have been subjected.

Chapter 4 including the explanation of the hydrological and hydraulic assessment, which was carried out for the main watercourses and related watersheds. The disclosure of the meaningful results was also included.

Chapter 5 is dedicated to the description of the WebGIS capabilities and implementation.

1. URBAN DEVELOPMENT OF COMO CITY

The city of Como is an Italian municipality that counts about 85,000 inhabitants; it is the town chief of the homonymous province located in Lombardy region. Worldwide it is famous for its lake and the silk industry, which are still the main drivers of the local economy. Like most of the Italian cities, Como boasts very ancient origins, coming from Roman time and a long development process, which crosses more than twenty centuries. The purpose of this chapter is to describe in a synthetic way the fundamental steps, which led to the actual situation. Particular care was addressed at the choices and needs that drove to the diversion and the burial of the watercourses.

1.1 FROM ROMANS TILL THE XIX CENTURY

The valley, where Como is located, ends in the southern part of the occidental branch of Como Lake, surrounded by wooded hills and mountains. According to the archaeologists, the first evidence of human settlements has been dated around the first half of the VII century BC. The Romans conquered the region in 196 BC; Tito Livio named the original settlement as *"Comum Oppidum"*. The birth of the city, as we know it today, was due to Giulio Cesare in 59 BC, who understood the strategic importance of the area for a further expansion of the empire beyond the Alps (http://it.wikipedia.org/wiki/Como). The initial shape of the city, renamed by Cesare *"Novum Comun"*, was a typical one for *Castrum Romanum*, characterized by straight roads crossing each other perpendicularly and forming squared lots. This peculiarity is still visible walking through the city centre.

The natural conformation of the valley and its evolution however cannot be completely understood without considering the numerous watercourses flowing through it before reaching the lake (Figure 1).

"…For a city located on the banks of a lake, in the bottom of a valley surrounded by mountains, from which numerous streams flow, the water problem is, and always has been, definitely, a fundamental problem."(Gianoncelli 1975)

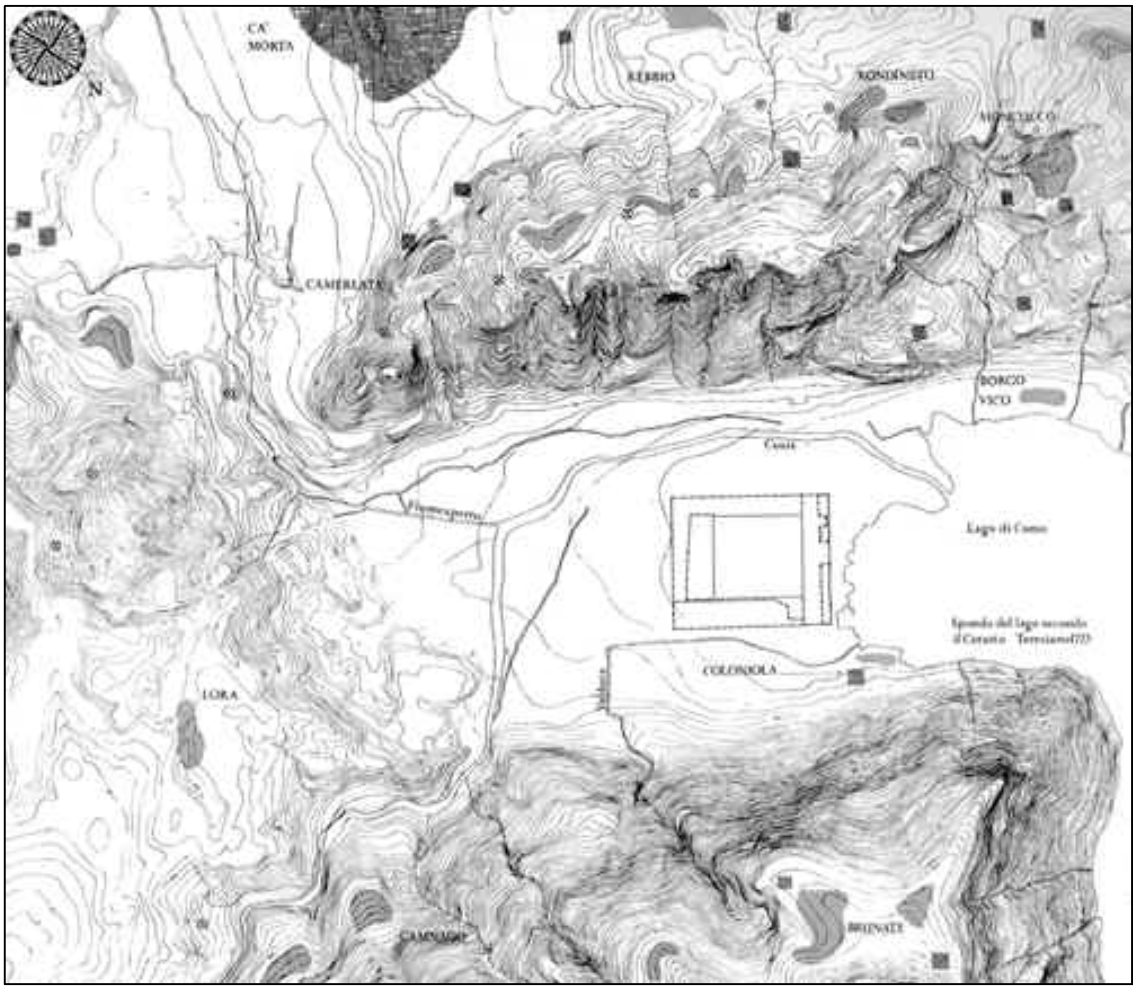

Figure 1: Novum Comum placed in the center of the valley (Caniggia 1963, Società Archeologica Comense).

The first hydraulic works in defence of the city are in fact attributed to Romans. The plain where they decided to build the *Castrum* probably appeared as a wetland, crossed by many watercourses (Jorio 2006). The most important ones were definitely Cosia Torrent, Valduce Torrent and Aperto Torrent. These had probably occupied the central axis of the valley and they were responsible for the filling of the alluvial plain with their debris. In order to remove any physical obstacle for the city development, diversions of riverbeds, out of the original position, as well as the reclamation of the wetland, became a priority for Giulio Cesare. Moreover, only with the Roman colonization, the technical potential of carrying out these kind of work became available (Gianoncelli 1975). Cosia and Aperto torrents were diverted to west side of the valley, in correspondence of the actual Monte Croce-Baradello Hillside, while Valduce Torrent was fixed in

the east side, draining all the streams coming from the actual Brunate Mountain. The central part of the plain was now ready to let the settlement grow. In 49 BC, the central Roman government declared Novum Comun "municipality" and the work for the construction of a massive city wall started, while technical and commercial districts were occupying the suburbs all around.

In the Early Middle Age, during the Western Roman Empire period, Como remained isolated without suffering any important pressure of the conquerors coming from central European countries. The city centre remained almost unchanged while outside the wall, a progressive increase of Lombard settlements occurred and the edification of numerous religious buildings started. These latter had been formed in suburban nuclei and they were called *"Corpi Santi"* of Como. Within the start of Late Middle Age, precisely on 27th August 1127, Como was sacked by Milan after ten years of war. The wall and many buildings were destroyed. Thirty years later, after the alliance with the emperor Frederick I Barbarossa, the city wall was reconstructed. Como witnessed a period of abundance and glory, participating in the assault of the city of Milan and obtaining its revenge due to the loss they have suffered. With the advent of the Lordships, Como passed first under the governance of Visconti family and then, during the second half of the 15th century, it was subdued to the Duchy of Milan.

Still it has not been established whether, during the medieval period, the position of city wall was modified, and how much, from the original Roman one. It was possible that a contraction along the eastern side happened, due to the frequent floods of Cosia and Valduce torrents which probably caused several structural failure along this part of the perimeter (Gianoncelli 1975). The maintenance of the ancient Roman water works did not stop even in the Municipality Age. In fact, a large number of municipal notices, dated in this period, were concerned for the restoration and securing of the main watercourses embankments. By Gianoncelli's opinion, the Roman works were so providential for the city but perhaps, because of their exaggerated artificiality, they involved great effort for their maintenance. At the beginning of the 16th century, Como suffered the expansionist ambitions of France, Spain, Austria and even the neighbouring Switzerland, which contended violently the city (Società Archeologica Comense 2012). The French governors ordered the restoration of the ancient fortifications and the construction of new ones to face the attack of the opponents but in 1521, the French invaders were forced to surrender to the Spanish troops. During the Spanish domination, the

fortifications, ruined by the conflict, were restored once again. Both the riverbed of Cosia Torrent and the trench surrounding the wall were dredged with defensive purpose too. Spanish domination was followed by Austrian control, during which Como enjoyed a period of stability. The ancient defence works were converted for public and private use, and finally in 1738 the trench around the wall was filled, becoming a tree-lined avenue. During subsequent periods, from Napoleon passing through the Kingdom of Lombardy-Venetia till the end of XIX century, this process of upgrading the old fortifications continued inexorable, while the city (Figure 2) did not face any particular expansion process, neither demographic nor for suburb areas. The only notable exception was the construction of majestic patrician villas near the lake on both sides of the valley.

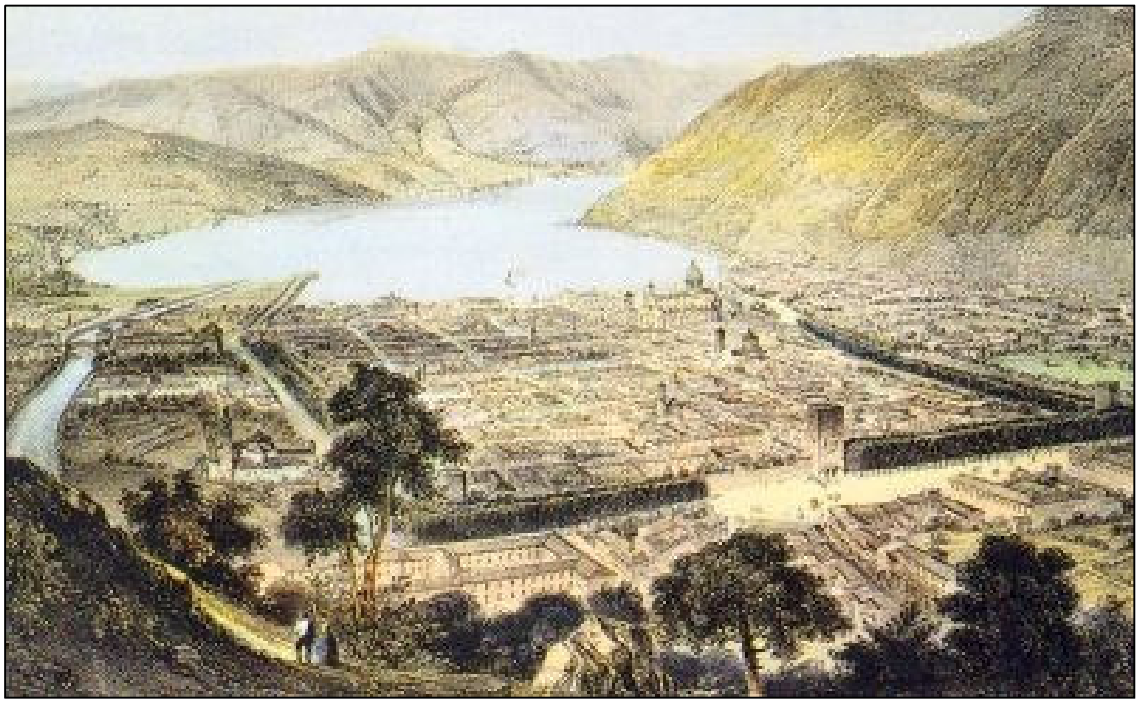

Figure 2: View of Como City in the first half of the XIX century (A. Gueston). Lithographed by J. Jacotter and printed in Paris by Lemercier (Larius, IV, 41/1).

1.2 THE LAST CENTURY

Modernization and expansion of the city in the XX century became essential topics, strongly supported by municipal councils, which led to first drafts of Como City's master plan. It is still the most widely used tool in urban planning management. Eng. G. Carcano drew up the first prototype of the master plan

in 1851. Finally, a complete and detailed document was written and executed in the twenties (Giussani & Catelli 1919). The interventions, listed in the first version of the plan, focused especially on the widening of the existing streets and the opening of new ones, in order to meet the needs of both pedestrian and vehicular traffic. This became a primary issue for all Italian cities in the first post-war period. For these reasons, the burial of urban reaches of the watercourses became necessary; followed by hygienic problems due to wastewater conveyed into them, coming from a constantly growing population. The work to bury the Valduce Torrent were already in act while for Cosia and Aperto torrents the first project was drawn up (Figure 3).

Birth and expansion of industrial poles in suburbs had already begun since years; the gradual multiplication of industrial buildings was a major concern of the subsequent plan, undertaken during the Fascist government (Ufficio Urbanistica Comune di Como 1937). Another focus of this period was the organization of agricultural lands as well as the creation of transport infrastructure. Consequently, planning began to include marginal areas of the valley and neighbouring municipalities, touching the inter-regional road and rail facilities. The aim was to create a broader and functional urban network, by connecting agricultural, industrial and touristic areas to the city centre.

Figure 3: Map of Como City 1:2,000. Piano regolatore e di ampliamento della città 1919, (Archivio RA Pu).

Once again, the complete burial of Cosia Torrent became fundamental to create a road joining Brianza Plain with the western shore of the lake and Switzerland, in order to divert the traffic from the walled city.

For the first time, in this master plan, fundamental issues such as solid waste disposal and collection of domestic and industrial wastewater were addressed. In particular this latter was conveyed in proximity of Cosia Torrent and disposed of into the lake using the watercourse as a large sewer collector, which was combined with tanks and cesspools, in order to encourage the agricultural recovery of the organic matter.

After the second World War Como extended over 3763 hectares, counting about 70,000 inhabitants (Marrazzi et al. 1967). The measures adopted in previous years led to inclusion of some neighbouring municipalities and development of the infrastructure network, which birth was needed starting from the thirties. The placement of industrial areas was not yet fixed. In the locations where infrastructure and water supply were easy to access, small productive centres started to concentrate.

These areas were in particular Camerlata Plain, where Aperto Torrent flows, and Cosia Valley. Within the late sixties, the work aimed at the burial of these two watercourses was completed. This is a perfect example how the presence of watercourses was significant for a city development. For Como City the environmental services provided by the watercourses were fundamental for the industry growth, typically for textile ones. In the following decades, the expansion of urban areas continued and Como achieved a peak of about 97,000 inhabitants in the seventies. Wastewater and sewerage management was upgraded by creating a centralized treatment plant, placed along Cosia Torrent in which the treated water was discharged.

Within the new Millennium, urban requirements changed. A growing attention towards the retraining of existing urban structure and the delimitation of constraint areas, for the protection of historical and environmental heritage, could be detected from the new master plan (Rota et al. 2001).

The demographic growth and the industrial expansion have progressively slowed, bringing the population around the actual stable value of approximately 85,000 inhabitants and leaving the shape of the city as we know it today.

1.3 GRADING OF THE STUDY AND SIMILAR CASES

The phenomenon of the burial of the watercourses, or more generally the complete distortion from their natural condition, does not regard just the city of Como. There are in fact countless similar cases in the world, but the purpose behind this custom is always the same: the urbanization. Nowadays this issue is studied in various scientific and humanistic disciplines, ranging from ecology to architecture, passing through archaeology and engineering. The understanding of all the effects caused by this particular situation it is still an open question. One of the first and most famous case study regards London, where almost all the tributaries of the Thames River flow under the city into culverts. This study begun during last century as historical investigation but now, a plan for the reclamation of the urban river environment was undertaken by a partnership between Environmental Agency (EA), Natural England and The River Restoration Centre (Heisse et al. 2009). In order to have a better understanding of the frequency of this phenomenon, just take into account the magazine report published by National Geographic, dedicated to the most important subterranean rivers, which flow under the major cities in the world. In this article they define as ironic that the watercourses which attracted populations to settle in a given area have become a victim of the concrete jungle expansion (Howard B. C. 2013). The European Union in the recent past has started to address the preservation and upgrading of urban watercourses, issuing guidelines and collecting the experiences of the member states (Environmental Agency 2011). Other relevant examples closely related to ecology and benefits arising from river ecosystem restoration, are observed in almost all continents. In Japan during the last two decades many projects were carried out, demonstrating also the economic return for the communities who have taken charge of these activities (Nakamura et al. 2006). An interesting American study defined this issue as *"The urban stream syndrome"*. It tried to find the correlation between human interventions and the related eco-hydrological changes, pointing out priorities and solutions (Aymond et al. 2005). All these work can be placed, more or less directly, in a large and modern research field called "Socio-Hydrology", which is defined as the science of human influence on hydrology and the influence of the water cycle on human social systems (Zlinszky & Timár 2013). Socio-hydrology is aimed as a discovery-based fundamental science, whos practice is informed through observing, understanding and predicting socio-hydrologic phenomena in real places in the landscape where real people live (Sivapalan et al. 2012).

The problem of watercourses confinement into artificial riverbeds is not correlated only with the ecosystem functionality nor with the recovery of historical memory. Often the impact of urbanization and extensive land exploitation, to the detriment of the rivers, had manifested with tragic or even catastrophic effects.

The last case of flooding in Italy due to inadequate hydraulic works dates back to October 2014. Bisagno River (Genoa), which urban reach was buried in the thirties, flooded causing millions of Euro of damage and even a casualty (http://it.wikipedia.org/wiki/Alluvione_di_Genova). The discharge during this flood event proved to be about twice the critical one estimated by the technical committee of the period, although some of the most distinguished Italian hydrologists formed it. Recent studies calibrated on the actual precipitation intensity and changes in land use had however forecasted a peak flowrate very close to the one that occurred. For this reason, an updated project based on current knowledge was put in place to improve the discharge capacity of the river. Unfortunately, due to bureaucratic issues, the work has been interrupted in 2009. In this case, Italian authorities are rendered involuntarily as one of the main causes of the tragedy.

Figure 4: The flood of Bisagno River, Genoa 10/10/2014, (ANSA).

This example helps to understand the attention that these hydraulic structures deserve and how it is difficult to evaluate their related problematics, because negatively and positively affected by a large number of variables.

Our study will therefore focus on few key points mentioned above. These include the reconstruction of the historical changes in urban watercourses (enriching what has been previously said), the effects of urbanization on peak flood discharges and the publication of the results in the most intuitive and direct way, to taking into account the positive effect of the public awareness on such issue.

2. SOFTWARE INVOLVED

The effects of urbanization on both the watersheds and watercourses of interest as well as the historical reconstruction phase need to be quantified and supported by objective data. Therefore, the use of Geographic Information System technologies (GIS) must be taken into account in data processing, in order to reduce the time required for this operation as well as to improve accuracy and repeatability of the analysis. Comparisons with similar hydrological and hydraulic studies (based on less recent or different techniques) as well as between geospatial data from different period of Como City history, proved to be essential in order to assess the reliability of the work.

The analysis's strategy was mainly based on the exploitation of GIS software. Most of the used information were geospatial data of different origin and nature so the use of GIS capabilities greatly facilitates their manipulation, storage and publication.

Different kind of software have been adopted for what it concerns the hydrological and hydraulic modelling even if the input data pre-processing was carried out within GIS environment. The combined use of specific software for hydraulic/hydrological modelling together with GIS systems is an increasingly used practice. The typical topics of these disciplines cannot disregard from their close interaction with morphological and topological features. Although several tools based on this concept were developed, it is not always easy the interchange of input/output data between these two kind of packages, often concerning technical issues related to the data format. Development of ad hoc hydrological and hydraulic model applications within the most diffused GIS would be therefore desirable, in order to promote their use even among average users.

2.1 QGIS FOR HISTORICAL MAP PROCESSING

Cartographic maps have always been needful tools for the historical reconstruction of events. Wars, floods and political control of the territory were, and still are, some of the main reasons for cartographic production.

The advantage of maps is definitely their possibility to provide complex information in a simple way to any kind of user. Preserving the original philosophy of the use of maps, conversion of paper maps in more suitable

digital format was carried out through GIS technologies. QGIS software (http://qgis.org/it/docs) was selected to assign this particular task (3.1.2).

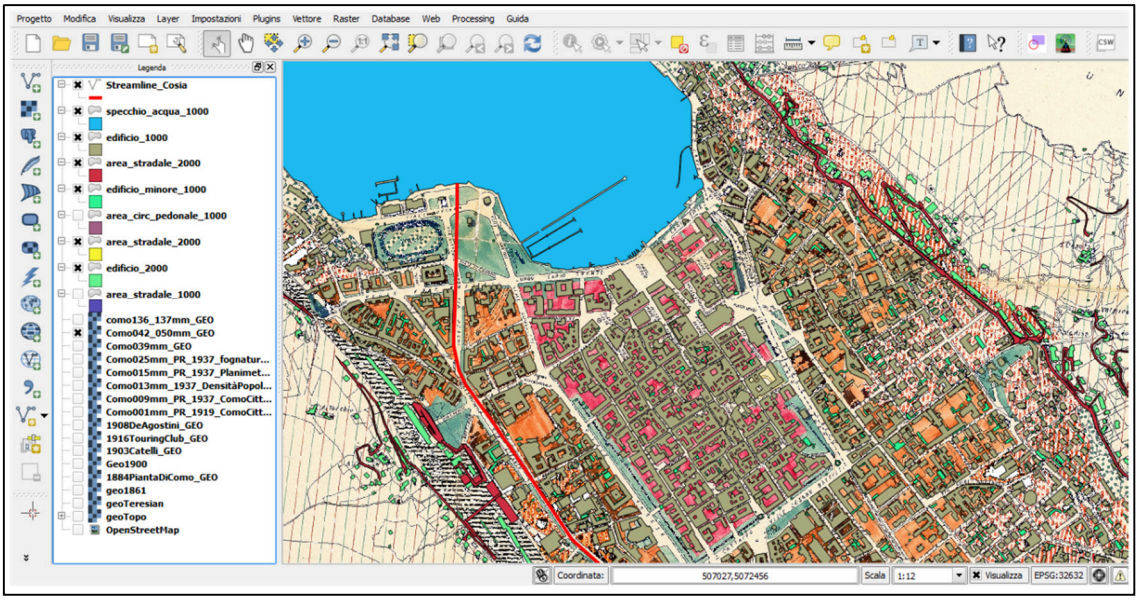

Figure 5: Screenshot of QGIS 2.4 user interface.

QGIS is a Free and Open Source Software (FOSS), released under GNU General Public License (GPL) (http://www.gnu.org); it is an official project of the Open Source Geospatial Foundation (http://www.osgeo.org). Free and Open Source mean that users do not have to purchase it and can freely distribute it to anyone else; moreover the source code is "transparent" so users are free to make changes and improvements to it. These possibilities are not available for property software.

Quantum GIS (original name of the software) was initially created in 2002 as a simple GIS viewer but has evolved into one of the premier FOSS GIS packages. It runs on all the main OS as Linux, MS Window, Unix and Mac OSX and it supports vector, raster and database formats, including ESRI shapefiles, spatial data in PostgreSQL/PostGIS, GRASS vectors and raster, or geotiff.

The use of QGIS was not limited only to the processing of the old maps; other basic functionalities were exploited in support to hydrological modelling and for manipulation and editing of vector and raster data.

2.2 ARCGIS FOR WATERSHEDS CHARACTERIZATION

The evaluation of peak flood discharges requires a priori knowledge on physiographic characteristics of the watersheds involved. This type of information can be obtained by processing, through specific algorithms, particular raster data called DTMs (Digital Terrain Models). Today, this kind of geoprocessing is integrated in many GIS software, including QGIS. For this particular case the use of ArcGIS (http://www.arcgis.com n.d.), a property software, was preferred because some advanced tools for hydrological modelling were not included in default tool packages of other FOSS GIS.

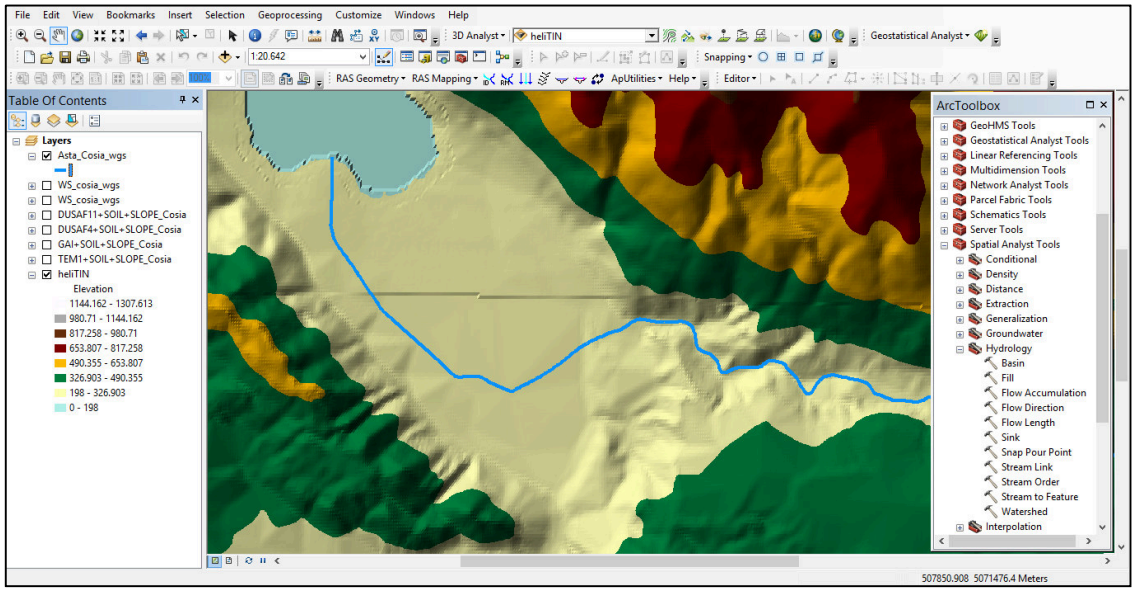

Figure 6: Screenshot of ArcMap 10.1 user interface.

ArcGIS is an integrated family of GIS software products for building a complete GIS. It is developed and distribute by ESRI (http://www.esri.com), a private American company leader worldwide in GIS software systems. ArcGIS provides a scalable framework for implementing GIS for a single user or many users on desktops, in servers over the Web and in the field. During this study, we exploited only the Desktop package, which is available as single user licence and runs under MS Window and Mac OSX. ArcGIS for Desktop consists of several integrated applications, including ArcCatalog, ArcMap, ArcToolbox and ArcScene. ArcCatalog is the data management application used to browse datasets and files. In addition to showing available data, ArcCatalog also allows users to preview the data on a map. ArcMap (Figure 6)

is the application used to view, edit and query geospatial data, and create maps. ArcToolbox contains geoprocessing, data conversion, and analysis tools. ArcScene is a 3D viewer that is well suited to generating perspective scenes that allow navigating and interacting with 3D feature and raster data.

Further information about the specific features employed will be described in the following chapters.

2.3 GEOPAPARAZZI FOR FIELD DATA COLLECTION

It was not easy to collect all the needed information regarding the watercourses only through GIS analysis. In our particular case, the DTM processing would be insufficient a priori, because the size of the riverbeds was often smaller than the DTM resolution itself. At the same time, the evaluation of the hydraulic roughness and the identification of the hydraulic works scattered on the watercourses would be difficult to perform. In the field of hydrology, measurement campaigns on site are still an essential tool for accurate analysis. Therefore, in order to address this need we decided to take advantage of new mobile technologies, collecting field data through the use of Geopaparazzi Android Mobile Application (http://geopaparazzi.github.io).

Geopaparazzi is a FOSS, released under GNU Lesser General Public License (LGPL), developed by HydroloGIS Environmental Engineering Company (https://sites.google.com/a/hydrologis.com) to perform very fast qualitative engineering and geologic surveys. The application is retrievable on Google Play Store. It allows to collect, export and share georeferenced tags and picture as well as GPS tracks, with the further possibility to import them into the main GIS application BeeGIS (http://www.beegis.org). The tags can be programmed by the user using JSON format (JavaScript Object Notation) to create complex templates, which can store multiple variables including strings, numbers, pictures and sketches. WGS84 geographic coordinates are automatically stored once the templates are filled in. Tags can be exported from the mobile device in KML (Keyhole Markup Language) or GPX (GPS eXchange Format) and displayed on BeeGIS or Google Earth (http://earth.google.com) as well as on other GIS software, like QGIS. The user is allowed also to choose the basemap on which perform the field survey from default providers such as OpenStreetMap (http://www.openstreetmap.org) and Bing Maps (http://www.bing.com) as well as editing own tail maps using a Desktop GIS.

Figure 7: Geopaparazzi map panel.

The information collected with Geopaparazzi were integrated inside both hydrological and hydraulic models as valuable input data to perform peak flood discharge estimation and routing (section 4.5 & 4.6).

2.4 HYDROLOGICAL MODELLING SOFTWARE

The hydrological modelling was based on the implementation of simple rainfall-runoff models for a single rain event, identified as critical or of particular interest for the case study.

The methodology adopted refers mainly to the Natural Resources Conservation Service Runoff Curve Number method (NRCS-CN). which was developed by the United States Department of Agriculture (http://www.usda.gov). NRCS is formerly known as the Soil Conservation Service (SCS), the name was change in 1994. This model was run exploiting the Window interface WinTR-55 provided by U.S. Department of Agriculture (USDA) (Figure 8).

In addition, peak flood discharges were also calculated with other lumped conceptual models using URBIS2003v.2 software (Figure 8), in order to compare the results. Complex models were not suitable because the studied watercourses are not gauged with flow-meters (chapter 4).

2.4.1 WinTR-55

WinTR–55 is a single-event rainfall-runoff, small watershed hydrologic model. The software is released free of charge but not it is not Open Source. The source code is based on MS Visual Basic 6.0 while a Graphical User Interface (GUI) is available for MS Window only. The model generates hydrographs from both urban and agricultural areas in selected points along the stream network. Hydrographs are routed downstream through channels and/or reservoirs according to the Muskingum-Cunge method (e.g. Chow et al. 1988; Tewolde & Smithers 2007). Multiple areas can be modelled within the watershed (U. S. Department of Agriculture 2009). Part 630 of the NRCS National Engineering Handbook (NEH) provides detailed information on NRCS hydrology (U. S. Department of Agriculture 2004) and it is the technical reference for this software.

2.4.2 URBIS2003v.2

URBIS2003v.2 software allows generating flood hydrographs, which develop within urban or natural basins as effect of a projected storm. The software does not require installation and runs on MS Window only. Department of Civil and Environmental Engineering of Politecnico di Milano (www.dica.polimi.it) developed this program in collaboration with Etatec Studio Paoletti s.r.l (www.etatec.it). Currently, a new version of the program called URBIS PRO is available and distributed under fee as commercial software.

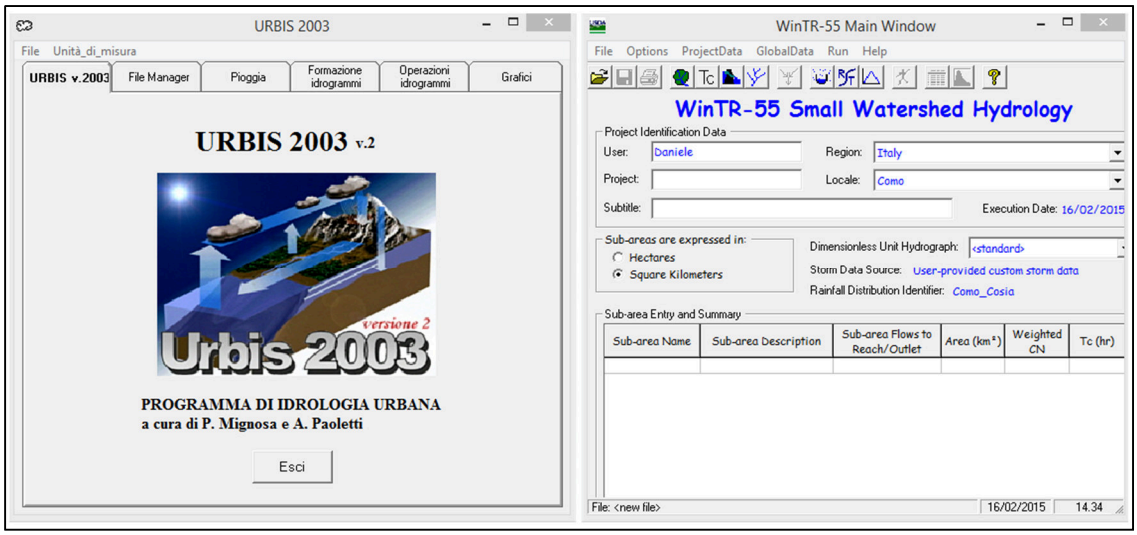

Figure 8: Main window of URBIS2003v.2 (right) and WinTR-55 (left).

The estimated peak flood discharges have been used in the hydraulic model as input data for the water profile simulations (section 4.5 & 4.6).

2.5 HEC-RAS AND HEC-GEORAS FOR HYDRAULIC MODELLING

The main purpose of the hydraulic modelling was to identify the water profiles elevation into streams for any selected flood scenario. This was necessary in order to assess the discharge efficiency of the buried channels and to identify the eventually overflow problems. The software selected to perform the hydraulic modelling was HEC-RAS (Hydrology Engineering Center – River Analysis System).

HEC-RAS allows to perform 1-D steady and unsteady flow calculation, sediment transport, mobile bed computations and water temperature modelling (http://www.hec.usace.army.mil/software/hec-ras 2010) . It was developed by U.S Army Corps of Engineers and it is released as Free but not Open Source software. It runs on MS Window only and a modular GUI is provided (Figure 9).

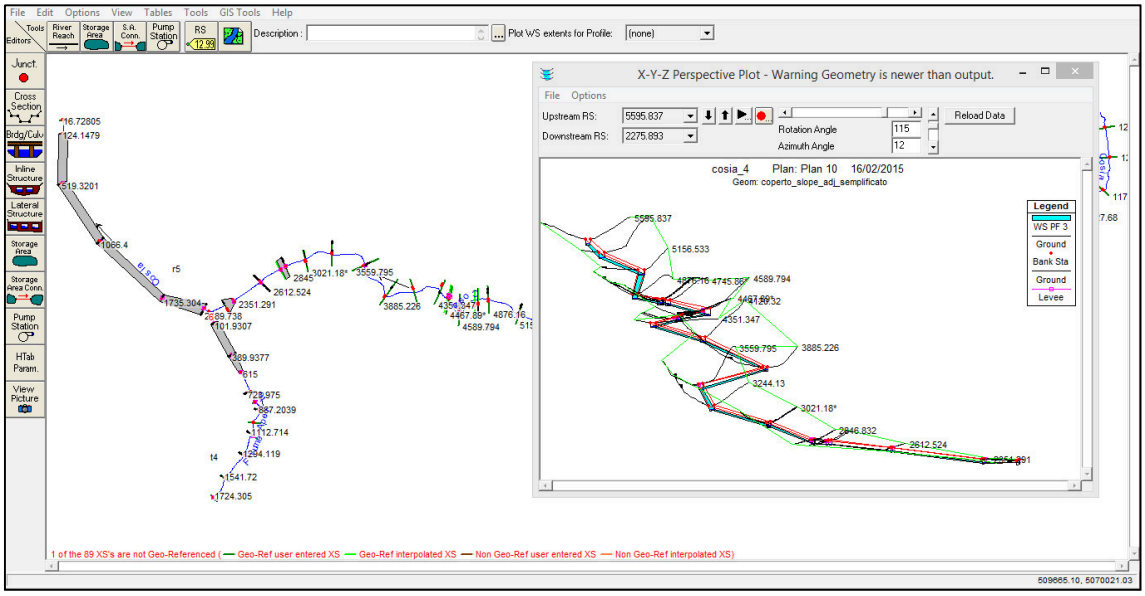

Figure 9: HEC-RAS geometry editor and 3D viewer panel.

The input data required are mainly topology and geometry for the watercourses under investigation. In order to address the editing of this kind of data some additional tools are available. These tools allow exploiting of GIS and Computer-Aided Drafting (CAD) systems to perform easily this task. One of

these plugin is HEC-geoRAS (Cameron & Ackerman 2012) and it works inside ArcGIS environment.

HEC-geoRAS is a Free but not Open Source application developed by HEC and it is based on ARC Macro Language (AML). This extension allows users with limited GIS experience to create an HEC-RAS import file containing geometric data from an existing DTM and complementary datasets (i.e. ArcGIS layers). Results of HEC-RAS simulations can be also post-processed using HEC-geoRAS to create for example inundation maps.

Simulations and data processing vary case by case due to the singularity of any watercourse. A detailed description of the analysis will be shown in section 4.6.

2.6 WEBGIS TECHNOLOGIES

The disclosure of the obtained results can be defined as an integral part of the study. Thanks to the Web Services diffusion, the possibility of sharing information has become virtually endless. We must keep in mind that most of the data used in this analysis were geospatial data and not all users are familiar with GIS technologies or with the use of maps. The best solution was therefore to implement a WebGIS to provide an easy access to these tools directly through the Web.

A WebGIS is GIS application accessible via the Internet which lets to view and query different kinds of geospatial data. It was created through the implementation of a specific architecture, which includes a Server and a Client Side. The Server Side is needed to access data and to elaborate requests coming from the Client, providing an HTML (HyperText Murkup Language) page as answer. The Client Side receives the information needed to execute the requested tasks of the users and sends back further requests to the Server. The Client lets the user to browse all the functionalities of the WebGIS. In order to allow geospatial data and functions to be interoperable between machines and be human-readable specific Web Services and Protocols have been developed. These are regulated and standardized by international associations as World Wide Web Consortium (W3C, http://www.w3.org), International Organization for Standardization (ISO, http://www.isotc211.org) and Open Geospatial Consortium (OGC, http://www.opengeospatial.org). Among all the services, some of the OWS (OGC Web Services) deserve to be remembered: WMS (Web Map Service) which is used to generate maps and

make them available as images (raster), WFS (Web Feature Service) that is used to generate maps and make them available as the real geographic features (vector) and WCS (Web Coverage Service) that generates geospatial coverages and through which the interchange of complete geospatial data (grid) via the Internet is possible.

GeoServer (http://geoserver.org) was selected to implement the Server Side. GeoServer is a Free and Open Source Server written in Java, allows users to process, edit and share geospatial data by mean of open standards. The Client based on the Leaflet JavaScript library (http://leafletjs.com) which is a Free and Open Source library for displaying map data in Web Browsers and building GIS like application in the Web (Figure 10).

The technical issues related to WebGIS programming was not among the purposes of the study. In chapter 5, practical functionalities of the system and the layers contained were explained in detail.

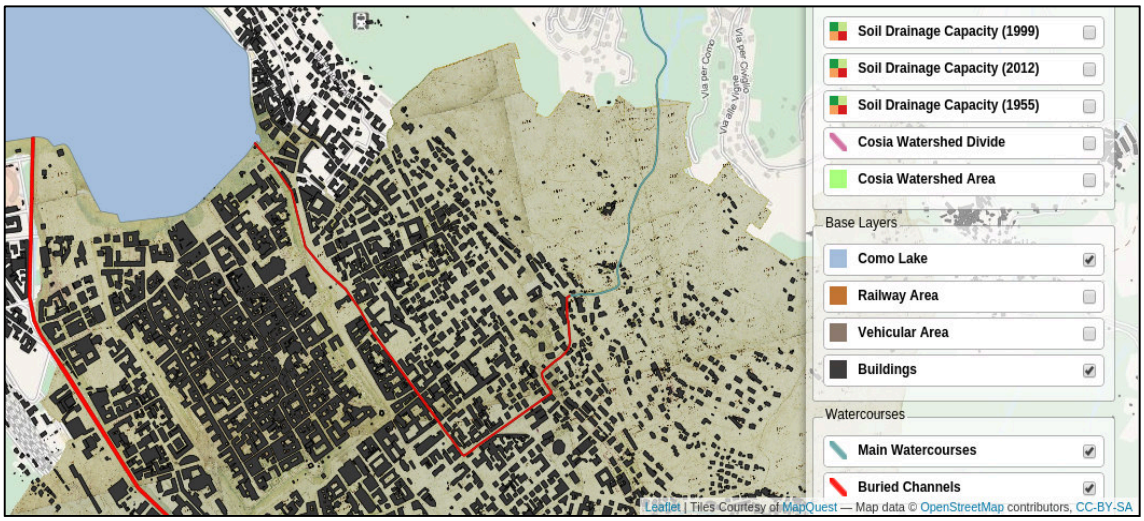

Figure 10: Screenshot of the WebGIS client interface based on Leaflet.

3. GEOSPATIAL DATA

The choice to exploit mainly GIS software capabilities surely comes from the availability and abundance of geospatial data for the case study. For Como City is available an impressive collection of historical maps, preserved mainly in public archives. The access to these documents is however not free of charge but provided as paid service or exceptionally permitted for public associations and institutions. Data necessary for hydrological and hydraulic modelling can be defined as Open Data, because most of them are freely obtainable by any user through specific geoportals (section 3.2.1). Some particular data (i.e. high-resolution DTMs) are instead not "open", but they were involved as complementary information. The distinction between historical maps and other geospatial data was important in order describe their manipulation and utilization. However, historical and hydrological information were often used together to conduct a cross-analysis of urban evolution and its effects on the watercourses.

3.1 HISTORICAL MAP COLLECTION AND PROCESSING

Thanks to the wide availability of historical cartography, the case of Como City development is well suited to be studied using maps and is often recalled in technical/educational urban archaeology literature.

"The rich history of large-scale mapping of Como (Lombardy) permits unusually detailed study of the changes that have occurred in the city's spatial structure as reflected in its built environment" (Conzen 2010).

Some of the maps came from past projects of Geomatic Laboratory, of Politecnico di Milano, Como Campus. This allowed an easy access to these data. Detailed information about the origins of the maps as well as their geometric and graphical properties were not mentioned below because not closely related with main object of this work. However, reference studies and projects were appointed for whom might be of interest.

3.1.1 The archives

The historical maps analysed in this work were provided to Politecnico di Milano mainly by two different archives, which released these documents

exclusively for research purposes. State Archive of Como (http://www.ascomo.beniculturali.it) provided maps representing the city centre of Como at the scale 1:1,000 (which were not used further because the studied torrents lie out of the them) and the suburbs at the scale 1:2,000. These belong to different cadastral series: the Theresian Cadastre (XVIII century), the Lombardo-Veneto Cadastre (mid-XIX century) with its updates and the New Lands Cadastre (1905). These maps represent one of the ancient examples related to the use of technical cartography for taxation control, which boosted the diffusion of land registers worldwide. Additionally, there was also, the oldest map of this area, the map that does not have cadastral meaning, but a purely topographic one: The topographic map of Como from the XVII century. The latter was kindly provided by Società Archeologica Comense (http://www.archeologicacomo.it).

The reference projects and studies from which we got the aforementioned data (in a suitable format for our analysis) deserve to be recalled: Web C.A.R.T.E. (http://webcarte.como.polimi.it), "Trasformazioni Cartografiche, Geocatalogo e Servizio Web di Visualizzazione dei Catasti Storici di Como" (Minghini 2010) and "A Simple WebGIS For Viewing the Evolution of The City Of Como" (Đurić 2014).

Master plan maps from the past century were instead processed within this work and provided by RAPu Archive (http://www.rapu.it). It consists in a virtual archive, collecting urban planning maps and related textual annexes, coming from all Italian territories. It aims to the dissemination of knowledge about Italian urbanistic heritage through the access of documents otherwise difficult to consult. From RAPu Archive Website (Figure 11), it is possible to download PDF documents and low-resolution maps in JPG format, while high-resolution maps are distributed under fee. We obtained them free of charge for research purpose only.

In this way it was possible to retrieve precious information about urban planning choices from different moments of the XX century, in particular: Piano Regolatore e di Ampliamento della Città di Como 1919 (Giussani & Catelli), Piano Regolatore e di Ampliamento della Città di Como 1937 (Ufficio Urbanistica - Comune di Como), Piano Regolatore Urbanistico Generale 1967 (Marrazzi et al.) and Piano Regolatore Urbanistico Generale 2001 (Rota et al.).

Additional old maps of the city centre have been used. These were originally included in the book "Como e il suo territorio" (G. Rumi et al. 1995) and published in the Website of the project "Como in the XVIII Century: Evolution of Como during The Centuries"(C. Muñoz & S. Altaf 2010). These maps were drawn by different authors with topographic intent only and not with a specific technical purpose as for cadastral ones. A detailed list of all the maps used is available in the following section (Table 2).

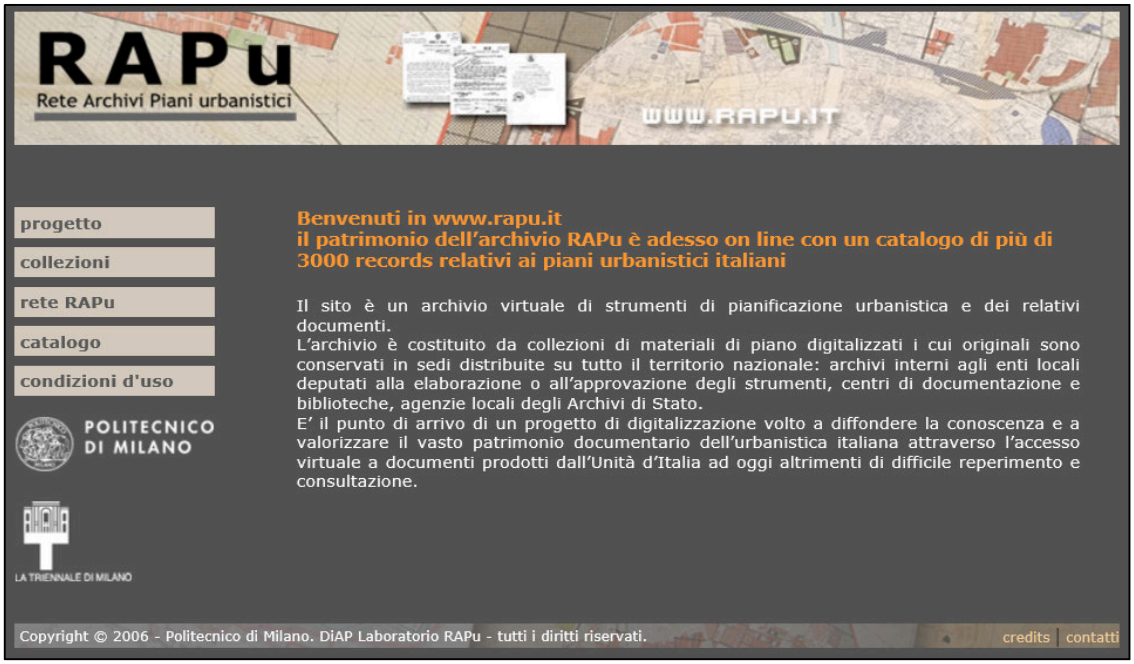

Figure 11: RAPu Archive homepage.

3.1.2 Manipulation needed for GIS environment

The analysis of historical maps within GIS required a previous specific processing on them. Maps have to be scanned, in order to create digital raster images, possibly with high-resolution scanners avoiding the loss of information to obtain an image as much as similar to the paper one. Some of the maps were originally composed by multiple sheets, which were mosaic using the FOSS GIMP (http://www.gimp.org).

After these simple but fundamental operations, it was necessary to assign to any pixel of the map a correct metric reference. When the metric reference is related to the system of earth coordinates or their map-projection counterparts, it is called georeference. This assignment was done using geometric

transformations, applied to points of the historical map with known or given coordinates. These points are called Ground Control Points (GCPs). GCPs are point features identified on the historical map, for which cartographic coordinates (i.e. coordinates expressed into a current reference and projection system) are also available. These coordinates can be directly obtained from a topographic or GPS survey, but typically they are derived from current digital cartography.

In this case, a subset of Como Municipality shapefiles was exploited (Table 1). These derive from a semi-implementation of the project "Topographic Database of the Municipality of Como" updated to 2006, not tested positive and therefore unofficial and free of certified guarantees of accuracy and fairness. It can be used exclusively as mere "background" useful for the preparation of thematic maps.

	Code	Description
1	A010101	Area of vehicular circulation
2	A010102	Area of pedestrian circulation
3	A020101	Buildings
4	A020106	Minor buildings
5	A040102	Water bodies

Table 1: Subset of Como Municipality shapefiles used for GCPs collection.

Once GCPs have been collected, a georeferencing transformation could be applied. This procedure was carried out taking advantage of Georeferencer GDAL (Geospatial Data Abstraction Library) QGIS plugin. It required manually collection of homologous points (Figure 12) that link locations on a raster image with corresponding locations in a correctly positioned vector dataset (that imply the user to have substantial knowledge about the geographic allocation of the raster image to correctly perform this task).

When a sufficient number of point was collected, a user-selected transformation was applied by the software in order to transform and resample the image.

The transformation was based on parameters, which were calculated before performing it. The larger is the number of the control points used for the computation of the parameters, the better statistical solution is achieved. A statistical estimate of the results was among the output of the process.

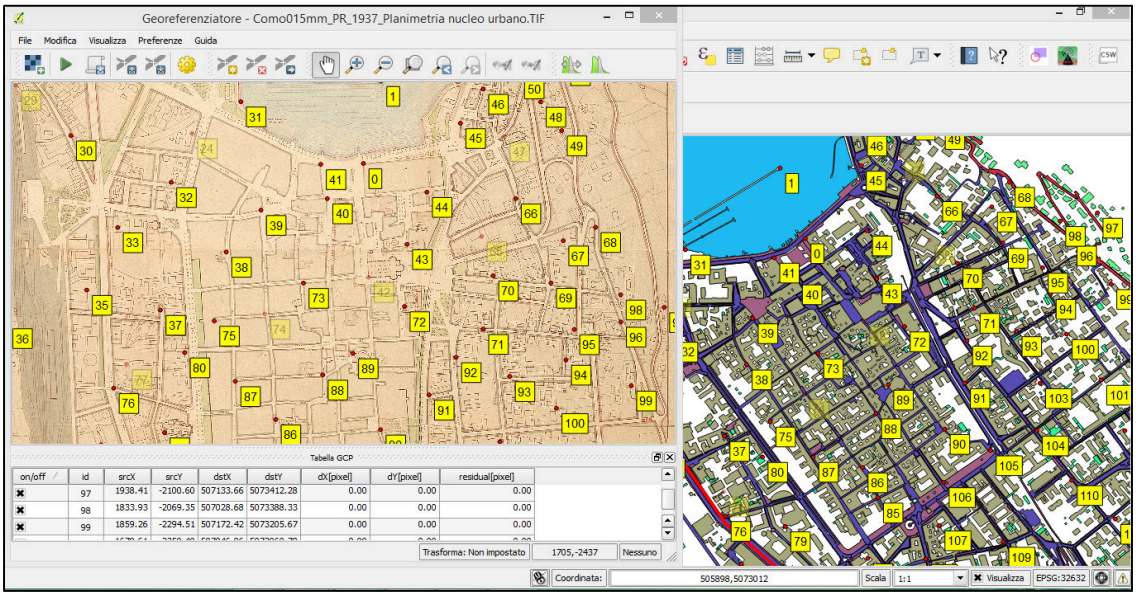

Figure 12: Homologous points collection with QGIS Georeferencer plugin.

The selected transformation derived from the well-known full polynomial system of equations:

$$X_k = \sum_{i=0}^{m}\sum_{j=0}^{n} a_{ij} x_k^i y_k^j , \qquad Y_k = \sum_{i=0}^{m}\sum_{j=0}^{n} b_{ij} x_k^i y_k^j$$

Equation 1: Polynomial system of equations

Where the summation convention in i, j was applied up to the order of the polynomial m, n. This system relates the coordinates of the control points X_k and Y_k in the geospace (or its mappings) with their coordinates x_k and y_k on the map to be georeferenced, where k (k= 1, 2, 3…) is the control point involved in the transformation. For each point k a set of two equations were taken. The required value of k for the solution of the system depends to the order of the polynomial used. The quantities a_{ij} and b_{ij} are the unknown parameters, which have been obtained by the transformation process and they are valid all over the map area. In a computational process, based on Least Squared adjustment, the number of control points should be always bigger than the unknown parameters. In order to evaluate the most suitable polynomial order (i.e. the one minimizes control point residuals), around 20% of GCPs collected have been subtracted from the points involved in the transformation and used

as checkpoints for the accuracy assessment. A specific MATLAB script, used also in the projects mentioned before, was involved to compute statistics (mean, standard deviation, minimum, maximum, and RMSE) for different polynomial orders (from 1 to 5). Based on these statistics, the scripts returned the most suitable polynomial order to apply. Unfortunately, Georeferencer plugin of QGIS is capable to apply only polynomial transformation of order 1, 2, 3. When the output of MATLAB computation indicated an order higher than 3, a further selection (between orders 1, 2, 3) was performed looking at the minimum RMSE for GCPs. The use of specific georeferencing software, in which polynomial transformations of order higher than three are allowed, could be taken into account to improve the results. The outcomes obtained with QGIS were anyhow enough suitable for the purpose of this work (Figure 13). This processing was applied on 12 historical maps (Table 2) while, for cadastral maps and topographic map of Como from the XVII century, existing processed images were included without any modification (*).

Figure 13: Map correctly placed in the geospace after georeferencing.

	Description	Source	Origin & Year	Sheets	Scale	Selected polynomial order	RMSE GCPs [m]
1	Zoning Map	RAPu Archive	Como Master Plan, 2001	2	1 : 5,000	2	8.371
2	Zoning Map	RAPu Archive	Como Master Plan, 1967	9	1 : 5,000	3	13.728
3	Zoning Map	RAPu Archive	Como Master Plan (update), 1952	1	1 : 10,000	2	22.404
4	General Planimetry	RAPu Archive	Como Master Plan, 1937	1	1 : 5,000	2	27.163
5	Average Population density Map	RAPu Archive	Como Master Plan, 1937	1	1 : 5,000	3	9.621
6	Black Sewage Schema	RAPu Archive	Como Master Plan, 1937	1	1 : 2,000	1	5.026
7	Urban Centre Planimetry	RAPu Archive	Como Master Plan, 1937	1	1 : 2,000	3	26.675
8	Urban Centre Planimetry	RAPu Archive	Como Master Plan, 1919	1	1 : 2,000	3	7.399
9	City Centre Map	Como e il suo territorio	Italian Touring Club, 1916	1	1 : 15,000	1	23.727
10	City Centre Map	Como e il suo territorio	De Agostini Geographic Institute, 1908	1	1 : 6,850	1	23.727
11	City Centre Map	Como e il suo territorio	Como Postal Almanac, 1903	1	(not available)	3	18.245
12(*)	Suburbs Map	State Archive of Como	Lombardo – Veneto Cadastre (update), 1900	(*)	1 : 2,000	(*)	(*)
13	City Centre Map	Como e il suo territorio	(not available), 1884	1	1 : 6,000	3	24.987
14(*)	Suburbs Map	State Archive of Como	Lombardo – Veneto Cadastre, 1861	(*)	1 : 2,000	(*)	(*)
15(*)	Suburbs Map	State Archive of Como	Theresian Cadastre, 1722	(*)	1 : 2,000	(*)	(*)
16(*)	Topographic Map of Como	Società Archeologica Comense	Giovio Family's Private Archive, XVII century	(*)	1 : 3,000 (approx.)	(*)	(*)
(*): map do not undergo processing within this study							

Table 2: List of historical maps involved.

3.2 VECTOR AND RASTER DATASET

One of the main benefits arising from the use of geospatial data was the possibility of obtaining accurate geometrical measurements, together with other information, from the analysed geographic features. Within any GIS software, many geoprocessing tools are available in order to assign different kinds of attributes to any analysed layer. Raster attributes were associated to each pixel (or grid cell), which also stores coordinates for a correct spatial positioning. Instead for vector data (shapefiles), additional information (i.e. those other than the pure element topology) were stored in database tables (.dbf), which represent one of the core metadata required by standard shapefile format.

A significant amount of digital cartography was involved in this study; any information has been used for specific assignment, during specific phases of the analysis. Therefore, any specific geospatial data was further described in its relative work section.

3.2.1 Data collection

Vector and raster data for Como Area were available in several geocatalogues and distributed through specific geoportals. A geoportal is a type of Web portal used to find and access geospatial information and associated geographic services (display, editing, analysis, etc.) via the Internet. Of particular interest for this work was the Lombardy Region geoportal (http://www.cartografia.regione.lombardia.it/geoportale) from which we obtained almost all the vector layers used. These mainly regard land use, pedology and stream flow-paths of the studied area and they revealed fundamental during the analysis.

Necessary information (including stream lengths and watershed areas) were extracted and stored in these layers. These have been used for the hydrological and hydraulic modelling (chapter 4).

Raster data, different from historical maps, were collected. These were DTMs, from which physiography of basins and watercourses (elevations and slopes in particular) were detected. Three Different DTMs of the area, with different cell-resolution, were tested to perform watersheds detection (section 4) and flow-paths extraction (section 3.2.2).

Figure 14: Lombardy Region geoportal homepage.

These Different DTMs are: 1) Heli-DEM (http://www.helidem.eu) DTM, it is freely obtainable through a dedicate geoportal (Figure 15) by means of WCS. The cell-size is 20x20 m. It is available in different reference frames (the European ETRF89 and the Italian Roma40) and gridded either in cartographic or geographic coordinates.

2) TINITALY/01 (http://www.tinitaly.pi.ingv.it). It is a DTM in Triangular Irregular Network format (TIN), created for the whole Italian territory in the UTM32-WGS84 coordinate system, and converted in grid format with 10x10 m cell-size (Tarquini et al. 2012). It is not freely available by the Internet but released under request by the owners for research purpose only.

3) DTM_LIDAR 2x2 m cell-size. It is available in reference frames Roma40 and covers only Lake Como backdrop and banks. Lombardy Region (http://www.regione.lombardia.it) developed this project merging a LIDAR

(Laser Imaging Detection and Ranging) survey of the area with the bathymetry of the Lake, performed by IIM (Navy Hydrographic Institute of Genoa). This DTM is distributed under fee and we obtained it freely only for research.

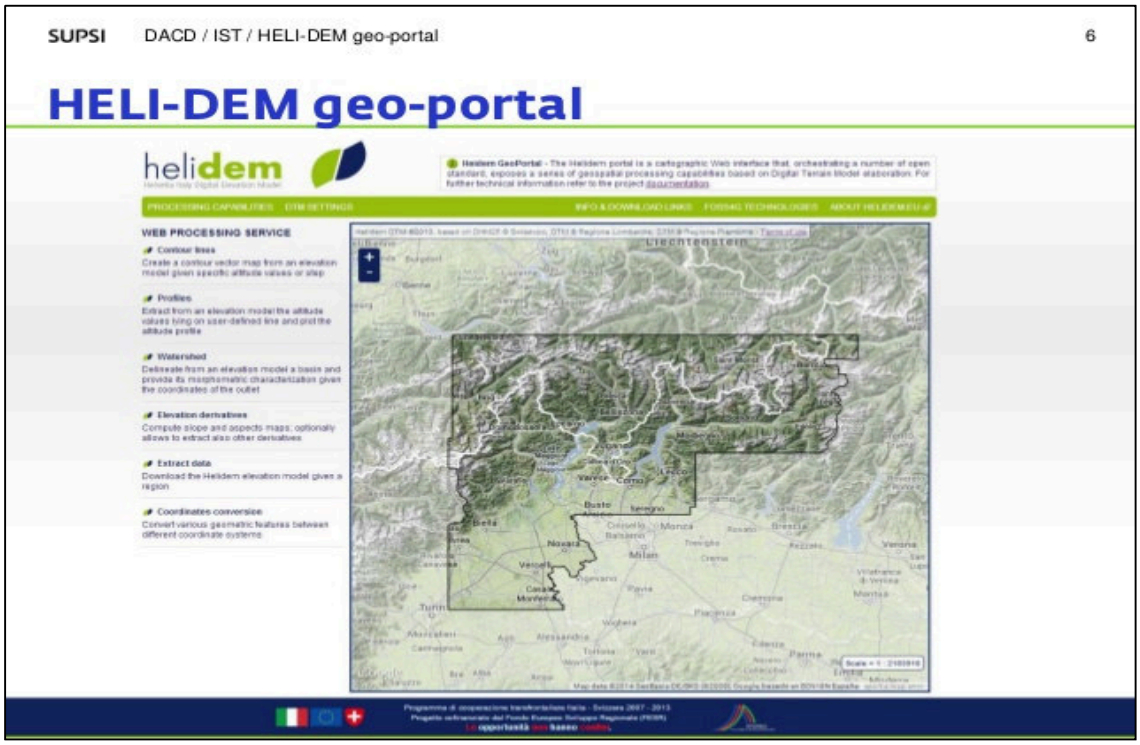

Figure 15: Heli-DEM geoportal.

3.2.2 Editing and extraction of additional data

Not all the necessary data were available directly from the geoportals. In some cases, original layers needed also a customization in order to address specific needs. One of the main trouble in dealing with minor watercourses often is the absence of existing cartography regarding them (especially in digital format). Como case was not an exception. Only Cosia Torrent was included inside drainage network layers available in Lombardy Region geoportal. Valduce Torrent as well as the tributaries of Cosia (including Aperto Torrent) were not comprehended because of their modest dimensions with respect to main watercourses of the region. In order to retrieve information on these latter, specific processing on the available data were performed.

The simplest operation was the manual editing of the watercourses (in vector format) from both historical maps and existing basemaps (i.e. OpenStreetMap)

in which these features were visible. This assignment was achieved using the Editing Toolbox of ArcGIS. An equivalent Toolbox is available also in QGIS. For the buried channels, supplementary information about their spatial position (i.e. master plan textual annexes and technical report from Municipality Archive) revealed needful. In this way, not only linear dimensions and topology of the minor watercourses became available but also changes in their flow-paths during time (perhaps due to human intervention) were detected (see section 3.3).

The extraction of the drainage network from the processing of DTMs was another possible procedure, conceptually more rigorous. Relying on the fact that superficial water runs off on the topographic surface along the direction of maximum slope (i.e. from higher to lower gravitational potential following the steeper gradient), a combination of algorithms to automatically identify water streamlines was developed inside almost all GIS software (Tarboton, D; Bras, R.L; Iturbe 1991). This procedure was carried out with ArcGIS Hydrology Toolbox. Starting from a DTM, these steps were required: 1) Create a depressionless DTM using *Fill tool* in order to remove any possible imperfection (sinks). 2) Create a grid, where to each cell is assigned a value representing the direction of flow. Using *Flow Direction tool*, for every 3x3 cell neighbourhood (Figure 16b), the grid processor finds the lowest neighbouring cell from the centre and assigns a value to the central cell that indicate this direction (Figure 16c). These numbers have no numeric meaning but are just coded directional values that indicates the steepest descent based on elevation.

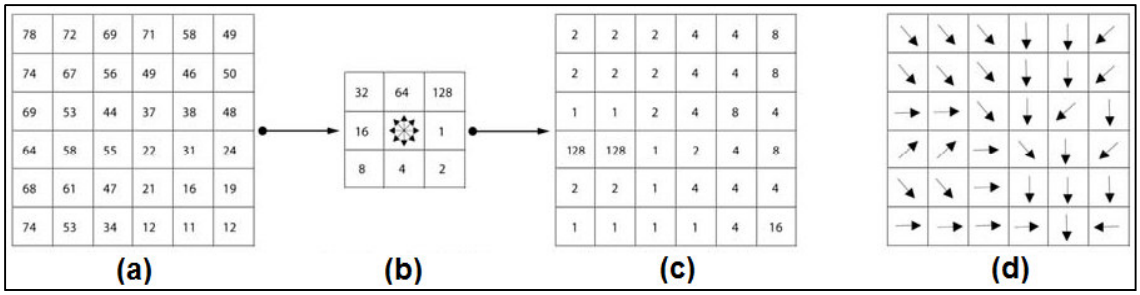

Figure 16: Flow Direction process. a) Elevation grid. b) Flow Direction coding. c) Flow Direction grid. d) Graphical representation of the Flow Direction grid.

3) Compute the flow into each cell using *Flow Accumulation tool*. The resulting grid stores in any cell a value that represents the number of cells flowing downstream into that particular cell. The main watercourses could be

recognized classifying the output raster, in order to display only the cells with high number associated (i.e. cells into which an important number of upstream cells flow). Lowering the classification break value also minor watercourses were displayed (Figure 17).

The drainage network was so extracted. This represent the most probable flow-path of the analysed watercourses but not necessarily their real position. Human intervention on the riverbeds had likely modified the slope-pattern respect to which the watercourses flow. For these reasons, further investigation on their correct positions were advisable. *Stream to Feature tool* was also involved in order to convert the flow-paths of interest in shapefile format.

Figure 17: Flow Accumulation raster (computed from HeliDEM) dipped over Como Valley. The white lines represent the flow-paths for two different classification break values: 100(left) and 5,000(right) upstream flow cells. In the first case the catchment area of any visible stream is ≥ 0.04 km² while, in the second case, it is ≥ 2 km².

The same geoprocessing was tested also using SAGA (System for Automated Geoscientific Analyses) GIS (http://www.saga-gis.org). It is a FOSS alternative to ArcGIS for hydrological analysis and it provides a comprehensive set of spatial algorithms (http://www.saga-gis.org/saga_module_doc/2.1.3/a2z.html). These can be also run directly from QGIS interface. The outcomes of Flow Accumulation process were comparable for the two GIS software (Figure 18). This test was carried out for simply evaluating the fairness of using FOSS to achieve this interesting result.

Other capabilities of ArcGIS Hydrology Toolbox were exploited in order to compute the watersheds of the studied torrents, retrieving information about their physiographic characteristics (section 4).

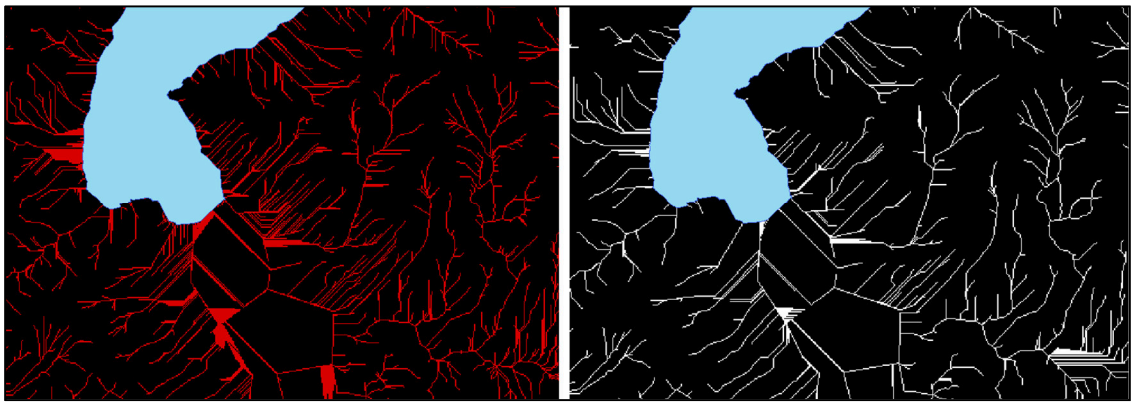

Figure 18: Comparison between Flow Accumulation rasters computed from TINITALY/01 DTM with SAGA GIS (left) and ArcGIS (Right). The calssification break value adopted is 100 (i.e catchment area ≥ 0.01 km²)

3.3 QUALITATIVE EVIDENCES OF CHANGES

The study of territorial evolutions as well as the investigation on the processes that have driven these changes are essential to ensure continuity in well-done land-management decisions (Turri 2002). These two phases, often uncorrelated, need instead to be carried out simultaneously and supported by objective proofs. Through the joint use of geospatial and historical data, both related to different moments of the city historical development, a precise reconnaissance about past and current territorial setting was achieved. A qualitative comparison between processed data revealed effective in order to detect urbanization steps as well as to bring objective evidences in support to the assumption (e.g. Gianoncelli 1975; Jorio 2006) about the original position of the watercourses.

The manual editing of the watercourse allowed a quick detection of changes in flow-path location between different epochs. Valduce Riverbed in different historical maps resulted to be drawn in different positions. The mismatches between the real position and the one retrieved from the maps were clearly visible from the Topographic Map of Como (Figure 19). Probably, these differences were due to the huge work for the maintenance of the channel after floods as well as to the intervention for private properties setting, which were crossed by the torrent. Instead, in the Theresian Cadastre Map, the position was

already similar to the actual one (Figure 20). Comparing Flow Accumulation rasters computed from different cell-size DTMs (i.e. 20 m, 10 m and 2 m), the original flow-path of the studied torrents could be detected. Considering the main stream (Cosia Torrent), the flow-path extracted from the three different DTMs crosses the city center, while its real flow-path passes through the west side of the valley. This observation can justify the validity of the hypothesis on the original central position of the torrent (Figure 21).

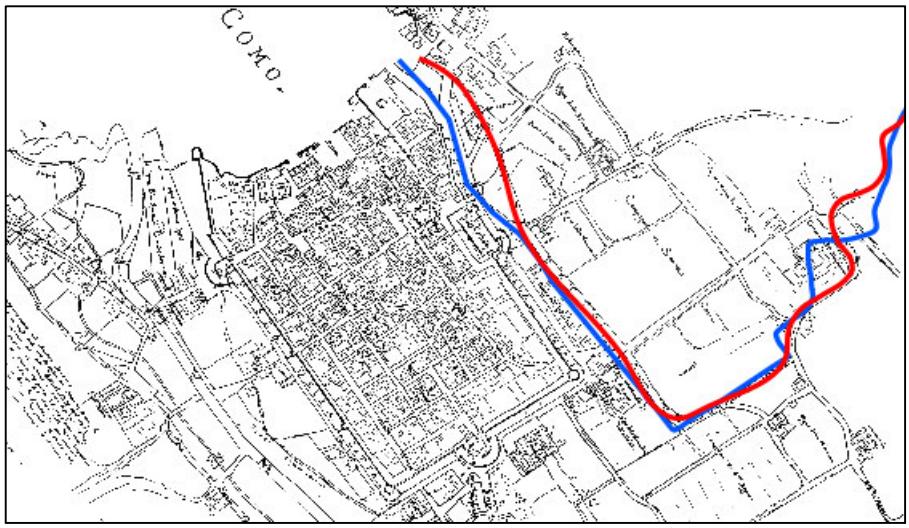

Figure 19: Valduce flow-path edited from Topographic map of Como, XVII century (red line) and real Valduce flow-path (blue line).

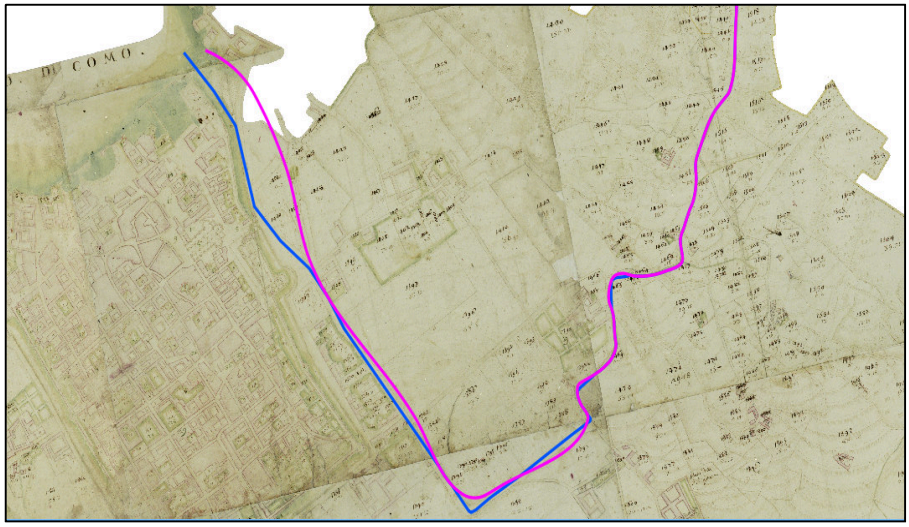

Figure 20: Valduce flow-path edited from Theresian Cadastre map, 1722 (purple line) and real Valduce flow-path (blue line).

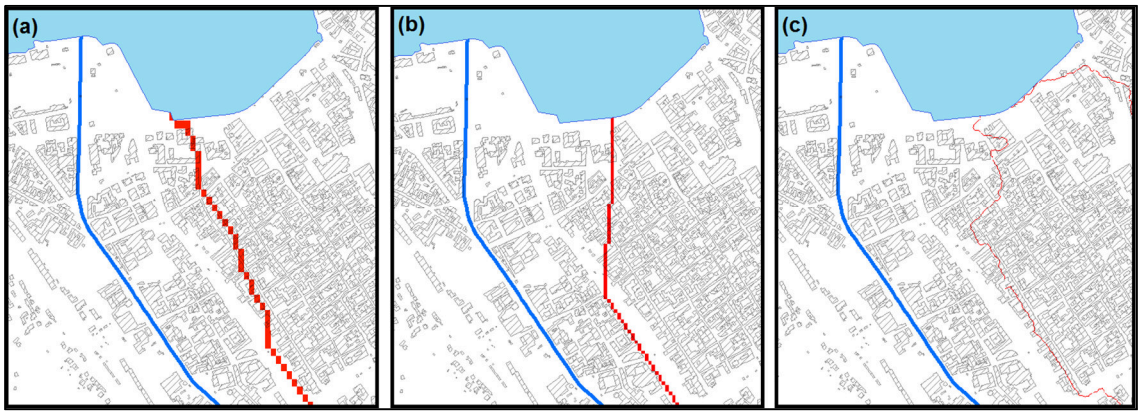

Figure 21: Cosia flow-path within the city centre (red line) computed from a) HeliDEM 20m, b) TINITALY/01 10m, c) LIDAR 2m DTMs. The blue line represents the real flow-path.

The city evolution steps found their geographical proof inside the maps. Inclusion of neighbouring municipalities, suburbs expansion and the burial of watercourses were easy identified both temporally and spatially, by comparing different period maps of the same area (Figure 22)

Figure 22: Particular of Como south suburb in Theresian Cadastre, 1722 (left) and Como Master Plan, 1952 (right). Note how the watercourses in the oldest map are clearly visible while their path disappears, covered by roads, in the more recent map.

4. HYDROLOGICAL AND HYDRAULIC ASSESSMENT

The analysis of the historical evolution of watercourses can be considered as a starting point for further investigations. The collection of existing data as well as the extraction of new one (by means of geospatial data processing) were key steps to ensure a valuable dataset for any further scientific study. Birth and expansion of the built environment cannot avoid hacking of the original settings for the territories in which these phenomena occurred. One of the well-known effects of the urbanization is definitely the soil sealing due to the widening of impervious areas. This normally results in an increasing surface runoff that affects the watersheds. Consequently, after intense rainfalls, higher peak flowrates are expected to run into streams in shorter times. The burials of the watercourses surely were designed with the best available knowledge and technology of the period in which these works were done (i.e. early XX century). However, it must be consider that in the following decades, hydrology and hydraulics sciences went rapidly forward and nowadays, new more accurate tools to improve hydrological analysis and hydraulic simulations are available. On the other hand, studies carried out almost a century ago, could not take into account the drastic changes that happened in the last period on the most relevant hydrological variables. For these reasons, in order to check if the discharge capacity of the buried channels is still enough even after the alterations brought by the urbanization process, a specific hydrological and hydraulic assess for the main watercourses and the related watersheds was here included.

The purpose of this study was to detect the changes, which occurred in land use within the watersheds of interest, by means of specific Rainfall-Runoff Models (RRMs), to quantify the resulting peak flood discharges. RRMs are standard tools in engineering and environmental science to evaluate catchment response to land use variability. Even if numerous hydrological variables may had changed along time (i.e. last seventy years); here, only the land use evolution was taken into account. This choice lies in the fact that the latter is directly related with the urban planning choices, and not with more complex regional or global climatic phenomena, which are influencing the water cycle (i.e. temperature variation, precipitation intensity, etc.). In this way, a rough simplification in flood discharge estimation was introduced; however, the results perfectly highlighted the "pure" human influence on surface runoff after

a specific rain-event (i.e. project storms). Practically, this means that by keeping the project storm fixed, we quantified the expected peak flowrates related with different land use scenarios, expressed by the land use data of three different years: 1955, 1999 and 2012 (section 4.2). In this way, the results can be easily related to the birth of industrial facilities, new residential areas, etc. that happened historically along the period in the watersheds of interest.

Flow-measurement records are not available for the studied torrents. Therefore, Empirical RRMs (i.e. models purely based on the information retrieved from the data or "black box") could not be suitable, due to the lack in calibration/validation data. In order to overcome this limitation, Parametric RRMs are commonly adopted. The RRMs involved in this study are called *Lumped* because they aggregate different hydrological processes developing within the watershed (i.e. rainfall, infiltration, evapotranspiration etc.) into a single parameter for the entire study area, which can therefore often not be derived directly from field measurements. Parametric models have a structure that is specified prior to their use and hence such models are commonly termed *Conceptual* (or "grey box"). These make up the vast majority of models used in practical applications (Wagener et al. 2004). The dependence of parameters calibration on flow-measurements makes their use difficult in ungauged basins. However, a wide set of experimental formulas and results is available, this helps the parameter assessment starting from the watershed characteristics with which they are linked to. In this study, due to the lack of streamflow data, this approach resulted as the only suitable one. Anyway, in order to reach better accuracy, calibration procedures are highly advisable. The computed peak flood discharges were used in order to assess the discharge efficiency of the buried channels through steady-flow simulations with HEC-RAS (see section 4.6). The hydraulic model for the main watercourses was developed starting from DTM analysis and improved using field observations collected with Geopaparazzi.

4.1 PHYSIOGRAPHICAL CHARACTERISTICS OF THE WATERSHEDS

Watershed physiography is one of the well-studied feature of hydrology. Maps representing the drainage areas have been involved since the beginning of such studies, in order to compute measurements and correlate them with watershed and drainage network characteristics by means of specific indices. The digital cartography has brought significant advantages in carrying out these

computations, which are now included within GIS environment. Other important information about watershed hydrology regard also the land use as well as rainfall distribution over the area under investigation. These items were discussed in section 4.2 & 4.3

The first step in the watershed analysis was to identify its divide. The divide can be defined as the line that separates one drainage basin from another; it follows the ridges or summits that form the exterior of the drainage basins. It delimitates an area of diversion or drainage area; that hat contributes water to the watershed (Adrien & Nicolas 2004). Often, surface water divide and groundwater divide within the same watershed do not overlap as they follow different paths. In this study, we pointed our attention only on surface runoff thus we identified only the surface divide (called also *topographic divide*), by means of a DTM analysis. Heli-DEM DTM was used to carry out this physiographic analysis. Starting from the Flow Accumulation raster it was possible to set appropriate outlet points for the watercourses, which paths are clearly underlined in section 3.2.2. An outlet point layer in ArcGIS was edited and placed it in the correct position (e.g. stream junctions and lake land locks). *Snap Pour Point tool* was employed in order to assign the outlet position to the Flow Accumulation raster. Finally, *Watershed tool* was used to delineate the watershed area (Figure 23). The watershed raster was computed automatically by the software. The grid calculator assigns "noData" value to any cell that do not flow towards the outlet point. To the cells in the watershed area, a value equal to the sum of all the cells within the watershed is associated. The watershed rasters were converted into shapefiles in order to facilitate geometric measurements on them.

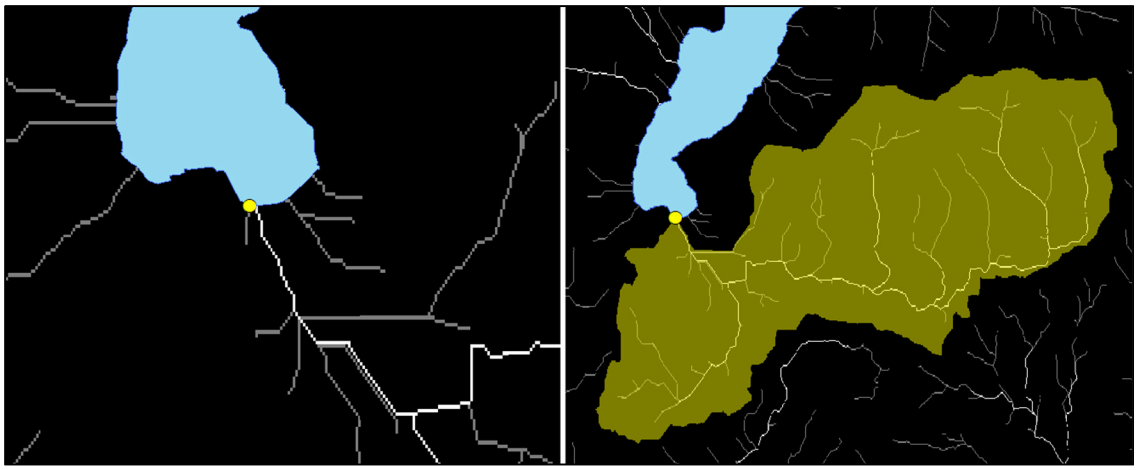

Figure 23: Outlet point identification on the Flow Accumulation raster (left) and watershed area delineation (right) with ArcGIS.

Due to the Roman diversion of the riverbeds some handworks on the extracted shapefiles was needed to get the model of the actual drainage network. The Roman works shifted the outlets of the main watercourses in a different position with respect to the ones indicated by the Flow Accumulation raster, as shown in section 3.3.

A specific set of algorithms to perform the same tasks is available in SAGA GIS (http://www.saga-gis.org/saga_module_doc/2.1.3/ta_channels_1.html) either in other FOSS GIS. Anyhow, these software require different input parameters; thus, ArcGIS procedure, with the available pre-processed data, was the fastest to be implemented.

In the watershed shapefile tables were included fundamental information such as perimeter [km], area [km²], average slope [%] and average/Min/Max altitudes [m a.s.l]. This was achieved by exploiting the 3D Analysis Toolbox and the *Calculate Geometry tool* of ArcGIS. The same procedure was applied also to the watercourse shapefiles, for which: stream lengths [km], average slopes [%] and stream order were computed (see section 4.1.1).

Cosia and Valduce watersheds together represent the drainage area of all the shallow water flowing in the Como Valley. A schematic view of the two watersheds is shown in Figure 24. These watersheds were described by means of standard physiographic indices in section 4.1.1 & 4.1.2

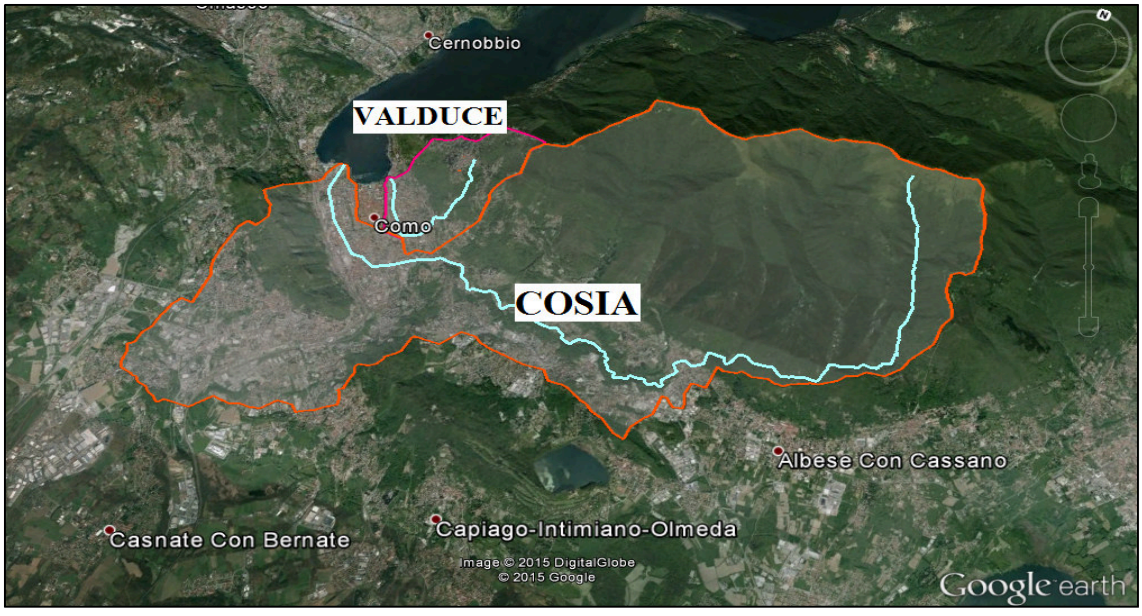

Figure 24: Watersheds (area inside the red and purple divides) and main watercourses (light blue lines) under investigation.

4.1.1 Cosia Watershed

Cosia Watershed includes Brunate-Bollettone mountains (east side of Como Valley), Monte Croce-Baradello hills (west side) as well as the southern suburbs of the city and Camerlata Plain. Its area is 36.35 km² (A) and its divide (P) measures 34.06 km. The altitude of the highest point of the basin is 1307 m a.s.l (h_{max}) while the lowest altitude point (i.e. the outlet) is 197 m a.s.l (h_{min}). It is a sub-basin of the bigger Adda Watershed, which flows into the Po River. It is bounded by the Seveso Watershed (south-west), Lambro Watershed (south-east) and by the Lake Como (north). Its main watercourse is the Cosia Torrent which pass through five different municipalities (i.e. Albavilla, Albese con Cassano, Tavernerio, Lipomo and Como) and it measures 14.8 km (L). Cosia Torrent receives water from numerous minor streams, which are characterized by enhanced torrential regime and thus their flowrates are affected by high variability. In order to identify the most important tributaries, we classified the Flow Accumulation raster with a break value of 5,000 (i.e. catchment area ≥ 2 km²). In this way, four main tributaries were identified: Rondina Torrent, Valloni Torrent, Vallaccia Torrent and Aperto Torrent (Figure 25).

Figure 25: Cosia Torrent (blue line) principal tributaries (light blue lines). 1) Rondina Torrent, 2) Valloni Torrent, 3) Vallaccia Torrent, 4) Aperto Torrent.

At this scale of analysis, Cosia Torrent resulted of the Second Order, based on Horton & Strahler Method. The stream order was automatically computed using the *Stream Order tool*, included in the Hydrology Toolbox of ArcGIS.

The shape of a watershed is a fundamental hydrological information. This influences the shape of its characteristic hydrograph (i.e. flow vs time curve). For example, a long shape watershed generates, for the same rainfall, a lower outlet flow, as the concentration time (see section 4.4) is higher. A watershed having a fan-shape presents a lower concentration time, and it generates higher flow (Musy & Higy 2011). Different geomorphologic indices have been proposed in order to describe the watershed shape. The most commonly adopted is the Gravelius's index K_G, which is defined as the relation between the perimeter (P) of the watershed and that of a circle having a surface equal to the watershed (A):

$$K_G = \frac{P}{2\pi\sqrt{A}} \approx \frac{0.28P}{\sqrt{A}}$$

Equation 2: Gravelius's index

K_G values close to 1 mean fan-shape while values higher than 1 indicate long shape. For Cosia Watershed, it resulted to be equal to 1.6038, thus long shape.

The relationship between areal information and elevation were also needed in order to complete the watershed description. These were retrieved by the interpolation of the watershed and watercourse shapefiles with the DTM. This task was performed exploiting *Adding Surface Information tool,* included in ArcGIS 3D Analysis Toolbox, and the *Hypsometry tool,* which is a FOSS Python script (http://arcscripts.esri.com/details.asp?dbid=16830). It can be free downloaded and run inside ArcGIS. The latter let to compute automatically the Hypsometric curve (Graph 1a). This dimensionless curve showed the proportion of land area that exists at various elevations by plotting relative areas $A_i/A (0 \leq A_i \geq A)$ against relative altitude $H_i/H_{max} (0 \leq H_i \geq H_{max})$. In order to compute it, the relative altitude $H_{max} = (h_{max} - h_{min})$ was split into n intervals and to each of them the enclosed watershed area was associated. Knowing h_{max} and h_{min} of the watershed it was possible to draw the Hypsographic curve, that represents the watershed area distribution with respect to the absolute altitude h_i, as it is shown in Graph 1b. The average

altitude h_m, which is defined as the average of the watershed altitudes weighted on area, was computed starting from these data and it is equal to 580 m. a.s.l.

$$h_m = \frac{\sum_i^n (h_i + h_{i+1}) . A_{i,i+1}}{2A}$$

Equation 3: Watershed average altitude.

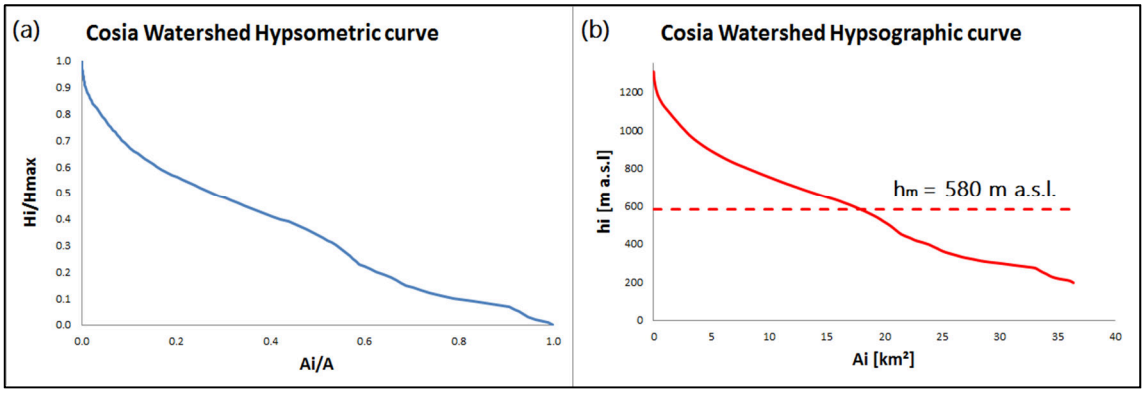

Graph 1: Hypsometric curve (a) and Hypsographic curve (b) of Cosia Watershed.

Another important information, that the Hypsographic curve gives, is the watershed evolution stage, which can be estimated by its integral, called Hypsometric integral. Values of the Hypsometric integral higher than 0.6 are considered as typical for the early evolution stage of the watershed while, values lower than 0.4 indicate senile evolution stage. Intermediate values are associated to maturity or equilibrium stage (Ferro 2006). Cosia Hypsometric integral, computed by the trapezoidal method, turned out to be equal to 0.345 that corresponds to senile evolution stage.

The average slope i_m of Cosia Watershed, equal to 35 %, was obtained by means of the *Adding Surface Information tool* of ArcGIS, while the average slope i_a of the main stream (Cosia Torrent) is 8.2 %. The elevation profile of the watercourse was also obtained with the same procedure (Graph 2). The length of the main stream from the divide to the outlet L_d was also calculated because required for further computations (see section 4.4).

Physiographical information are commonly requested as input data in hydrological modelling. For the implementation of conceptual models in

ungauged watersheds these information are essential in order to carry out peak discharges estimation. Cosia Watershed parameters are shown in Table 3.

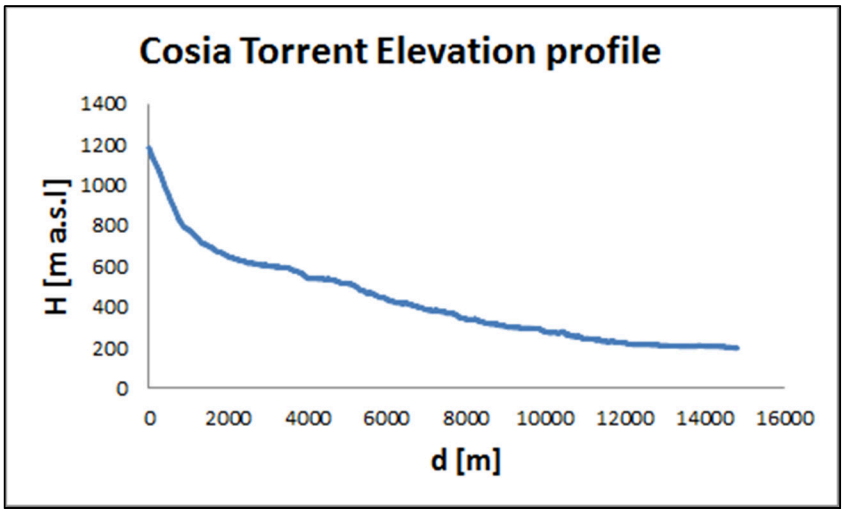

Graph 2: Cosia Torrent elevation profile; d represent the distance from the source.

Area (A) [km²]	36.35
Perimeter (P) [km]	34.06
Main stream length (L) [km]	14.8
Main stream length up to the divide (L_d) [km]	14.98
Max absolute altitude (h_{max}) [m a.s.l.]	1307
Min absolute altitude (h_{min}) [m a.s.l.]	197
Relative altitude from the outlet (H_{max}) [m]	1110
Average altitude (h_m) [m a.s.l.]	580
Average slope (i_m) [%]	35
Main stream average slope (i_a) [%]	8.2
Main stream order (Strahler) [/]	2
Gravelius's index (K_G) [/]	1.6038
Hypsometric integral [/]	0.345

Table 3: Physiographical characteristics of Cosia Watershed.

4.1.2 Valduce Watershed

Valduce Watershed is placed at the east side of the Como Valley; it drains the Brunate Mountain as well as the east side of the city centre. Valduce Watershed

extends over 2.80 km² and its divide is 7.17 km long. The highest altitude is 985 m a.s.l while the lowest altitude is 197 m a.s.l. It is a less important watershed with than the Cosia one and its main stream (Valduce Torrent) measures is only 2.94 km long. It origins from two little springs placed near the centre of Brunate Municipality and it reaches Como City by flowing through a steep rocky riverbed, characterized by many waterfalls. In order to identify its flow-path, a small break value of 100 (i.e. catchment area ≥ 0.04 km²) was used in the classification of the Flow Accumulation raster due to the small dimensions of the watershed and of its drainage network. Valduce Torrent flows underground for a significant portion of its path. Therefore, the DTM was not able to underline the real path of the torrent. The detection of the precise position of the buried channel required the use of historical maps. Actually, modern geospatial data related to this little torrent are not available. The tributaries of Valduce Torrent are mostly negligible streams that contribute to the total flow of Valduce Torrent only during intense rainfalls. Thus, Valduce Torrent was assumed to be the only stream drains the entire watershed (Figure 26).

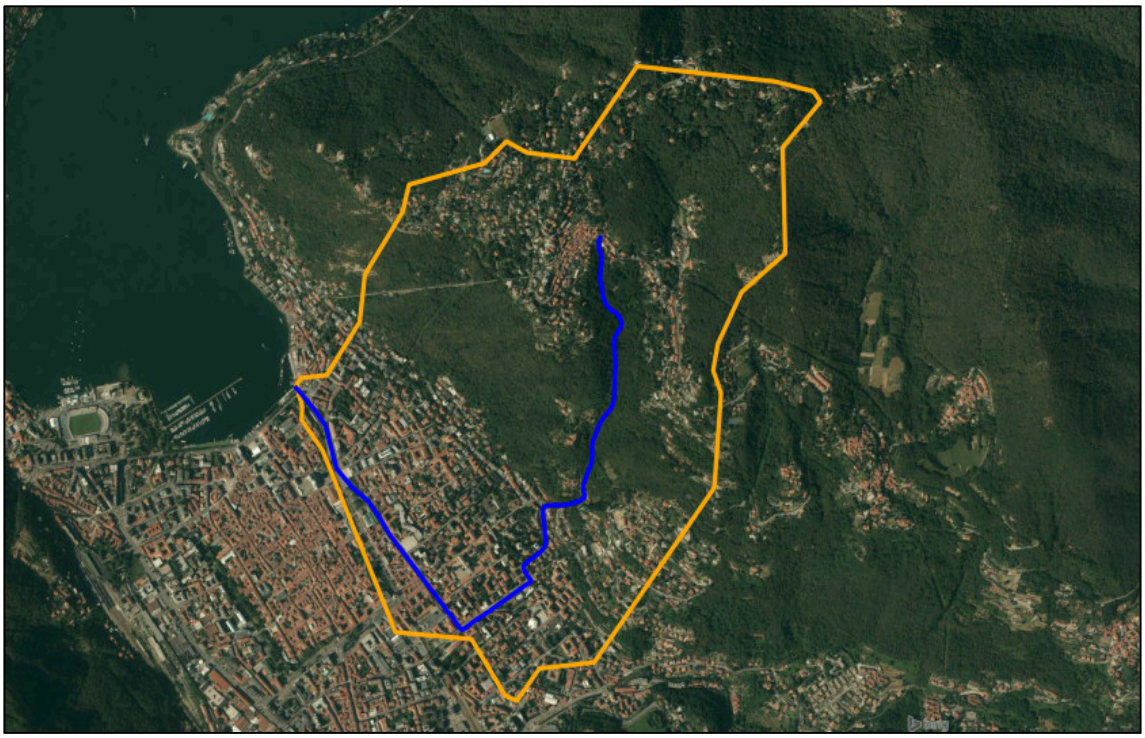

Figure 26: Valduce Watershed (orange divide) and Valduce Torrent (blue line).

By applying the same procedure described for the Cosia Watershed, the main physiographical characteristics of the Valduce Watershed were obtained. These are summarized in Graph 3, Graph 4 and Table 4.

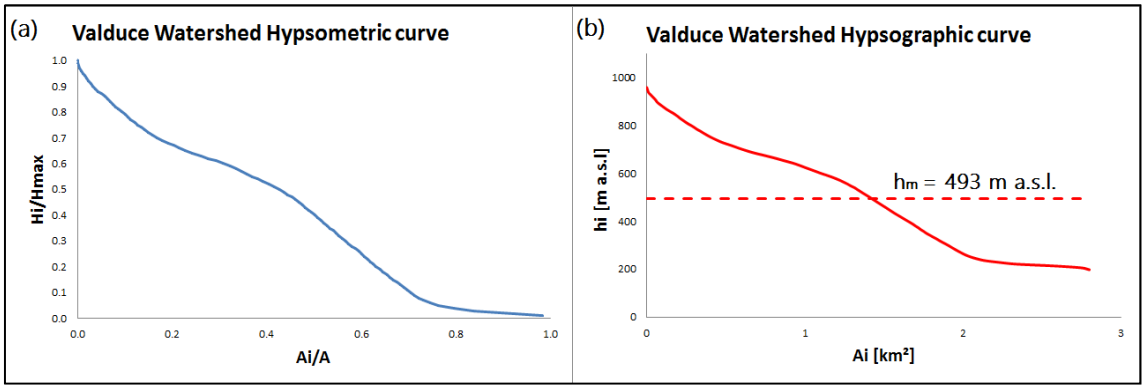

Graph 3: Hypsometric curve (a) and Hypsographic curve (b) of Valduce Watershed.

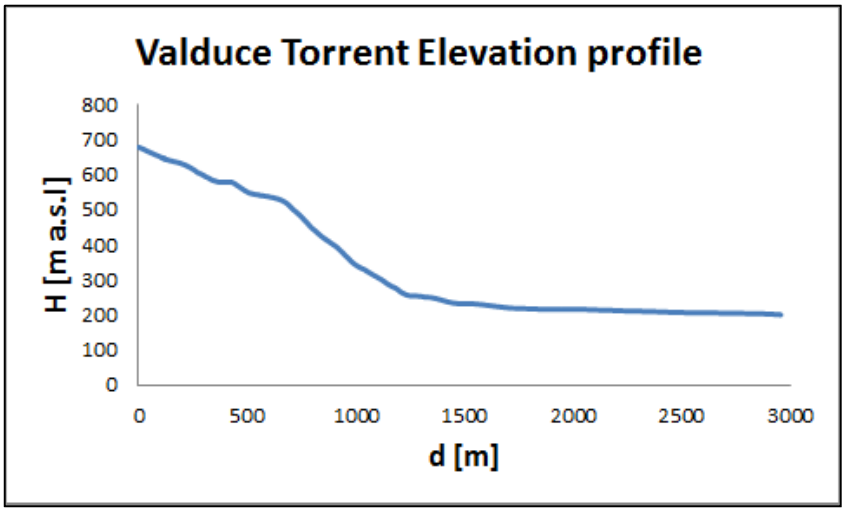

Graph 4: Valduce Torrent elevation profile, d represent the distance from the source.

Area (A) [km²]	2.80
Perimeter (P) [km]	7.17
Main stream length (L) [km]	2.94
Main stream length up to the divide (L_d) [km]	3.85
Max absolute altitude (h_{max}) [m a.s.l.]	985
Min absolute altitude (h_{min}) [m a.s.l.]	197
Relative altitude from the outlet (H_{max}) [m]	788

Average altitude (h_m) [m a.s.l.]	493
Average slope (i_m) [%]	41
Main stream average slope (i_a) [%]	18
Main stream order (Strahler) [/]	1
Gravelius's index (K_G) [/]	1.1998
Hypsometric integral [/]	0.389

Table 4: Physiographical characteristics of V alduce Watershed.

Notice that the Valduce Watershed parameters indicate a shape close to the fan-shape and both the watershed and the riverbed slopes are steeper than for the Cosia Watershed. The Hypsometric integral underlines a senile evolution stage; its value is higher than the one of the Cosia Watershed (i.e. Valduce Watershed seems to be "younger").

4.2 LAND USE AND SOIL TYPE DATA

The land use within a watershed is one of the most important parameters influencing the shallow water behaviour. *"Land use is characterised by the arrangements, activities and inputs people undertake in a certain land cover type to produce, change or maintain it"* (FAO 1999). Therefore, land use changes are directly connected with the land management and planning or, more in general, with human choices.

In order to study changes in land use along time in the study area, land use data of different periods were collected. These data were retrieved as shapefiles from Lombardy Region geoportal. They cover all the regional territory. Land use layers were provided by Ente Regionale per i Servizi all'Agricoltura e alle Foreste (ERSAF) and recorded within the database Destinazione d'Uso dei Suoli Agricoli e Forestali (DUSAF). The land use layers have been obtained by means of aerial photos interpretation. The shapefiles have been created with a scale of 1:10,000. DUSAF classification for land use layers consider a hierarchical structure of five levels. Levels 1, 2, 3 are defined in the same way of Corine Land Cover, (these let to compare land use data at interregional scale) while levels 4 and 5 describe local characteristics relying on auxiliary datasets which were involved during the aerial photos interpretation to improve the information detail (Fasolini et al. 2010).

In this study, land use data coming from three different time periods were involved. These are: 1) Land Use, 1955, which was obtained by the

interpretation historical aerial photos, which were shot by Italian Military Geographical Institute (IGM). 2) DUSAF 1.0, 1999 and 3) DUSAF 4.0, 2012. In this way, three different land use scenarios were considered, which were useful in the study of land use changes occurred in the last sixty years. The land use layers were clipped on the study area by means of intersection with the watershed shapefiles, in order to reduce the file dimensions and facilitating their manipulation. (Figure 27).

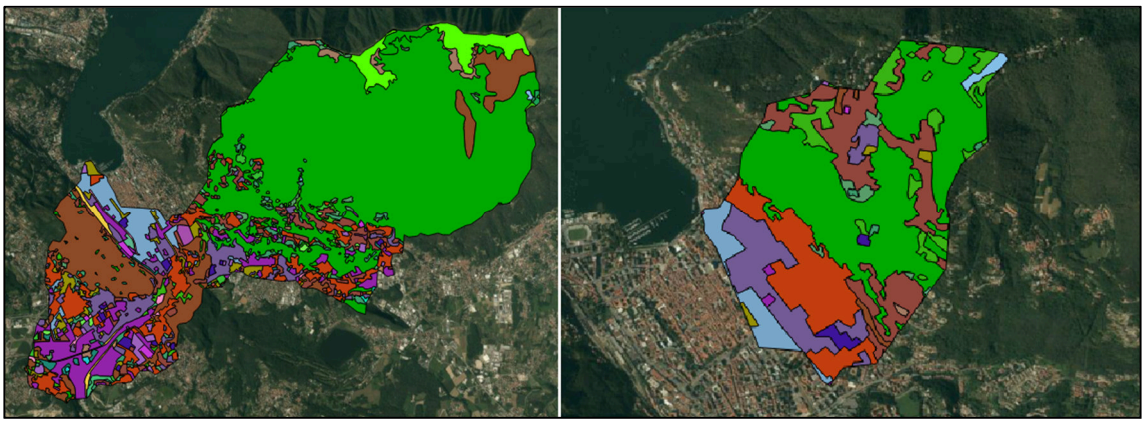

Figure 27: Land use DUSAF 4.0 clipped on Cosia Watershed (left) and Valduce Watershed (right). Different colours represent different land use classes.

The main effect of land use changes is the modification of the infiltration capacity of the soil, thus the modification of runoff characteristics. Usually, the urbanization process is characterized by the arise of new impervious areas. Residential settlements, roads and parking as well as industrial facilities are ever obstacles for rainfall catching by the ground. Moreover, lack in vegetation or bared lands lose their efficiency in catching part of the rainfall. Thus, the surface runoff volume increases while the time it takes to reach the drainage network normally decreases, yields in higher peak flowrates to be conveyed by streams and channels.

The purpose of this study was to quantify the runoff capacity changes in the considered watersheds, due to changes in land use. Different land use scenarios, corresponding to the three land use data, were considered. In order to quantify the soil runoff capacity, Curve Number (CN) parameter (U. S. Department of Agriculture 2004) was used. This is a number ranging from 1 to 100 and represents the properties of the type of soil and land use within a portion of land (Adrien & Nicolas 2004). For the same rainfall, higher CN values

potentially result in higher volume of surface runoff. This parameter is one of the input data required by NRCS methodology, used for peak discharge estimation as described in section 4.5.

NRCS tabulated the CN values based on the land use and the soil type. The latter was classified in four different classes (i.e. A, B, C and D), based on the soil saturated hydraulic conductivity (K_{sat}) as shown in Table 5. These classes are called Hydrologic Soil Groups (HSGs). CN values were calibrated through a huge number of experiments, carried out by USDA along the second half of the last century.

HSG	Conductivity range [in/ h]
A	$K_{sat} > 0.3$
B	$0.15 < K_{sat} \geq 0.3$
C	$0.05 < K_{sat} \geq 0.15$
D	$K_{sat} \leq 0.05$

Table 5: Hydrologic Soil Group conductivity ranges.

The soil type of the study area was detected from the Pedological map at the scale 1:250,000, provided by ESRAF through the Lombardy Region geoportal. The Pedological map was also clipped on the watershed areas (Figure 28). It contains polygons, with relative attributes, describing the soil type and soil physical characteristics. Unfortunately, K_{sat} is not included among these information and the soil classification did not match directly with HSGs.

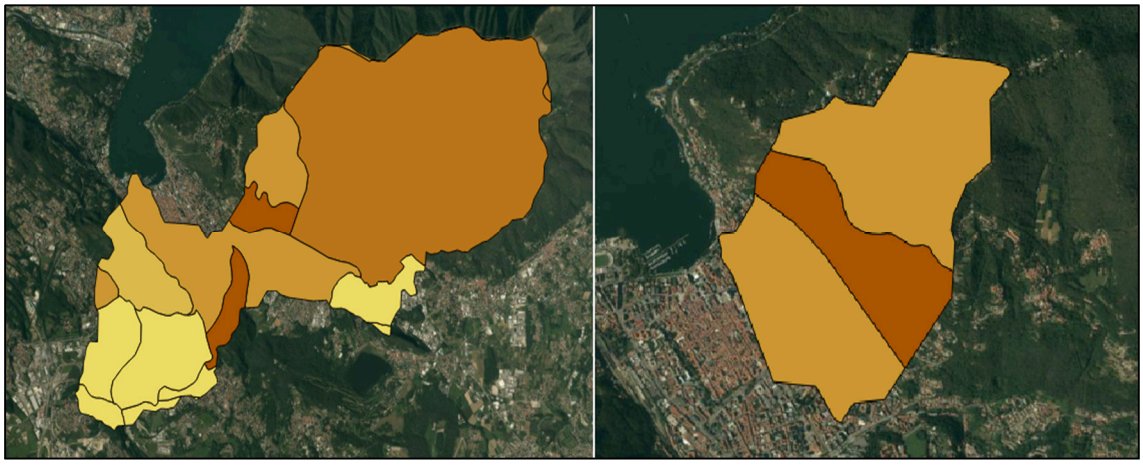

Figure 28: Pedological map dipped on Cosia Watershed (left) and Valduce Watershed (right). Different colours represent different soil type classes.

In order to attribute the HSG to each soil type, K_{sat} was calculated for the Pedological map classes, based on their typical clay and sand fractions. In order to compute the saturated hydraulic conductivity we exploited a Web Application available in ARPA Sardinia Website (http://www.sar.sardegna.it/servizi/agro/idrosuoli.asp). An average K_{sat} was computed for each soil class included in the Pedological map (Table 6). The translation was performed assigning to each of them an appropriate HSG.

	Pedological map soil type code	**Description**	**Average % sand / % clay**	**Average K_{sat} [in/ h]**	**HSG**
1	A	Clay	20\60	0.075	C
2	AL	Silty Clay	5\45	0.122	C
3	FLA	Silty Clay Loam	15\35	0.150	C
4	FL	Silt Loam	20\15	0.736	A
5	L	Silt	5\5	1.724	A
6	FA	Clay Loam	35\30	0.146	C
7	F	Loam	45\20	0.323	A
8	FSA	Sandy Clay Loam	60\25	0.165	B
9	AS	Sandy Clay	45\50	0.043	D
10	FS	Sandy Loam	65\10	1.055	A
11	SF	Loamy Sand	85\5	2.815	A
12	S	Sand	95\5	3.480	A

Table 6: Pedological soil-classes translated to HSGs.

The creation of CN maps required also an appropriate translation of the DUSAF classification in order to set appropriate CN values. This translation required less effort with respect to the Pedological map because DUSAF land use classes and NRCS ones resulted to be easily comparable (Table 7). Thus, in the attribute tables of both land use and soil type shapefiles were included NRCS land use class and HSG information.

	NRCS land use class	**DUSAF land use class**
1	Meadow—continuous grass, protected from grazing and generally mowed for hay	• Aree verdi incolte • Praterie naturali d'alta quota assenza di specie arboree ed arbustive • Prati permanenti • Prati permanenti in assenza di specie arboree ed arbustive • Seminativi semplici

2	Agricultural lands	♠ Colture orticole a pieno campo ♠ Colture orticole protette. ♠ Orti familiari
3	Woods	♠ Boschi di conifere a densità media e alta ♠ Boschi di latifoglie a densità media e alta ♠ Boschi di latifoglie a densità bassa ♠ Boschi misti a densità bassa ♠ Boschi misti di conifere e di latifoglie ♠ Boschi misti a densità media e alta
4	Woods—grass combination (orchard or tree farm)	♠ Castagneti da frutto ♠ Frutteti e frutti minori ♠ Praterie naturali d'alta quota con presenza di specie arboree ed arbustive sparse ♠ Seminativi arborati ♠ Vigneti ♠ Altre legnose agrarie
5	Brush—brush-weed-grass mixture with brush the major element	♠ Cespuglieti con presenza significativa di specie arbustive alte ed arboree ♠ Cespuglieti e arbusteti ♠ Cespuglieti in aree di agricole abbandonate ♠ Formazioni ripariali
6	Open space (lawns, parks, golf courses, cemeteries, etc.)	♠ Cimiteri ♠ Impianti sportivi ♠ Parchi e giardini
7	Fallow (bare soil)	♠ Aree degradate non utilizzate e non vegetate ♠ Cave
8	Urban districts	♠ Impianti di servizi pubblici e privati ♠ Insediamenti di grandi impianti di servizi pubblici e privati ♠ Impianti tecnologici ♠ Insediamenti industriali, artigianali, commerciali ♠ Insediamenti industriali, artigianali, commerciali e agricoli con spazi annessi ♠ Insediamenti ospedalieri
9	Impervious areas	♠ Reti ferroviarie e spazi accessori ♠ Reti stradali e spazi accessori ♠ Aree portuali (*) ♠ Bacini idrici naturali (*)
10	Newly graded areas, (pervious areas only, no vegetation)	♠ Cantieri
11	Residential districts by average lot size 2 acres	♠ Cascine
12	Residential districts by average lot size 1 acre	♠ Tessuto residenziale sparso

13	Residential districts by average lot size 1/2 acre	• Tessuto residenziale rado e nucleiforme
14	Residential districts by average lot size 1/3 acre	• Tessuto residenziale discontinuo
15	Residential districts by average lot size 1/4 acre	• Tessuto residenziale continuo mediamente denso
16	Residential districts by average lot size 1/8 acre or less (town houses)	• Tessuto residenziale denso
17	Farmsteads—buildings, lanes, driveways and surrounding lots	• Insediamenti produttivi agricoli
(*)	No translation found. These classes were arbitrary treated as impervious areas. For Cosia and Valduce watersheds, they represent less than 0.0001 % of the total area.	

Table 7: Translation table from DUSAF to NRCS land use dasses.

Finally, by means of the *intersection tool* applied to land use and soil type shapefiles, we obtained a single layer containing both those information (Figure 29). Moreover, the surface extension of any sub-polygon of these maps was computed and added to the attribute tables. Proper CN value was assigned to any sub-polygon using NRCS-CN tables (U. S. Department of Agriculture 2004).

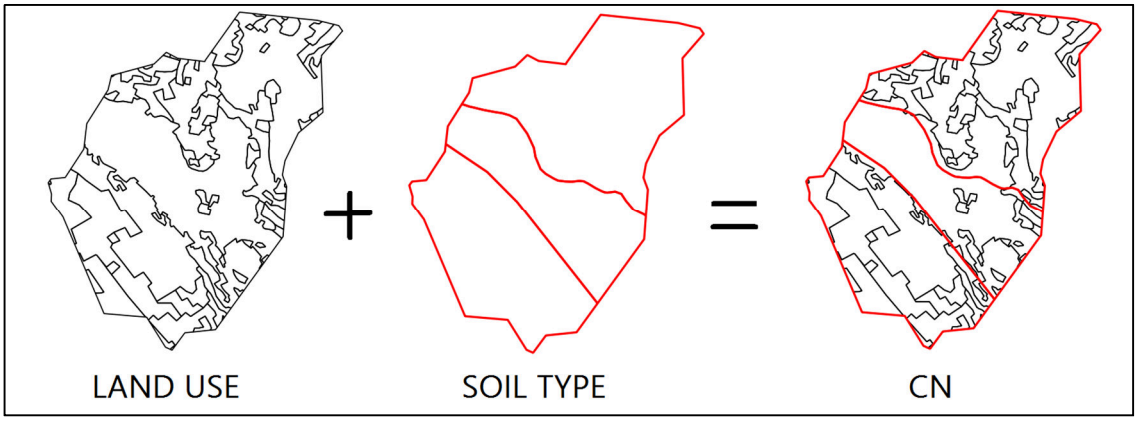

Figure 29: Intersection between land use and soil type shapefiles for Valduce Watershed.

In Table 8 is reported the simplify CN table used for the land use classes involved in this study.

Actually, the selection of CN values for some of the land use classes required also information about hydrologic soil condition, percentage of connected

impervious areas and land treatment (U. S. Department of Agriculture 2004). These data were not available for the entire study area and almost impossible to retrieve with accuracy. In order to overcome this limitation, two different CN values have been assigned when the aforementioned information was requested. The two CN value considered represent the highest (CN_max) and the lowest (CN_min) values among the possible ones related to a land use class and HSG characterizing any sub-polygon. When just one CN value was possible, both CN_max and CN_min have been corresponded to this value. Each land use scenario (i.e. 1955, 1999 and 2012) has been split in two sub-scenarios from the runoff point of view: one representing the worst (CN_max) and one the best (CN_min) condition.

	NRCS Land use class	**Hydrologic soil condition/ Soil treatment/ Impervious area connected [%]**	**CN for HGS**			
			A	**B**	**C**	**D**
1	Meadow-continuous grass, Good protected from grazing an generally mowed for hay	/	30	58	71	78
2	Agricultural lands	Poor: Factors impair infiltration	66	76	82	85
		Good: Factors encourage infiltration.	62	73	80	84
3	Woods	Poor condition (grass cover < 50%)	45	66	77	83
		Fair condition (grass cover 50% to 75%)	36	60	73	79
		Good condition (grass cover > 75%)	30	55	70	77
4	Woods—grass combination (orchard or tree farm)	Poor condition (grass cover < 50%)	57	73	82	86
		Fair condition (grass cover 50% to 75%)	43	65	76	82
		Good condition (grass cover > 75%)	32	58	72	79
5	Brush—brush-weed-grass mixture with brush the major element	Poor condition (grass cover < 50%)	48	67	77	83
		Fair condition (grass cover 50% to 75%)	35	56	70	77

		Good condition (grass cover > 75%)	30	48	65	73
6	Open space (lawns, parks, golf courses, cemeteries, etc.)	Poor condition (grass cover < 50%)	68	79	86	89
		Fair condition (grass cover 50% to 75%)	49	69	79	84
		Good condition (grass cover > 75%)	39	61	74	80
7	Fallow	bare soil	77	86	91	94
8	Urban districts	Commercial and business	89	92	94	95
		Industrial	81	88	91	93
9	Impervious areas	Paved parking, roofs, driveways, etc. (excluding right-of-way)	98	98	98	98
		Gravel (including right-of-way)	76	85	89	91
		Dirt roads (including right-of-way)	72	82	87	89
10	Newly graded areas, (pervious areas only, no vegetation)	/	46	65	77	82
11	Residential districts by average lot size 2 acres	12	77	86	91	94
12	Residential districts by average lot size 1 acre	20	51	68	79	84
13	Residential districts by average lot size 1/2 acre	25	54	70	80	85
14	Residential districts by average lot size 1/3 acre	30	57	72	81	86
15	Residential districts by average lot size 1/4 acre	38	61	75	83	87
16	Residential districts by average lot size 1/8 acre or less (town houses)	65	77	85	90	92
17	Farmsteads—buildings, lanes, driveways and surrounding lots	/	59	74	82	86

Table 8: Curve Number table used in the study.

Notice that CN values are also influenced by the moisture condition of the soil. To take into account this fact, NRCS identified three different condition for soil moisture. These are called Antecedent Moisture Conditions (AMCs) and represent dry (AMC I), average (AMC II) and wet (AMC III) soil moisture condition. In order to assess the proper AMC, it is necessary to know the

amount of rain that has fallen in the five-day period antecedent to the rain event under investigation.

The critical amount of rain that distinguishes the three classes varies accordingly also to the vegetative period (Table 9). The NRCS CN table contains CN values related to AMC II (CN_{II}). Correction factors have to be applied in order to take into account different moisture conditions (Equation 4a & 4b) and compute CN values for AMC I (CN_I) and AMC III (CN_{III}).

AMC	**Total five days antecedent rainfall [cm]**	
	Dormant season	Growing season
I	Less than 1.3	Less than 3.6
II	1.3 to 2.8	3.6 to 5.3
II	More than 2.8	More than 5.3

Table 9: Antecedent Moisture Conditions.

$$a)\ CN_I = \frac{CN_{II}}{2.3 - 0.013\ CN_{II}};\ b)\ CN_{III} = \frac{CN_{II}}{0.43 + 0.0057\ CN_{II}}$$

Equation 4: Correction factors for AMC I (a) and AMC III (b).

The project storms, used for peak discharge estimation, were given as the Probable Maximum Precipitation (PMP) for the studied watersheds. Due to the small size of the watershed under investigation, the maximum PMP duration was fixed up to 24 hours (see section 4.3). For a given geographic location, catchment area, return period etc. PMP is theoretically the greatest depth of precipitation (Mishra & Singh 2003). Therefore, the project storms may never occur in the study area and the assessment of antecedent rainfalls made no sense to be performed. For this reason, only CN_{II} values were consider to evaluate the surface runoff in average moisture conditions. However, CN_{III} values could be involved to estimate the runoff in a very unfavourable situation.

CN maps were used in order to compute the average CN value ($\overline{CN}$) for each watershed or sub-watershed of interest. $\overline{CN}$ was the required parameter in NRCS-CN methodology for peak discharge estimation (section 4.5). Each watershed area A includes n sub-polygon containing a specific CN value.

$\overline{CN}$ was computed as a weighted average of the sub-polygon CN (CN_i) on the related area (A_i):

$$\overline{CN} = \frac{\sum_i^n CN_i \,.A_i}{A}$$

Equation 5: Average CN

The changes of soil runoff capacity were clearly underlined just by comparing CN maps from different periods, as shown in Figure 30. The main changes have been detected in the area surrounding Aperto Torrent and near the medium-low course of Cosia Torrent. These were exactly the places where, during the second half of the XX century, new industrial facilities and residential areas developed (as before mentioned in section 1.2). The differences between the two sub-scenarios (i.e. CN_max and CN_min), observed by comparing same period data (Figure 31), demonstrated instead to not be so relevant.

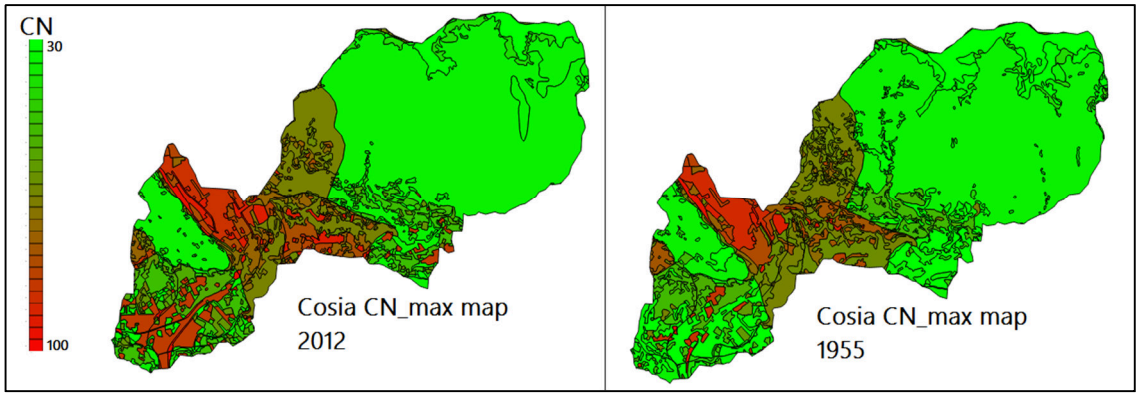

Figure 30: Comparison between different land use scenarios (2012 and 1955, CN_max) for Cosia Watershed.

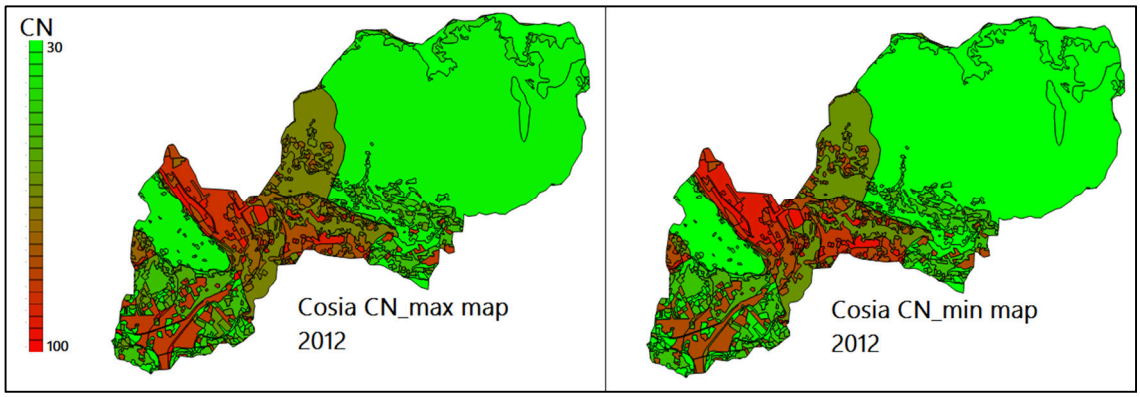

Figure 31: Comparison between different land use sub-scenarios (CN_min and CN_max, 2012) for Cosia Watershed.

In order to quantify the differences between scenarios and sub-scenarios, in terms of peak discharge, specific $\overline{CN}$ were computed for each of them (Table 10). These data were used to run the hydrologic models whose outputs were compared in order to determine the magnitude of the changes brought by the urbanization.

	Cosia Watershed $\overline{CN}$			**Valduce Watershed $\overline{CN}$**		
	1955	**1999**	**2012**	**1955**	**1999**	**2012**
CN_max	52	56	57	79	80	80
CN_min	42	46	47	75	76	76

Table 10: $\overline{CN}$ values for Cosia and Valduce watersheds.

4.3 PROJECT STORMS

The quantitative forecast of heavy rainfalls that might fall over the watersheds, is a necessary information for hydrological modelling (DeMichele, C., Rosso & Rulli 2005). For computing the peak flood discharge, the estimation of critical storms (PMPs) is required and to get the latter, information about both temporal and spatial distribution of the expected amount of rainfall falling over the watershed is needed. Usually, this information is obtained by statistical elaboration of rainfall records available for the study area. The common way to describe rainfall patterns of a given place is the Depth, Duration and Frequency (DDF) curve. This curve describes, in a synthetic way, the maximum rainfall depth (h) for a given duration θ and return period T. The latter is defined as the average interval of time units within which the magnitude of a particular event (e.g. a storm) will be equaled or exceeded (Adrien & Nicolas 2004). The mathematical relation between these variables is usually expressed as:

$$h\,(\theta;T) = a \cdot \theta^{n}$$

Equation 6: DDF curve.

The parameter a is called pluviometric coefficient and it is a function of the return period T. The parameter n is called scale factor and it takes the same value for all return periods. Instead, both n and a vary with the geographic location considered. The Hydrographic Service of ARPA Lombardia provides rainfall distributions and related parameters, for the study area. These data cover the entire region and they can be accessed through a specific WebGIS (http://idro.arpalombardia.it/pmapper-4.0/map.phtml).

The DDF parameters are associated to grid cells that measure approximately 2.5 km². Any cell of the grid was assumed as homogenous rainfall area and the associated DDF curve, for $\theta \leq 24$ hours and $T \leq 200$ years, could be computed (Figure 32). The DDF parameters were obtained by statistical elaboration from rainfall records collected by the rain gauge network managed by ARPA Lombardia. The statistical model used to obtain the DDF curve is the Generalized Extreme Value probability distribution (GEV) and the curve parameters, associated to each rain gauge, were spatially distributed over the region by means of geostatistical extrapolation (DeMichele, C., Rosso & Rulli 2005).

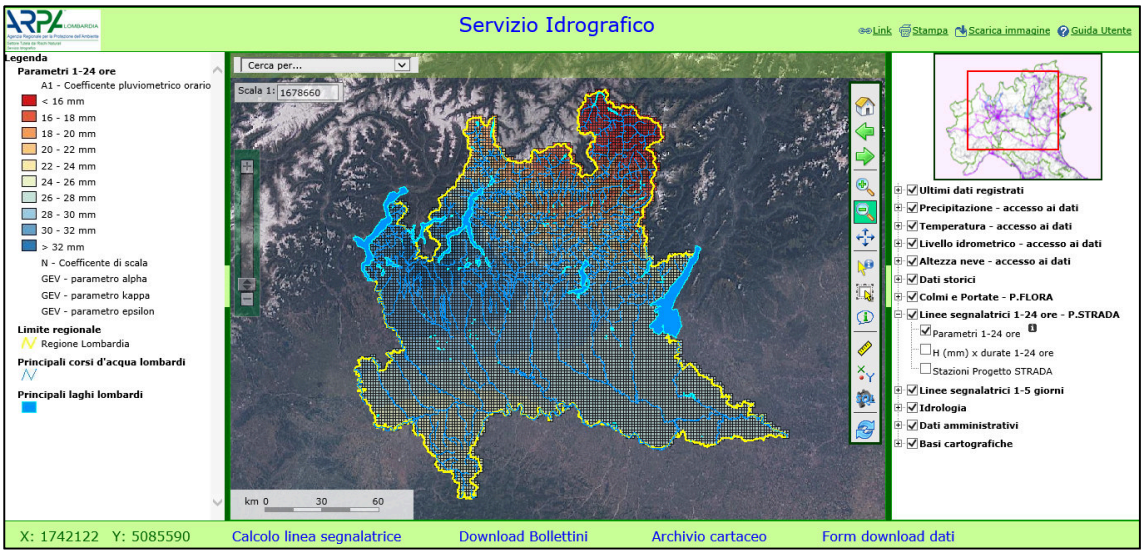

Figure 32: ARPA Lombardia WebGIS.

All the parameters, including hourly pluviometric coefficient a_1 and n as well as the GEV coefficients α, k and ε, could be retrieved as table, simply querying the cells. Table of maximum rainfall h for $\theta \leq 24$ hours and $T \leq 200$ years could be also obtained in the same way. The DDF curve for each cell was computed applying the Equation 7a. The dependence on T of the pluviometric coefficient $a(T)$ is expressed in Equation 7b.

$$a)\ h(\theta;T) = a(T) \cdot \theta^{n} \quad ; \quad b) \begin{cases} a(T) = a_1 \cdot w_t \\ w_t = \varepsilon + \dfrac{\alpha}{k}\left\{1 - \left[\ln\left(\dfrac{T}{T-1}\right)\right]^{k}\right\} \end{cases}$$

Equation 7: DDF curve based on the GEV distribution.

The aforementioned grid for the study area was reconstructed with QGIS (Figure 33). Notice that the watersheds under investigation are influenced by more than one cell (i.e. rainfall homogeneous area). Thus, the aim was to find at least two DDF representative for Cosia and Valduce watersheds since the hydrologic models required these data as input (section 4.5).

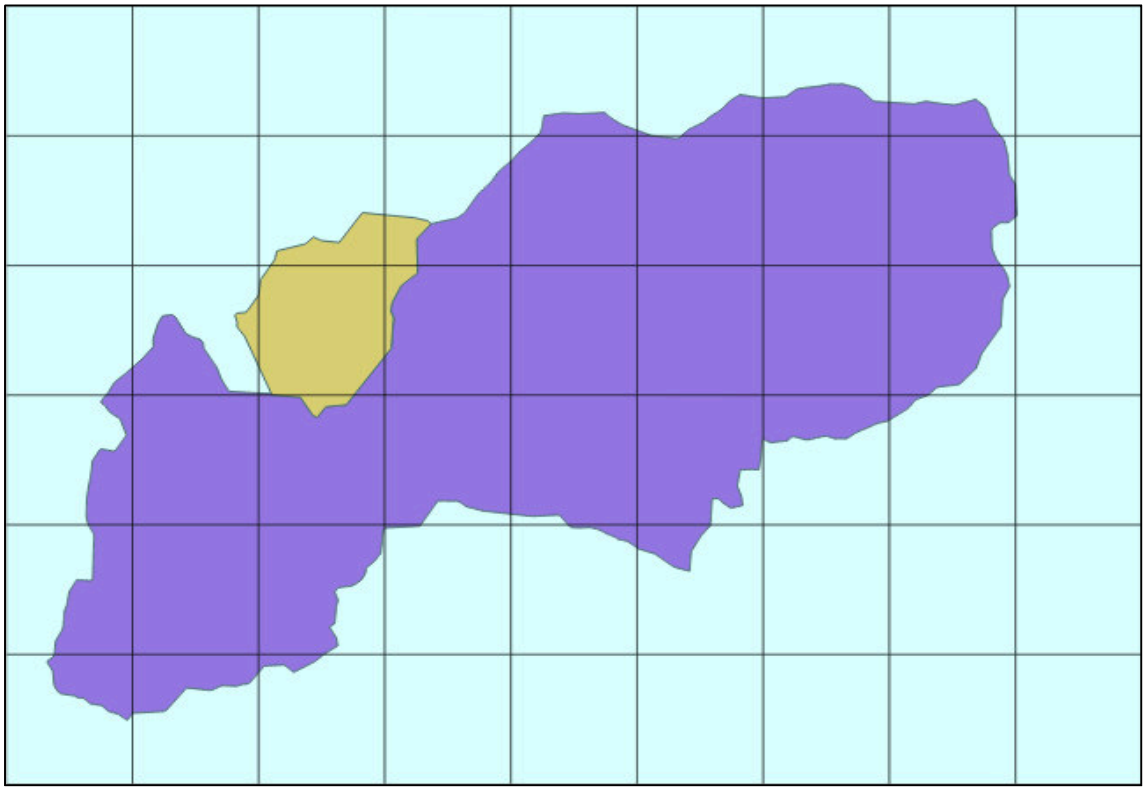

Figure 33: Reconstructed DDF parameter grid (6x9 cells) covering the study area.

Return periods of the design storms have been selected in order to study events with short (T=2 years), medium (T=20 years) and large (T=200 years) return periods. In order to assess the DDF curves, an average rainfall depth $\bar{h}\,(\theta = 1,2,\ldots 24;\ T = 2,20,200)$ was adopted. The average rainfall depth was computed weighting any cell contribution $h_i(\theta;T)$ on the cell surface A_i. Not all the cells of the reconstructed grid were involved but just the m cells overlapping the watershed area A with a portion of their surface A_i.

$$\bar{h}\,(\theta;T) = \frac{\sum_i^m h_i \,.\, A_i}{A}$$

Equation 8: Average rainfall depth over the watershed.

The reliability of using the average rainfall depth for the whole watershed was previously tested by calculating the variation of $h_i(\theta;T)$ among all the grid cells on the watershed. That was done for T= 2, 20, and 200 years and θ =1, 2, 3, …, 24 hours. Maximum and minimum $h_i(\theta;T)$ as well as $\bar{h}(\theta;T)$ values for 24 different durations and 3 return periods were thus calculated considering the entire grid. The maximum difference $h_{i,max}(\theta;T) - h_{i,min}(\theta;T)$ was found to be less than 8 % of the average depth (for T equal to 20 years and θ equal to 24 hours), as it is shown in Table 11. This variability among the cells was considered low enough to consider the average rainfall depth as representative for the whole watershed.

θ [h]	T [y]	$\bar{h}(\theta;T)$ [mm]	$h_{i,min}(\theta;T)$ [mm]	$h_{i,max}(\theta;T)$ [mm]	max diff. [mm]	max diff. [%]
1	2	30.11	29.60	30.28	0.68	2.25
	20	54.45	54.19	54.78	0.59	1.09
	200	76.35	75.27	76.99	1.72	2.25
2	2	37.96	37.65	38.27	0.62	1.64
	20	68.65	68.31	69.27	0.96	1.40
	200	96.26	95.77	97.12	1.35	1.40
3	2	43.47	42.98	43.89	0.91	2.10
	20	78.62	77.93	79.83	1.90	2.41
	200	110.23	109.32	111.33	2.01	1.82
4	2	47.86	47.19	48.45	1.26	2.63
	20	86.55	85.57	88.28	2.71	3.13
	200	121.36	120.04	122.68	2.64	2.18
…						
24	2	87.12	84.50	90.79	6.30	7.23
	20	157.56	153.22	165.75	12.53	7.95
	200	220.91	214.93	230.25	15.32	6.93

Table 11: Test on rainfall depth variability among the cells of the reconstructed grid.

The average depth $\bar{h}(\theta;T)$ has been thus computed for the two watershed, considering the contributions $h_i(\theta;T)$ of the overlapping cells, for the selected T and θ =1, 2, 3…, 24. The results are shown in Table 12.

In order to estimate the DDF parameters for the two watersheds (i.e. a and n), $\bar{h}(\theta;T)$ values were used as observation dataset to fit the DDF curve by using Ordinary Least Square (OLS) method. Thus, the parameter values $\hat{a}$ and $\hat{n}$ (Figure 34 & Table 13) were estimated.

	Cosia Watershed average rainfall depth [mm]			Valduce Watershed average rainfall depth [mm]		
θ[h]	$\bar{h}(\theta;2)$	$\bar{h}(\theta;20)$	$\bar{h}(\theta;200)$	$\bar{h}(\theta;2)$	$\bar{h}(\theta;20)$	$\bar{h}(\theta;200)$
1	30.1	54.4	76.2	30.2	54.4	76.5
2	38.0	68.7	96.2	38.0	68.5	96.3
3	43.5	78.7	110.2	43.5	78.5	110.3
4	47.9	86.6	121.4	47.9	86.3	121.4
5	51.6	93.4	130.8	51.6	93.0	130.7
6	54.9	99.3	139.1	54.8	98.8	138.9
7	57.8	104.5	146.5	57.7	104.0	146.2
8	60.5	109.3	153.2	60.3	108.8	152.9
9	62.9	113.7	159.3	62.7	113.1	159.0
10	65.2	117.8	165.1	65.0	117.1	164.6
11	67.3	121.7	170.4	67.1	120.9	170.0
12	69.3	125.3	175.5	69.0	124.5	174.9
13	71.2	128.7	180.3	70.9	127.8	179.7
14	72.9	131.9	184.8	72.7	131.0	184.2
15	74.7	135.0	189.1	74.4	134.1	188.4
16	76.3	138.0	193.3	76.0	137.0	192.5
17	77.9	140.8	197.2	77.5	139.8	196.5
18	79.4	143.5	201.1	79.0	142.5	200.2
19	80.8	146.1	204.7	80.5	145.1	203.9
20	82.2	148.7	208.3	81.8	147.6	207.4
21	83.6	151.1	211.7	83.2	150.0	210.8
22	84.9	153.5	215.1	84.5	152.3	214.1
23	86.2	155.8	218.3	85.7	154.6	217.3
24	87.4	158.1	221.4	87.0	156.8	220.4

Table 12: Average rainfall depth for Cosia and Valduce watersheds.

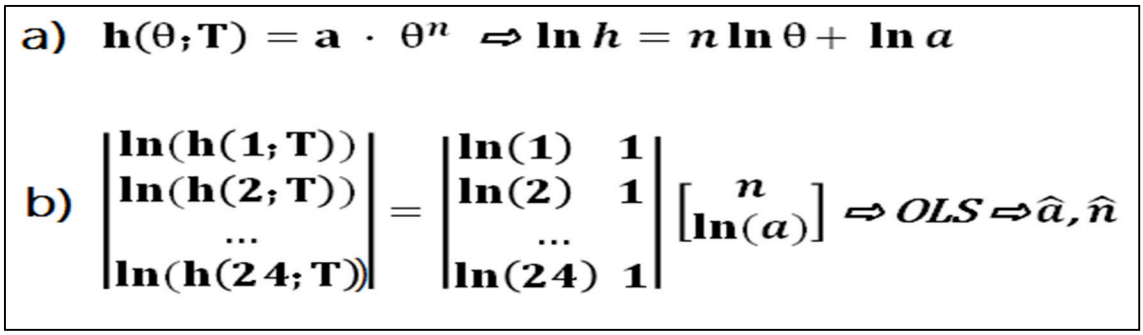

Figure 34: OLS adjustment for DDF parameters estimation. a) DDF linearization, b) parameters estimation.

	Cosia Watershed DDF			Valduce Watershed DDF		
T	2	20	200	2	20	200
$\hat{a}$	30.10	54.42	76.25	30.18	54.42	76.49
$\hat{n}$	0.34	0.34	0.34	0.33	0.33	0.33

Table 13: Estimated DDF parameters.

4.4 Time of Concentration

In order to complete the necessary dataset required for the estimation of peak discharges, it was necessary to assess the Time of Concentration (tc) of each watershed. The time of concentration is defined as the time required surface water to move from the hydraulically most distant point of the drainage area to the outlet or the design point. The peak discharge usually occurs during a storm having θ equal to time of concentration. In fact, in this case all the areas of the watershed contribute runoff to the station or point under consideration (Adrien & Nicolas 2004).

The tc is an essential parameter, especially for ungauged watersheds (Grimaldi et al. 2010). Several empirical formulas are available in literature (e.g. Ferro 2006, Chow 1959) in order to compute tc. These are based on specific physiographical characteristics of the watershed (Table 3 & Table 4). The authors of the selected formulas obtained them by studying small watersheds (i.e. dimensions similar to the ones of the study watersheds). These formulas are: Tournon's formula (Equation 9), Kiprich's formula (Equation 10), Pezzoli's formula (Equation 11), Ferro's formula (Equation 12). The latter is an empirical

relation computed by the author through the interpolation on many different tc equations.

Kiprich's formula was not used for Cosia Watershed because it is suggested for very small watersheds but it fitted better to the Valduce Watershed. Pezzoli's formula was used only for Cosia Watershed, for the opposite reason.

$$tc\,[h] = 0.396 \cdot \frac{L}{\sqrt{i_m/100}} \cdot \left(\frac{A \cdot \sqrt{i_a/100}}{L^2 \cdot \sqrt{i_m/100}}\right)^{0.72}$$

Equation 9: Tournon's formula.

$$tc\,[h] = 0.00035 \cdot \left(\frac{L_d}{\sqrt{i_a/100}}\right)^{0.77}$$

Equation 10: Kiprich's formula.

$$tc\,[h] = 0.055 \cdot \frac{L}{\sqrt{i_a/100}}$$

Equation 11: Pezzoli's formula.

$$tc\,[h] = 0.00037 \cdot \left(\frac{L/1000}{\sqrt{i_a/100}}\right)^{0.8}$$

Equation 12: Ferro's formula.

Actually, the NRCS-CN methodology provides different procedures in order to compute tc. The original tc expression, developed within this methodology, is the Mockus's formula (Equation 13) which is also called the Watershed Leg method (U. S. Department of Agriculture 2004). In this formula, tc assumes a similar, but not equal, meaning with respect to other RRMs. The parameter used in NRCS-CN methodology to describe the time at which the peak discharge occurs it is called Time to Peak (ta), It can be derived from time of concentration and the duration of the rainfall producing the runoff tp (Equation 14). A detailed description of the NRCS-CN methodology and the aforementioned parameters was included in the following section (4.5.1).

$$tc\ [h] = 0.57 \cdot \frac{{L_d}^2}{{i_m}^2} \cdot \left(\frac{1000}{\overline{CN}} - 9\right)^{0.7}$$

Equation 13: Mockus's formula.

$$ta\,[h] = 0.5tp + tL; \qquad tL\,[h] = 0.6 \cdot tc$$

Equation 14: NRCS-CN formula for ta.

It is important to notice that in the Mockus's formula, tc depends also on the $\overline{CN}$ of the watershed; therefore, a specific tc has to be calculated for any land use scenario and sub-scenario. In this study, the Mockus's formula was adopted to compute tc within WinTR-55 model (section 4.5.1). To estimate the peak discharge with URBIS2003v.2 (section 4.5.2) instead, an average $\overline{tc}$, computed from Equation 9, 10, 11 and 12 (Table 14), was used.

	Tournon $tc[h]$	Kiprich $tc[h]$	Pezzoli $tc[h]$	Ferro $tc[h]$	$\overline{tc}[h]$
Cosia Watershed	1.95	/	2.71	2.10	2.26
Valduce Watershed	0.43	0.67	/	0.37	0.49

Table 14: Time of concentration for Cosia and Valduce watersheds.

4.5 PEAK FLOOD DISCHARGES

The surface runoff is the portion of precipitation that reaches the nearest channel by flowing over the ground surface (Adrien & Nicolas 2004). The runoff, which is conveyed into streams or channels, generates a flood wave that run to the watershed outlet. The peak of this wave represents the peak discharge, which has to be assessed in order to evaluate the discharge efficiency of the buried channels involved in this study.

The first step in peak discharge calculation is to identify the portion of rainfall that is expected to become runoff. The design project storm volume was compute by means of the DDF curve. This rainfall volume was distributed along time and all over the watershed area through a synthetic hyetograph. A hyetograph is defined as the graph that plots the rainfall volume over the watershed along a time scale (Dixey 1975). Actually, part of this volume is

retained by the ground; therefore, the runoff is generated only when the total rainfall volume results to be higher than the volume which can be subtracted by infiltration. The portion of rainfall that becomes runoff is called excess rainfall R_e. The R_e distribution over an area along time is described by a specific hyetograph, called net hyetograph.

The NRCS-CN methodology was used to compute the net project hyetograph (i.e. the net hyetograph related to the project storms). This method relays on simple equations, which let modelling the ground rainfall retention by using the $\overline{CN}$ parameter. Thus, it was possible to compute R_e as a function of the soil initial abstraction I_a. The latter is assumed a fraction λ of the maximum soil retention capacity S. Usually, the value of λ is set to 0.2. The hypothesis, on which this method is based, is expressed by the proportionality between the ratios of the excess rainfall R_e over the total rainfall volume R, purified from the initial abstraction I_a, and the infiltrated volume Fover the maximum soil retention capacity S.

$$\frac{R_e}{R - I_a} = \frac{F}{S} \; ; \begin{cases} if\ R < I_a \rightarrow R_e = 0 \\ F = R - I_a - R_e \\ I_a = \lambda S = 0.2S \\ S = 25.4\left(\frac{1000}{\overline{CN}} - 10\right) \end{cases} \rightarrow R_e = \frac{(R - 0.2S)^2}{R + 0.8S}$$

Equation 15: NRCS-CN equations (R_e, R and S are expressed in [mm]).

NRCS-CN methodology is the standard procedure for computing R_e whit WinTR-55 software, while URBIS2003v.2 allows choosing among different methods. However, NRCS-CN was applied also with URBIS2003v.2 software in order to compute the net project hyetographs.

Once R_e is computed, the peak discharge at the watershed outlet can be estimated. The product R_e depth by the watershed area gives the total runoff volume of the flood wave running to the watershed outlet. The shape of this wave was described by means of hydrographs; these are the graphical representations of flowrates, occurring in a specific point of a watershed (e.g. the outlet), versus time.

Instantaneous Unit hydrographs (IUH) are involved, in order to quantify the response of the watershed to an input rainfall volume. An instantaneous unit

hydrograph is a hydrograph of direct surface runoff from a unit excess rainfall occurring in unit time, uniformly over the watershed area (Dixey 1975). IUH shape depends on the watershed physiography as well as on the rainfall distribution over the watershed area. To take into account this, the IUH is multiplied by specific factors, which represented both watershed and rainfall characteristics, to compute the peak discharge. URBIS2003v.2 software allows choosing among three different IUH generation methods (section 4.5.1). The NRCS methodology, which is implemented in the WinTR-55 software (section 4.5.1) is based instead on the NRCS dimensionless unitary hydrograph (DUH), called also Mockus's unitary hydrograph (Ferro 2006).

4.5.1 WinTR-55 model

WinTR-55 is a single event rainfall-runoff, small watershed hydrologic model. The model was first issued by the SCS (now NRCS) in January 1975 whit the Technical Release 55 (TR-55)-Urban Hydrology for Small Watersheds. It represented a simplified procedure for calculating storm runoff volume and peak discharges. TR-55 has been improve with different revisions during time and the software WinTR-55 was developed to facilitated the computational procedures (U. S. Department of Agriculture 2009). The peak discharge estimation is based on the NRCS DUH (Figure 35).

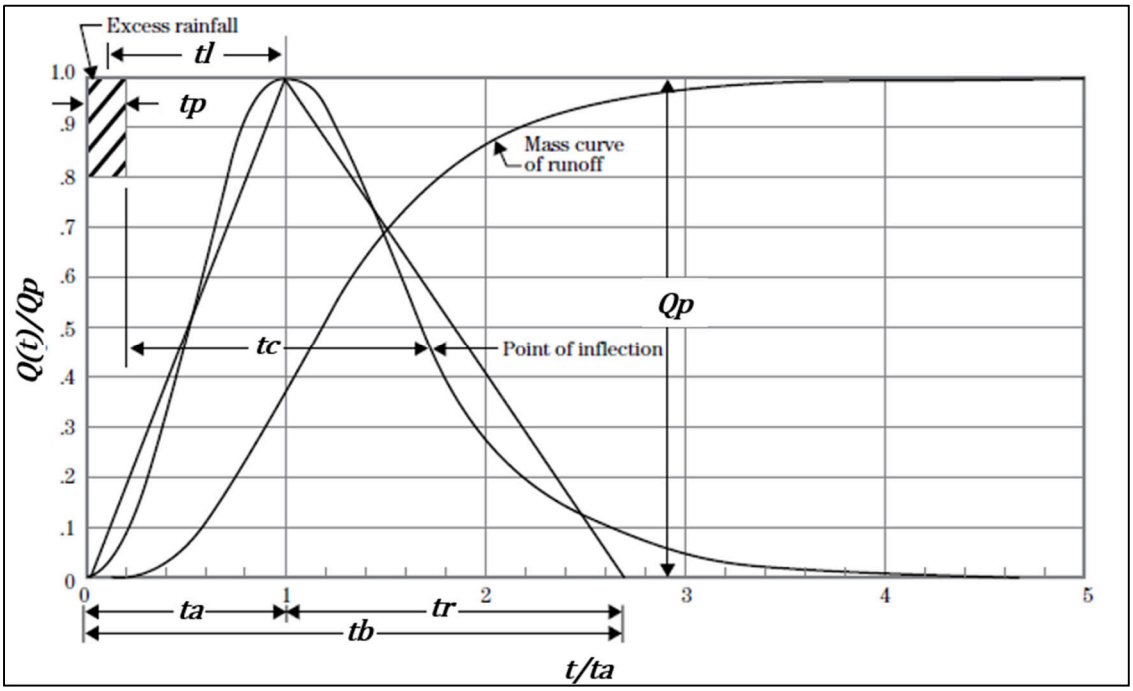

Figure 35: NRCS Dimensionless Unit Hydrograph.

An equivalent triangular hydrograph (i.e. a triangular-shape hydrograph with equal time to peak ta and peak discharge Q_p) is associated to the NRCS DUH, to obtain the peak discharge equation. Other characteristics of the NRCS DUH are the Lag time tl, which is defined as the time distance between the hyetograph centroid and the peak discharge, as well as the Base time tb, which is duration time of the triangular hydrograph. The value of tl can be assessed by the relation $tl = 0.6tc$, while tb is computed assuming that the 37.5% of the hydrograph area (i.e. runoff volume) is included in the rising side ($0 \leq t \geq ta$) thus $tb = 2.67tc$. The difference ($tb - ta$) is called exhaustion time tr and it is given by $tr = 1.67tc$. These characteristics are referred to the standard NRCS DUH and were assessed in this case study in order to compute the peak discharges. Mockus's DUH represents the default DUH for WinTR-55 software.

Different DUHs are available to fit different kinds of watershed. These are characterized by different time distribution of the runoff volume with respect to the standard one, which yields different values for Q_p. The peak discharge formula, using the standard DUH, is available in Equation 16, where A is the watershed area. Once Q_p and ta were computed, the peak hydrographs can be plot by multiplying the DUH axis for these two quantities.

$$Q_p[m^3/s] = 0.208 \frac{R_e[mm] \cdot A[km^2]}{ta\,[h]}$$

Equation 16: Peak discharge equation for standard NRCS DUH.

WinTR-55 software allows to model a single watershed area as well as to split the watershed in up to ten sub-watersheds. For each sub-watershed, a hydrograph is generated. These hydrographs can be routed through a maximum of ten reaches. These represent the major flow paths of watershed, connecting the upland sub-watershed with the watershed outlet. The hydrograph routing method, which is included in this software, is the Muskingum-Cunge method (e.g. Chow et al. 1988; Tewolde & Smithers 2007). In order to perform the hydrograph routing, physical characteristics of a representative cross-section for the reaches have to be included among the input data. Sub-watersheds and reach hydrographs were combined by the software, as needed to represent the accumulation of flow, from the uplands to the watershed outlet.

The simplest model run involves a single watershed area. NRCS suggests the use of this simple run only for very small watershed (i.e. $A \leq 20$ km²) or for watershed having homogeneous characteristics in term of land use. Moreover, using the single area procedure, only the peak discharge at the watershed outlet can be computed. The Cosia Watershed includes different tributaries and heterogeneous land use within its area; thus, the latter procedure was not suitable for Cosia Watershed but it was for the small Valduce Watershed, which peak discharge was computed by modelling the watershed as a single area.

The peak discharge computation required input data such as the project storms, expressed as dimensionless DDF curve together with the total 24-hour rainfall depth for each T, as well as the watershed A, $\overline{CN}$ and tc. Thus, hydrographs and Q_p related to the land use scenarios (i.e. 1955, 1999 and 2012) and sub-scenarios (i.e. CN_min and CN_max) were computed (Figure 36).

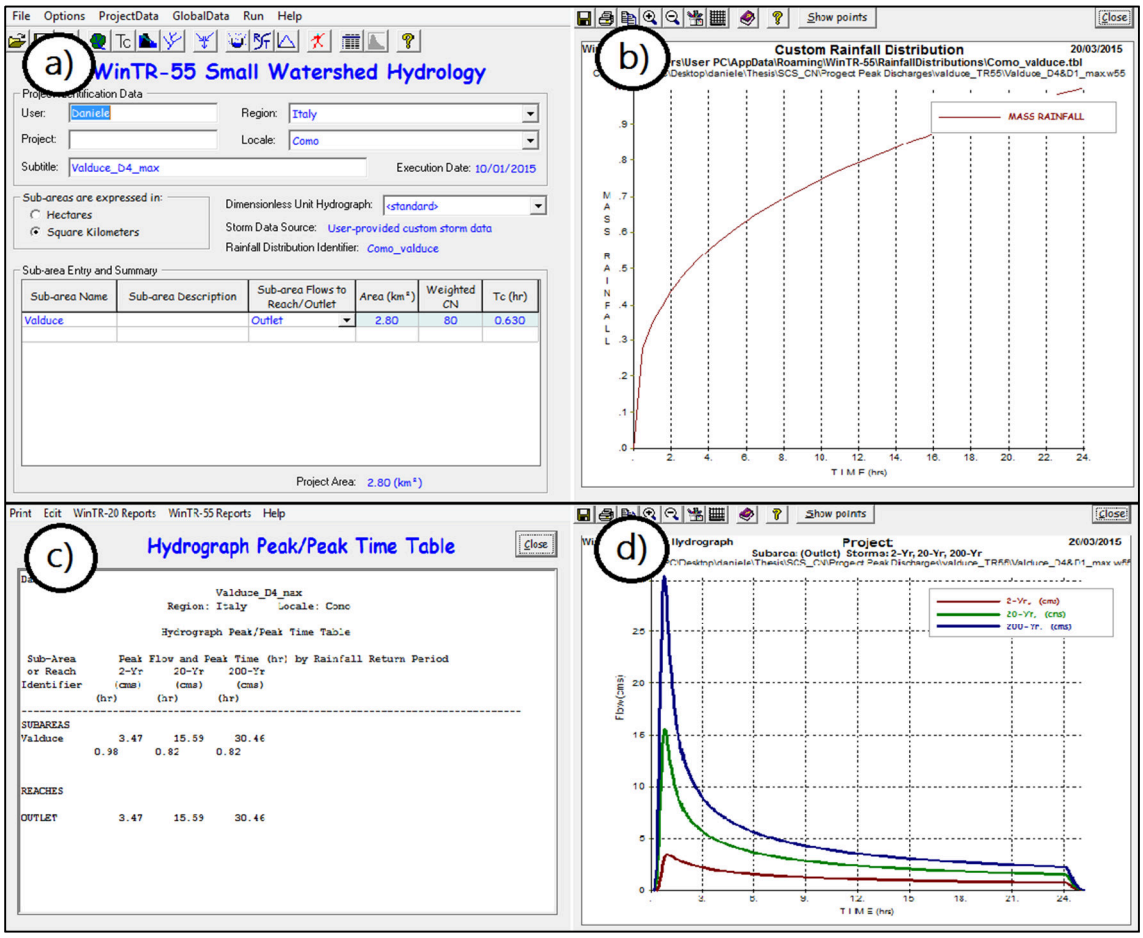

Figure 36: WinTR-55 Valduce Watershed input data windows: a) Watershed characteristics, b) dimensionless DDF. WinTR-55 output windows: c) Hydrograph peak time table, d) Hydrographs.

Actually, the software only allows simulation of 24-hour storms, uniformly distributed over the watershed area. This fixed duration assumed by the TR-55 methodology permits to explore the effects of the entire storm and the user do not have to deal with the additional task of assessing the storm critical duration. In fact, the latter is a specific characteristic of any sub-watershed and it may change between different land use scenarios. For other methods, this critical duration is normally assumed equal to tc.

Using the 24-hours storm, given by the DDF, it was possible to identify the maximum discharge contributions of all the sub-watersheds to the outlet.

Cosia Watershed was modelled as a composed area one (Figure 37) in which the peak flow hydrographs were computed at the junctions (Oi) of each sub-watersheds (Ai) and routed towards the Cosia outlet through four different reaches, representing different reaches of Cosia Torrent.

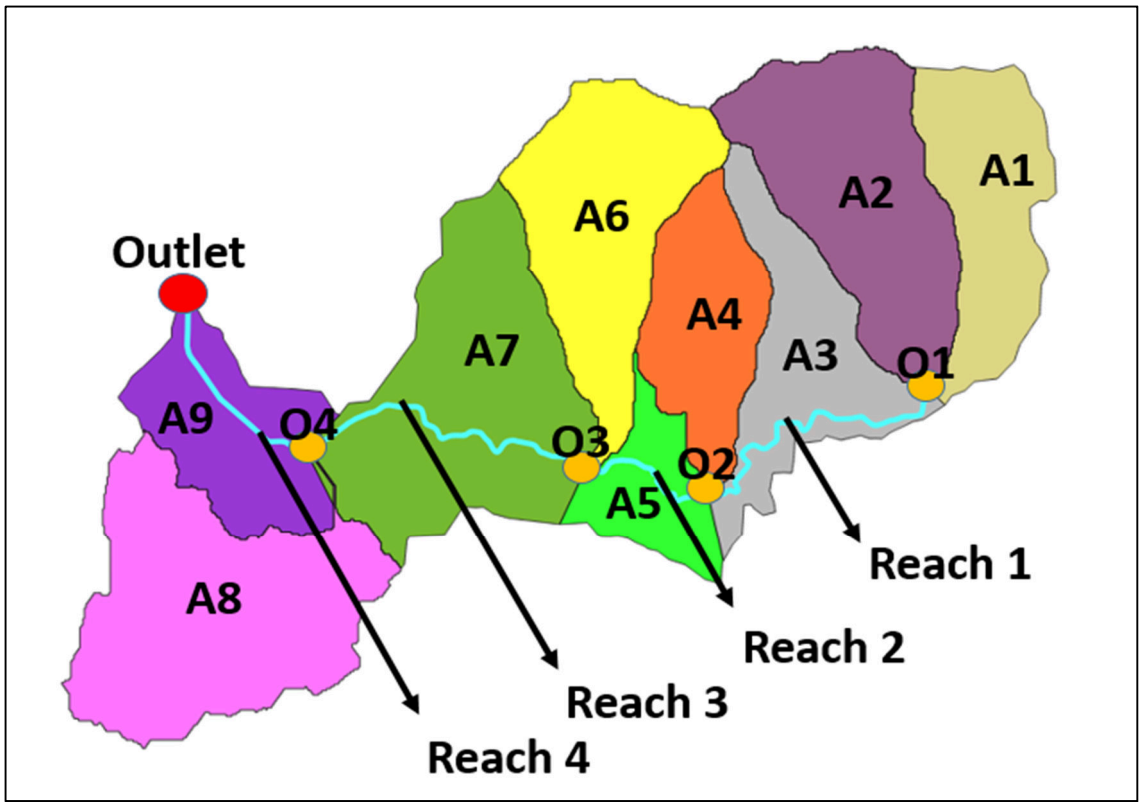

Figure 37: Cosia Watershed divided in sub-watersheds (A i). Oi represent the hydraulic junctions between Cosia Torrent and its main tributaries.

The input dataset required for these calculation includes rainfall data, A, $\overline{CN}$ and tc for each sub-watershed as well as information about the physical characteristic of a representative cross-section for any reach considered. The sub-watersheds have been analysed with the same procedure used for the two main watersheds. Thus, physiographical indices, $\overline{CN}$ as well as tc were assigned. The information about the typical cross-sections for the reaches were collected during field surveys by using Geopaparazzi (Figure 38).

Geopaparazzi allowed collecting of georeferenced tags, which were programmed to store simple information, including cross-section geometries and hydraulic roughness. At many points along the Cosia Torrent path, the measurements were performed using a laser meter. These data were collected filling the tag templates, which were displayed on a mobile phone screen (Figure 39). Pictures and sketches of the cross-sections were stored also in the same templates.

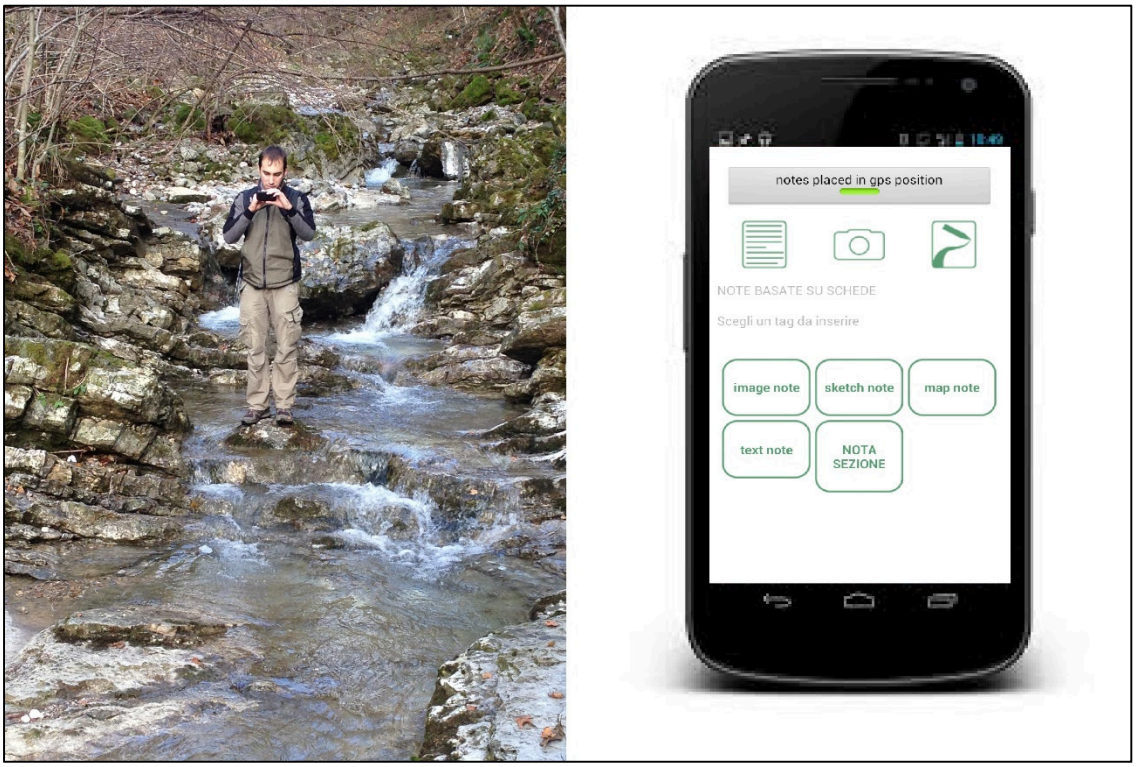

Figure 38: Fast field survey with Geopaparazzi.

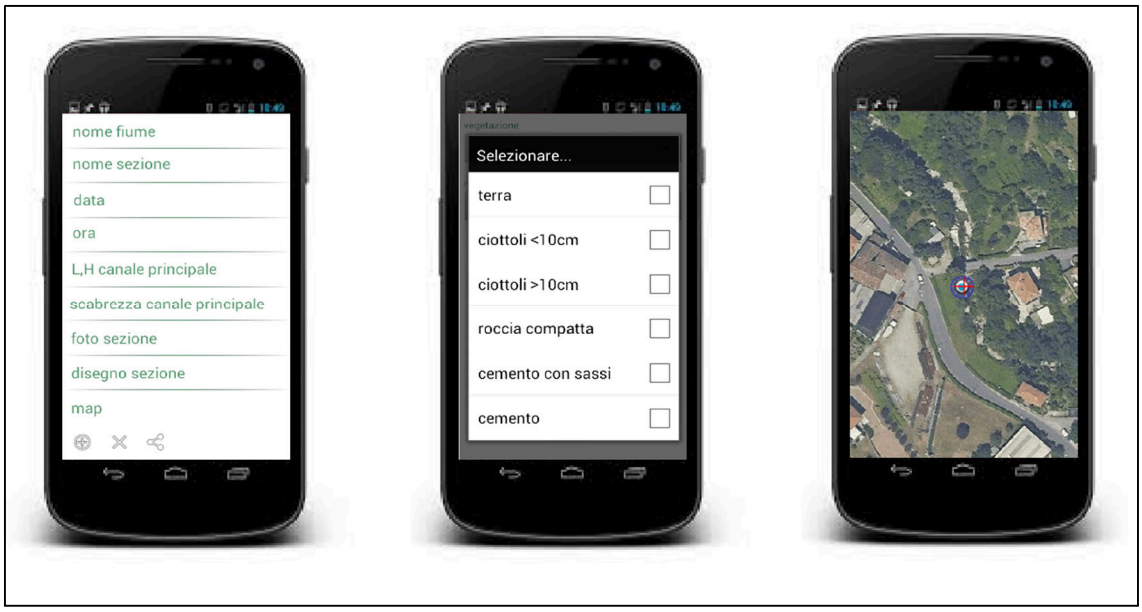

Figure 39: Examples of Geopaparazzi templates and tag positioning.

The filled tags were stored in the device memory and further imported as KMZ files in Google Earth. The tags could be placed on the map by means of geographic coordinates, which were automatically stored in the tag once the templates had been filled. The information was accessed simply querying the tags (Figure 40).

Figure 40: Exported KMZ tags displayed on Google Earth.

According to the collected data, a typical cross-section was identified for each reach, in terms of hydraulic roughness, bottom width, friction slope and average side slopes (Figure 41).

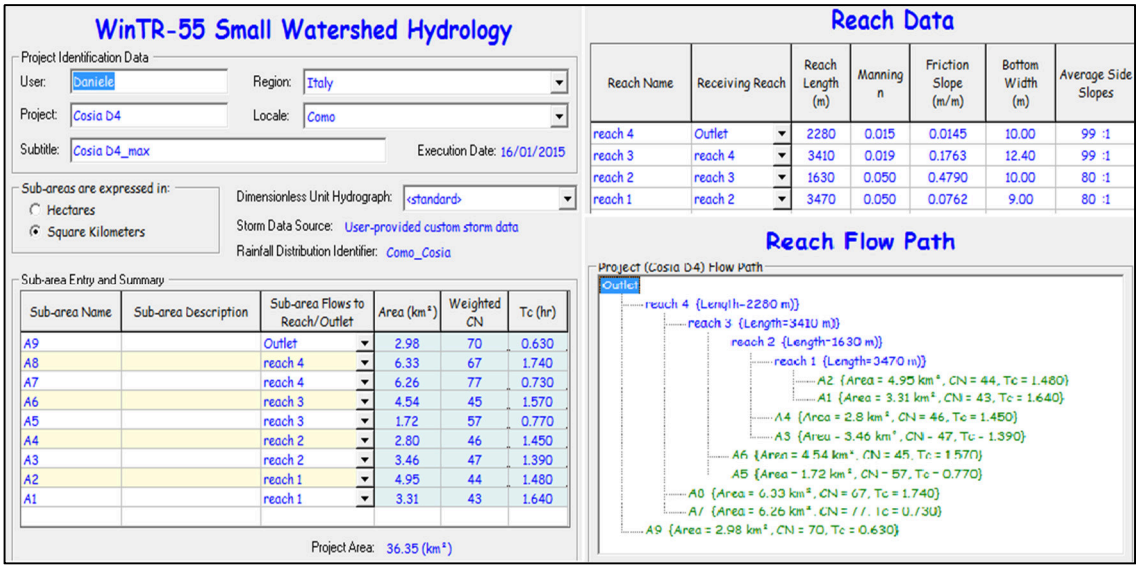

Figure 41: WinTR-55 Cosia Watershed input data windows.

The single area procedure was tested also for the Cosia Watershed, in order to compare the results of the two approaches.

The comparison demonstrated that if the Cosia watershed is analysed as single area, the contributions of the impervious areas (e.g. A7, A8 and A9) in terms of average CN, resulted to be "smoothed" by the wide wooden upland areas, as A1, A2 and A6. That can be explained by looking at the relation $R_e = f(R, \overline{CN})$, adopted by the NRCS, which is not a linear function as shown in Graph 5. Therefore, by lowering the $\overline{CN}$ value, the excess rainfall from an equal precipitation R, shows a not linear decrement. In that way, runoff contributions from impervious areas, which can be abundant even for small R, become negligible if an uncorrected CN averaging procedure is used.

For this reason, the peak discharges computed for Cosia Watershed by using the single area procedure were considered not reliable. A summary for the computed peak discharges (T=2, 20 and 200 years) at the watershed outlets, for different land use scenarios and sub-scenarios, is available in Table 15.

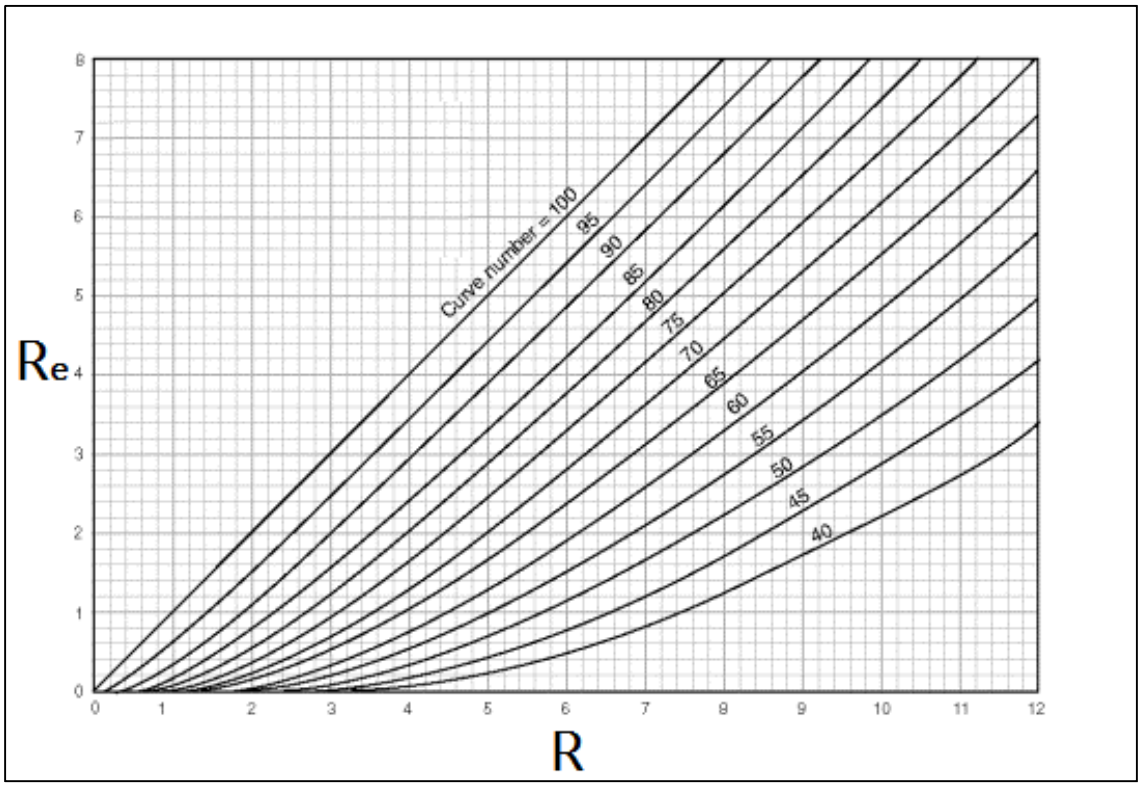

Graph 5: NRCS $R - R_e$ relation plotted for $\lambda = 0.2$ (Hawkins et al. 2009).

	T [y]	Land use Scenario	CN_max	CN_min
Cosia Watershed Q_p (single area)	**2**	**1955**	3.71	1.11
		1999	5.08	2.12
		2012	5.49	2.38
	20	**1955**	19.40	9.43
		1999	25.38	12.74
		2012	27.01	13.67
	200	**1955**	44.38	23.50
		1999	56.19	30.70
		2012	59.26	32.62
Cosia Watershed Q_p (multiple areas)	**2**	**1955**	5.24	3.06
		1999	6.85	4.02
		2012	7.25	4.37
	20	**1955**	27.48	16.54
		1999	33.72	20.76
		2012	35.46	22.22

	200	**1955**	60.02	39.78
		1999	74.39	49.46
		2012	77.56	52.54
Valduce Watershed Q_p	**2**	**1955**	3.04	1.93
		1999	3.47	2.13
		2012	3.47	2.13
	20	**1955**	14.36	10.04
		1999	15.53	10.94
		2012	15.53	10.94
	200	**1955**	28.57	21.60
		1999	30.34	23.06
		2012	30.34	23.06

Table 15: $Q_p[m^3/s]$ at the watershed outlets, computed with WinTR-55.

The peak discharges, running the model as multiple areas, were computed also for each sub-watershed (Ai) and hydraulic junction (Oi) (Table 16). The discharges at the junction included the contribution of all the sub-watersheds placed upland of the junction, while the sub-watershed discharges accounted only for the single area contribution. These were used in order to set up the hydraulic simulation in section 4.6.2.

	T [y]	**Land use Scenario**	**CN_max**	**CN_min**
O1 Q_p	**2**	**1955**	0.16	0.00
		1999	0.29	0.00
		2012	0.33	0.00
	20	**1955**	1.79	0.59
		1999	2.21	0.59
		2012	2.32	0.65
	200	**1955**	4.87	1.97
		1999	5.97	1.97
		2012	6.26	2.09
O2 Q_p	**2**	**1955**	0.53	0.00
		1999	0.65	0.00
		2012	0.69	0.00
	20	**1955**	4.17	1.11
		1999	4.38	1.28
		2012	4.50	1.41

	200	**1955**	11.20	3.61
		1999	11.72	3.91
		2012	12.05	4.14
O3 Q_p	**2**	**1955**	0.72	0.00
		1999	1.10	0.13
		2012	1.12	0.16
	20	**1955**	5.48	1.81
		1999	6.90	2.18
		2012	6.96	2.41
	200	**1955**	14.70	5.55
		1999	18.22	6.23
		2012	18.38	6.66
O4 Q_p	**2**	**1955**	4.27	2.43
		1999	5.58	3.33
		2012	6.06	3.68
	20	**1955**	21.59	12.77
		1999	26.23	17.05
		2012	28.47	18.25
	200	**1955**	45.80	30.06
		1999	57.85	39.67
		2012	61.62	42.13
A1 Q_p	**2**	**1955**	0.08	0.00
		1999	0.12	0.00
		2012	0.12	0.00
	20	**1955**	0.75	0.23
		1999	0.89	0.23
		2012	0.89	0.26
	200	**1955**	2.04	0.79
		1999	2.39	0.79
		2012	2.39	0.84
A2 Q_p	**2**	**1955**	0.09	0.00
		1999	0.18	0.00
		2012	0.21	0.00
	20	**1955**	1.04	0.35
		1999	1.33	0.35
		2012	1.44	0.39
	200	**1955**	2.82	1.18
		1999	3.58	1.18

		2012	3.88	1.25
A3 Q_p	**2**	**1955**	0.12	0.00
		1999	0.21	0.00
		2012	0.21	0.00
	20	**1955**	0.93	0.29
		1999	1.27	0.43
		2012	1.44	0.46
	200	**1955**	2.51	0.91
		1999	3.40	1.19
		2012	3.88	1.26
A4 Q_p	**2**	**1955**	0.14	0.00
		1999	0.15	0.00
		2012	0.15	0.00
	20	**1955**	0.88	0.24
		1999	0.95	0.27
		2012	0.95	0.30
	200	**1955**	2.36	0.73
		1999	2.55	0.80
		2012	2.55	0.85
A5 Q_p	**2**	**1955**	0.12	0.00
		1999	0.22	0.13
		2012	0.24	0.16
	20	**1955**	0.69	0.33
		1999	1.29	0.74
		2012	1.40	0.93
	200	**1955**	1.85	0.91
		1999	3.38	2.00
		2012	3.65	2.45
A6 Q_p	**2**	**1955**	0.19	0.00
		1999	0.25	0.00
		2012	0.22	0.00
	20	**1955**	1.32	0.38
		1999	1.54	0.38
		2012	1.43	0.42
	200	**1955**	3.54	1.19
		1999	4.11	1.19
		2012	3.82	1.26

A7 Q_p	**2**	**1955**	4.27	2.43
		1999	4.73	3.20
		2012	5.26	3.47
	20	**1955**	21.59	12.77
		1999	23.86	16.54
		2012	25.88	17.71
	200	**1955**	45.76	30.06
		1999	49.78	36.90
		2012	52.98	38.91
A8 Q_p	**2**	**1955**	0.14	0.06
		1999	1.86	0.96
		2012	2.02	1.05
	20	**1955**	1.44	1.22
		1999	8.96	5.14
		2012	9.56	5.46
	200	**1955**	3.81	3.27
		1999	19.83	11.97
		2012	20.99	12.52
A9 Q_p	**2**	**1955**	1.06	0.69
		1999	1.41	0.69
		2012	1.28	0.75
	20	**1955**	5.99	3.85
		1999	8.01	3.86
		2012	7.35	4.12
	200	**1955**	15.27	10.03
		1999	19.06	10.11
		2012	18.02	10.65

Table 16: $Q_p[m^3/s]$ at the sub-watershed outlets (A i) and junctions (Oi), computed with WinTR-55.

4.5.2 URBIS2003v.2 models

URBIS2003v.2 software was used in order to estimate peak discharges also with other methods, in order to compare these results with the ones obtained with the WinTR-55. URBIS2003v.2 software is widely used by professional engineers in practical applications for peak discharge and design hydrographs assessment.

The software GUI includes multiple windows concerning the input data for a single storm and a single watershed. Thus, the program is able to compute only one hydrograph per run. For this reason, the watersheds were modelled as a single drainage area. Therefore, the peak discharges, obtained with this software, were used only with a comparison purpose in order to ensure the reliability of the peak discharge estimated with the WinTR-55. Rainfall input were included inserting the DDF parameters. The total amount of rainfall is obtained by specifying the critical storm durations for any return period, which normally is assumed equal to $\overline{tc}$ (Table 14). The excess rainfall R_e was computed by choosing the CN method, among the software's options; therefore, $\overline{CN}$ of the watershed was specified for any land use scenario. Thus for Cosia and Valduce watersheds, specific net hyetographs related to each land use each return period have been computed (Figure 42).

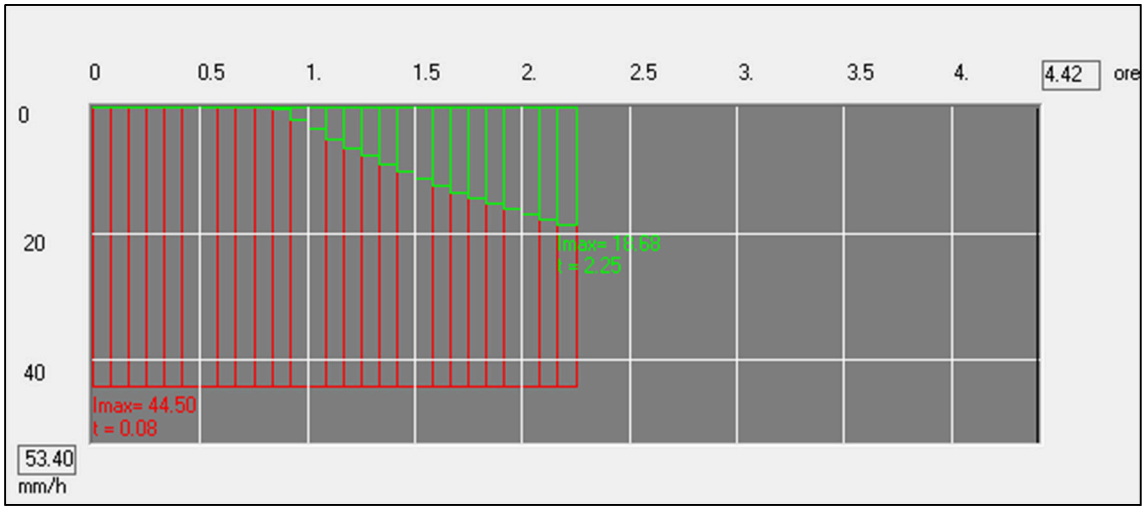

Figure 42: Example of hyetograph (red) and net hyetograph (green) computed with URBIS2003v.2.

To compute the IUH, URBIS2003v.2 considers three different models: 1) Linear reservoir model, 2) Kinematic model and 3) Nash model.

The linear reservoir model is based on the concept that the watershed can be assumed as a linear reservoir of volume $W(t)$, whit a net inflow $p(t)$ and an outflow $q(t)$. $p(t)$ represents the excess rainfall, while $q(t)$ is the correspondent outlet discharge. The storage characteristics of whole watershed is expresses by its own "linear reservoir routing constant" k that represents the relation between the reservoir volume and the discharge as $W(t) = k \cdot q(t)$.

The value of k was computed automatically by the software, starting from the $\overline{tc}$. The shape of linear reservoir IUH was reported in Equation 17.

The kinematic model is based on the same concept as for the time of concentration. Any different portion of the watershed area contribute to the outlet discharge according to its tc. The IUH is expressed as the ratio between contributing area in a unit time $A_t - A_{t-\Delta t}$ over the unit time Δt (Equation 18). A linear relation between area and time was selected for the studied watersheds.

Nash model is based on the linear reservoir concept but it considers the watershed as a cascade of n linear reservoir with an equal routing constant k. The value of n was set to 3, which is the default value for the software and k is computed as a function of $\overline{tc}$ through the relation $k = 0.5\overline{tc}/(n-1)$. The shape of Nash IUH is given in Equation 19.

$$IUH_{LR}(t) = \frac{1}{k} \cdot e^{\frac{-t}{k}}$$

Equation 17: Linear reservoir IUH.

$$IUH_{LK}(t) = \frac{A_t - A_{t-\Delta t}}{\Delta t}$$

Equation 18: Kinematic IUH.

$$IUH_N(t) = \frac{1}{k \cdot (n-1)!} \cdot \left(\frac{-t}{k}\right)^{n-1} \cdot e^{\frac{-t}{k}}$$

Equation 19: Nash IUH.

Specifying the watershed area, hydrographs and the related outlet peak discharges could be computed as shown in Figure 43. This was done for each land use scenario and sub-scenario (Table 17) by using the three aforementioned methods.

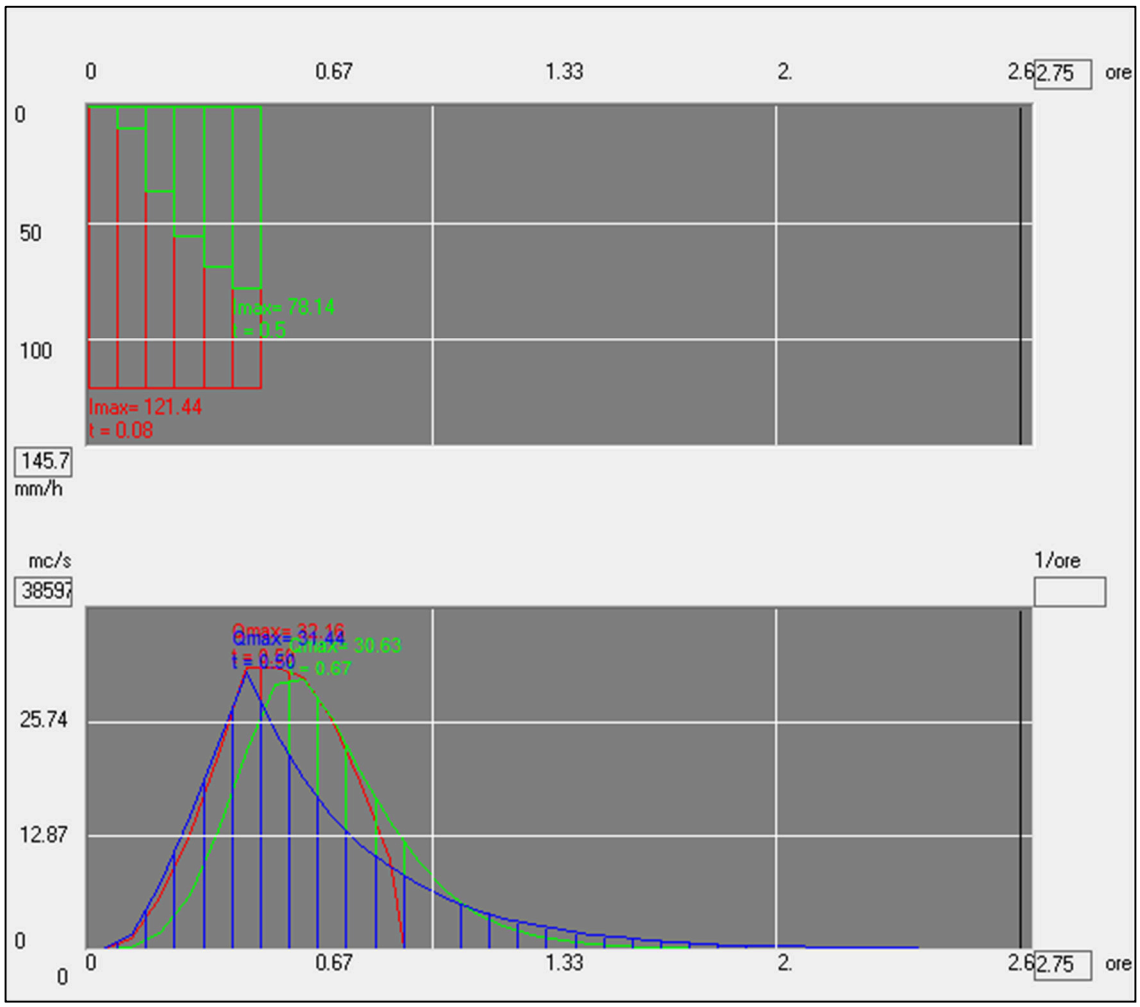

Figure 43: Example of hydrographs computed with URBIS2003v.2; Linear reservoir (blue), Kinematic (red) and Nash (green).

	T [y]	Land use Scenario		Linear reservoir	Linear Kinematic	Nash
Cosia Watershed Q_p	**2**	**1955**	**CN_max**	0.00	0.00	0.00
			CN_min	0.00	0.00	0.00
		1999	**CN_max**	0.00	0.00	0.00
			CN_min	0.00	0.00	0.00

		2012	**CN_max**	10.31	7.61	8.18
			CN_min	0.00	0.00	0.00
	20	**1955**	**CN_max**	12.72	10.46	11.00
			CN_min	0.00	0.00	0.00
		1999	**CN_max**	22.46	19.33	20.02
			CN_min	2.67	2.03	2.17
		2012	**CN_max**	25.22	21.93	22.63
			CN_min	3.90	3.00	3.21
	200	**1955**	**CN_max**	49.24	44.21	44.98
			CN_min	13.15	10.59	11.21
		1999	**CN_max**	67.43	62.64	62.78
			CN_min	25.70	21.73	22.65
		2012	**CN_max**	72.25	67.65	67.53
			CN_min	29.26	25.02	25.93
Valduce Watershed Q_p	**2**	**1955**	**CN_max**	2.55	2.18	2.32
			CN_min	1.04	0.84	0.90
		1999	**CN_max**	3.04	2.64	2.79
			CN_min	1.35	1.10	1.19
		2012	**CN_max**	3.04	2.64	2.79
			CN_min	1.35	1.10	1.19
	20	**1955**	**CN_max**	14.64	14.11	14.07
			CN_min	10.45	9.68	9.90
		1999	**CN_max**	15.42	15.40	15.24
			CN_min	11.42	10.69	10.86
		2012	**CN_max**	15.42	15.40	15.24
			CN_min	11.42	10.69	10.86
	200	**1955**	**CN_max**	29.79	30.23	28.98
			CN_min	23.65	23.22	22.84
		1999	**CN_max**	31.44	32.16	30.63
			CN_min	25.12	24.86	24.30
		2012	**CN_max**	31.44	32.16	30.63
			CN_min	25.12	24.86	24.30

Table 17: $Q_p[m^3/s]$ at the watershed outlets, computed with URBIS2003v.2.

4.5.3 Disclosure of the results

The comparison between peak discharges results for different land use scenarios and sub-scenarios as well as from different software and modelling strategies, lets to do important observations. The effects of urbanization on the peak discharge could be detected by comparing different land use scenarios related to an equal sub-scenario. It is evident that for Valduce Watershed, the land use did not face a drastic change between the three different scenarios. Therefore, the related increase in peak discharges, estimated with WinTR-55, was not considerable. In fact, the differences are less than 10% for the period 1955-2012. Cosia peak discharges computed with WinTR-55 instead increased approximately of 25% during the last sixty years (Graph 6). It can be notice that in Cosia Watershed, the urbanization process has brought a significant change in the soil runoff capacity.

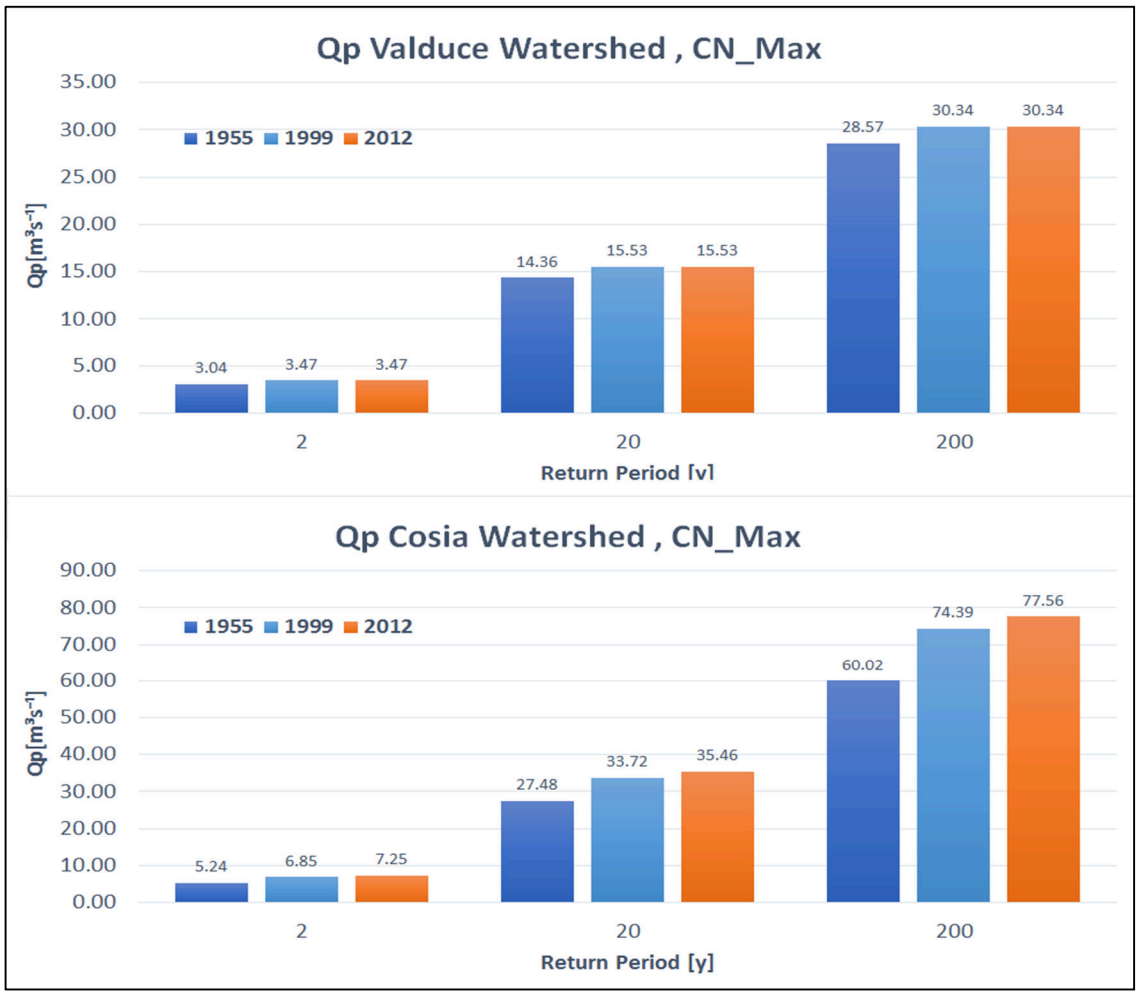

Graph 6: Cosia and V alduce peak discharges from the different land use scenarios.

The sensitivity of the NRCS-CN method, whit respect to the CN value, could be evaluated by looking at the peak discharges from different sub-scenarios (i.e. CN_max, CN_min).

The CN values for an equal land use class and HSG can vary also of 30 units. This was especially true for rural area classes, where CN values variability resulted to be the highest. The related peak discharges for Valduce Watershed, estimated with WinTR-55, resulted in a difference of about 25% between the sub-scenarios. This difference was larger than the one between the scenarios 1955 and 2012. Cosia peak discharges underlined differences ranging from 30% to 40% for different sub-scenarios (Graph 7). Once again, this difference was larger than the one between different land use scenarios. Therefore, detailed information about the soil hydrologic condition and land treatment proved to be necessary in order to estimate a precise value for the peak discharges.

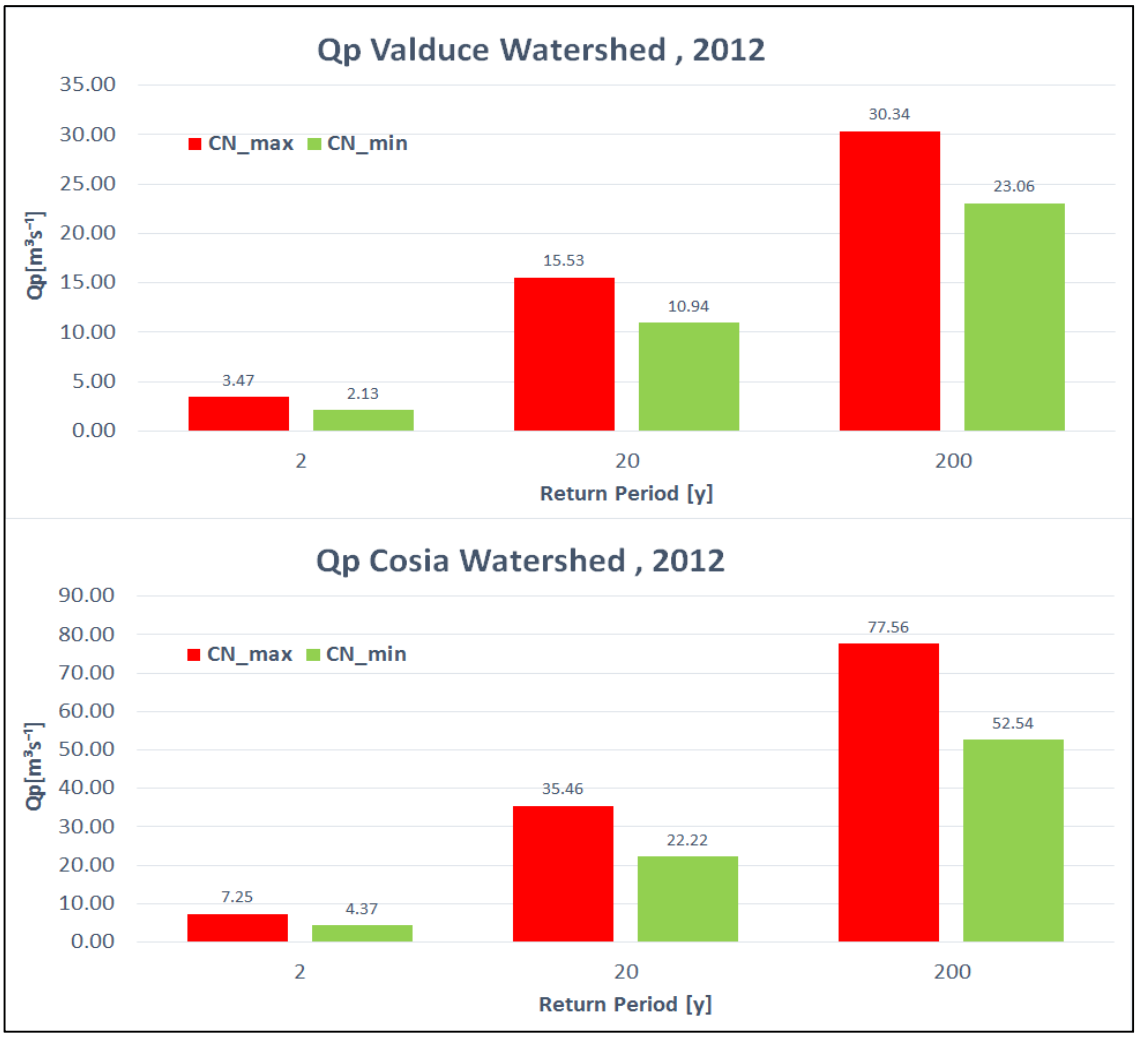

Graph 7: Cosia and V alduce peak discharges from different land use sub-scenarios.

The differences between peak discharges computed with different models could be also observed. Peak discharge values for Valduce Watershed resulted to be comparable (Graph 8).

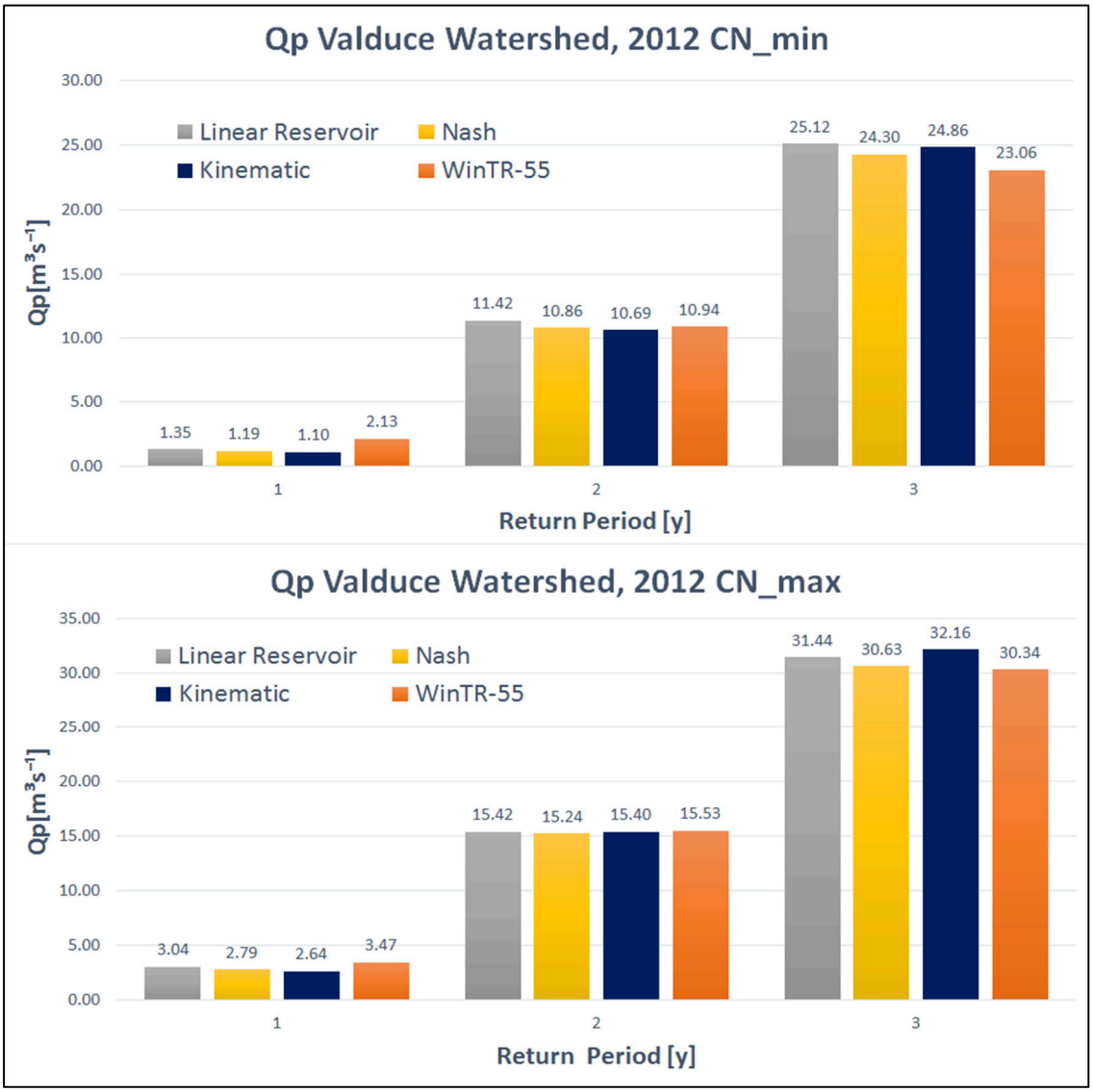

Graph 8: Valduce peak discharges from different models.

Cosia peak discharges showed higher variability among WinTR-55 and URBIS2003v.2 models. As mentioned in section 4.5.1, the use of a unique $\overline{CN}$ for the entire watershed area introduced inaccuracies. The initial abstraction of the urbanized area was probably overestimated. This could explained why null discharges were obtained from URBIS2003v.2 models, for storms with T=2 years in CN_min sub-scenario (Graph 9). Values closer to each other were

obtained for higher CN, as in CN_max sub-scenario. The disclosure in mathematical differences between the models was not among the purposes of this study. The peak discharge estimation was carried out with different methods in order to obtain feasible critical discharge values to be used for the hydraulic simulations. Therefore, the peak discharges estimated with the multiple area strategy of WinTR-55 were selected for the Cosia Torrent hydraulic simulations. In fact, these turned out to be the highest values for T=20 and 200 and they represented the worst cases for testing the conveyance of this torrent. Peak discharges computed with WinTR-55 were involved also for Valduce Torrent hydraulic model, as matter of coherence, even if these values were very close to the ones computed with URBIS2003v.2.

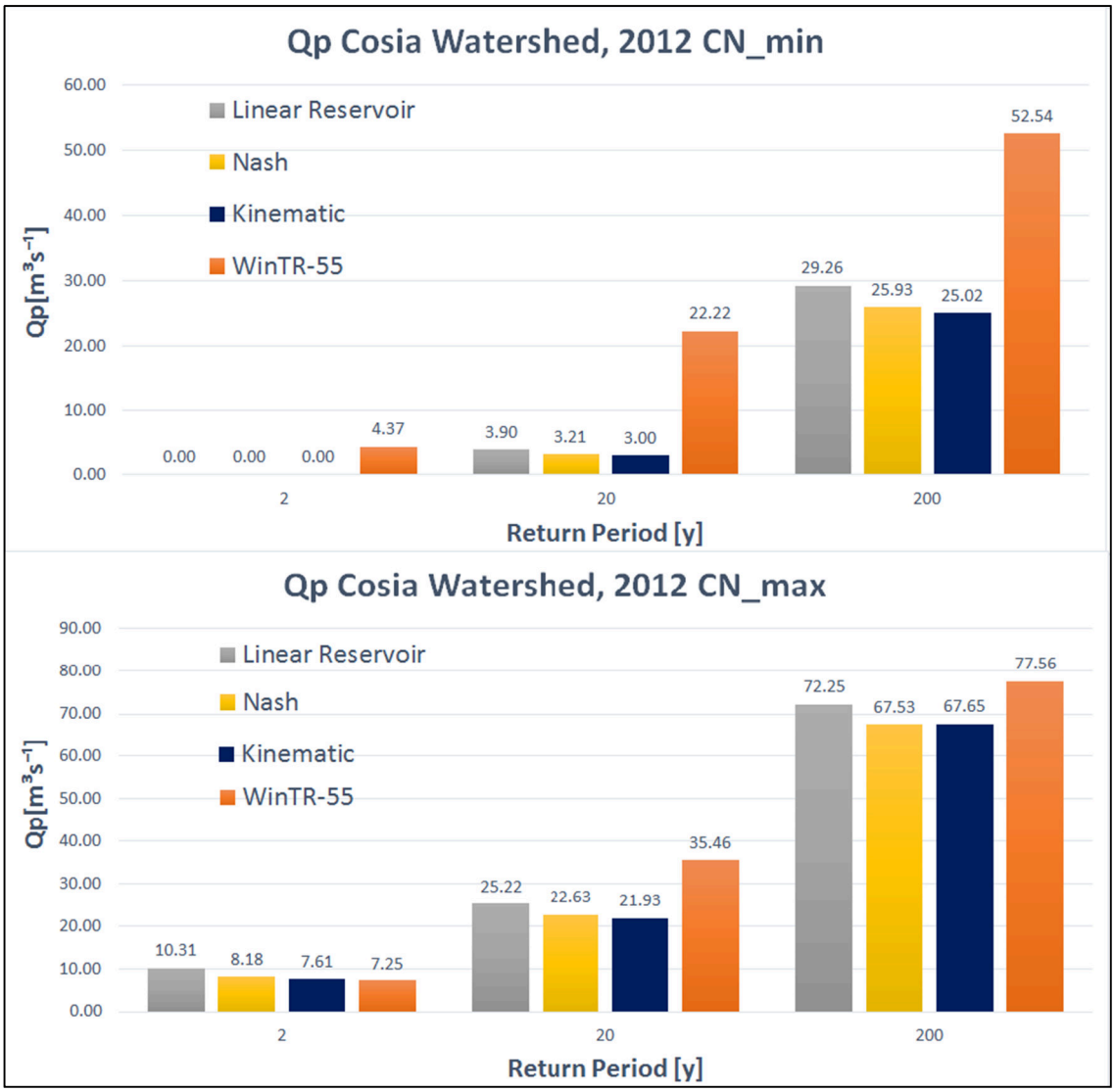

Graph 9: Cosia peak discharges from different models.

4.6 HYDRAULIC MODEL

The discharge efficiency of the buried channels was assessed by studying the residual conveyance of the channels for the computed peak discharges. The discharge efficiency can be estimated by computing the water profiles in these channels when the estimated peak discharges is running inside them. This task was achieved using HEC-RAS software. Surely, changes in peak discharges, which have been underlined between different land use scenarios, induced modification of the related water profiles; in particular, the increase of peak flowrates of the last sixty years may results in overflow problems that may affect the buried channels. Therefore, the modification of the residual conveyance could be read as the effect of urbanization on the hydraulic risk.

4.6.1 Pre-processing of input data with HEC-geoRAS

The hydraulic simulation of water profiles required data about the geometry and the hydraulic characteristics of the stream cross-sections. From the hydraulic point of view, these represented fundamental features in order to model the torrents. A detailed topographical survey, regarding Cosia and Valduce torrents, was not available; therefore, GIS software has been used in order to extract cross-section information from the available set of geospatial data.

HEC-RAS software provides different tools in order to design input data, describing cross-section geometry and hydraulic characteristics, by means of GIS processing. HEC-geoRAS is one of these tools (Cameron & Ackerman 2012). This plugin works inside ArcGIS environment and allows creating an HEC-RAS import file, containing geometric data, from an existing DTM and a complementary dataset. The complementary dataset includes shapefiles representing flow-paths, channel banks, cross-section positions as well as flow obstruction areas and hydraulic roughness map within the floodplains.

TINITALY/01 DTM was used for this particular task. Besides having higher cell resolution with respect to Heli-DEM, its default unit of measure is the meter and not the decimal degrees as for Heli-DEM. This allowed the exchange of files with HEC-RAS, which is not able to read pre-processed data in degree units. The LIDAR DTM (with 2m cell size) would be a better choice because its higher cell resolution but it was not available for the entire study area.

The DTM was converted into TIN (Triangulated Irregular Network) format with ArcGIS and a set of HEC-geoRAS layers was crated containing the torrent flow-paths, banks stations, cross-sections etc. They were drawn up by using the Editing Toolbox of ArcGIS, reconstructing the drainage network topology. The edited layers were interpolated with the TIN using the HEC-geoRAS Toolbox, adding to them elevation information as well as geographic coordinates in order to obtain the elevation profiles as well as the topological relationships for both flow-paths and cross-sections.

Additional information were included in specific layers such as hydraulic roughness maps, which are maps of polygons having as attribute the Manning's coefficients (e.g. Chow 1959) as well as obstruction areas (i.e. building features) near the torrents. An example of pre-processed data is included in Figure 44.

This procedure was carried out both for Cosia and Valduce torrents and the results were imported in HEC-RAS using HEC-geoRAS *Export RAS data tool* (Figure 45 & Figure 46) that allows converting the shapefile dataset into HEC-RAS input data format.

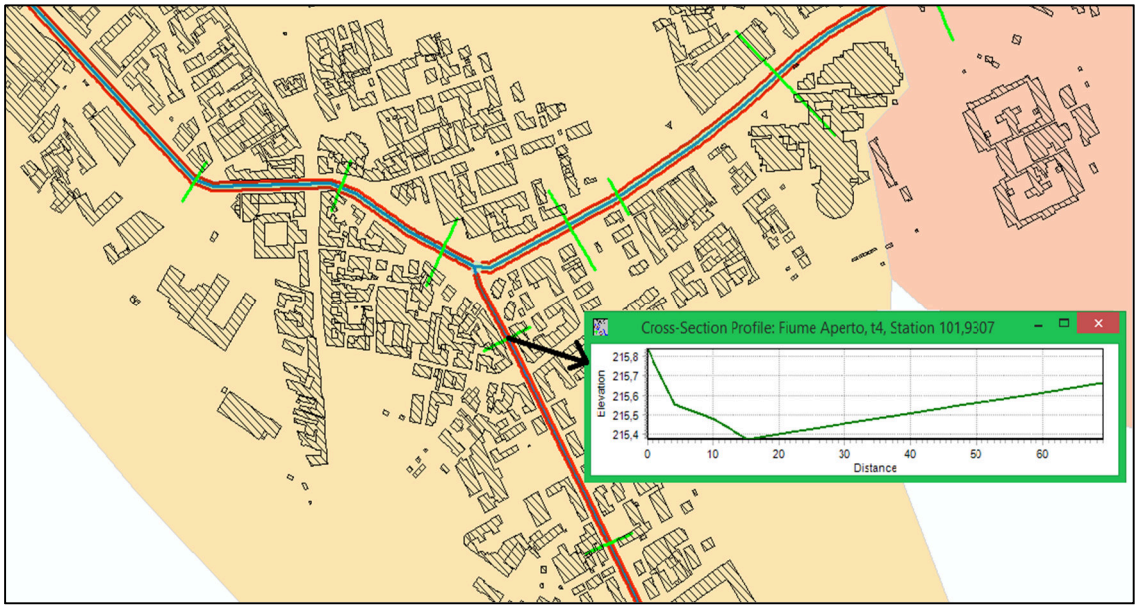

Figure 44: HEC-geoRAS data pre-processing. The visible features represent torrent flow-paths (blue lines), banks position (red lines), cross-section positions (green lines), obstruction areas (black stripes polygon), hydraulic roughness map (background pink polygons) and cross-section profiles (popup graph).

These geometric models of the torrents, developed with HEC-geoRAS, represented the input data required for the hydraulic simulations.

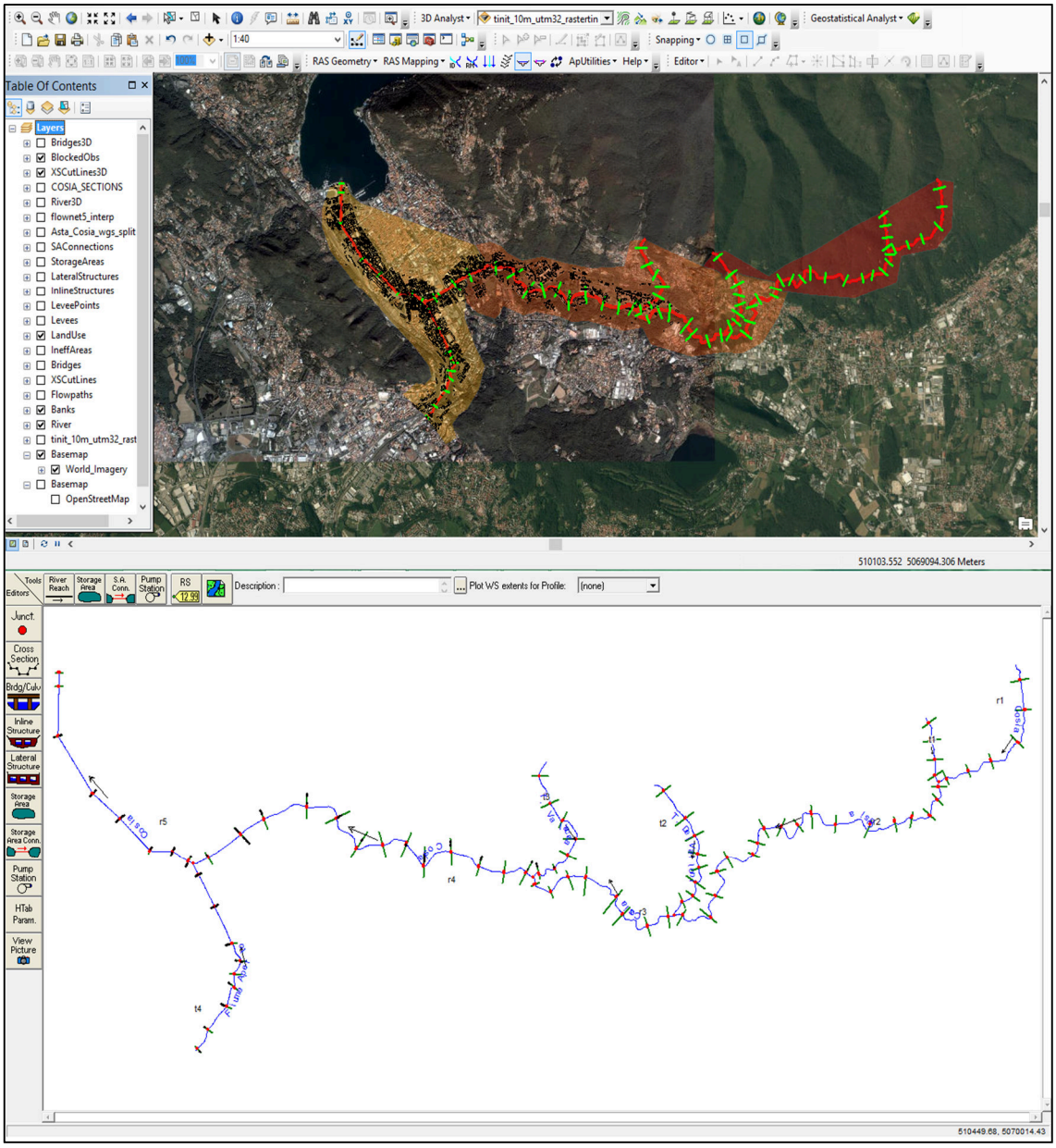

Figure 45: Cosia Torrent HEC-geoRAS layer dataset (up) and exported geometric model in HEC-RAS (down).

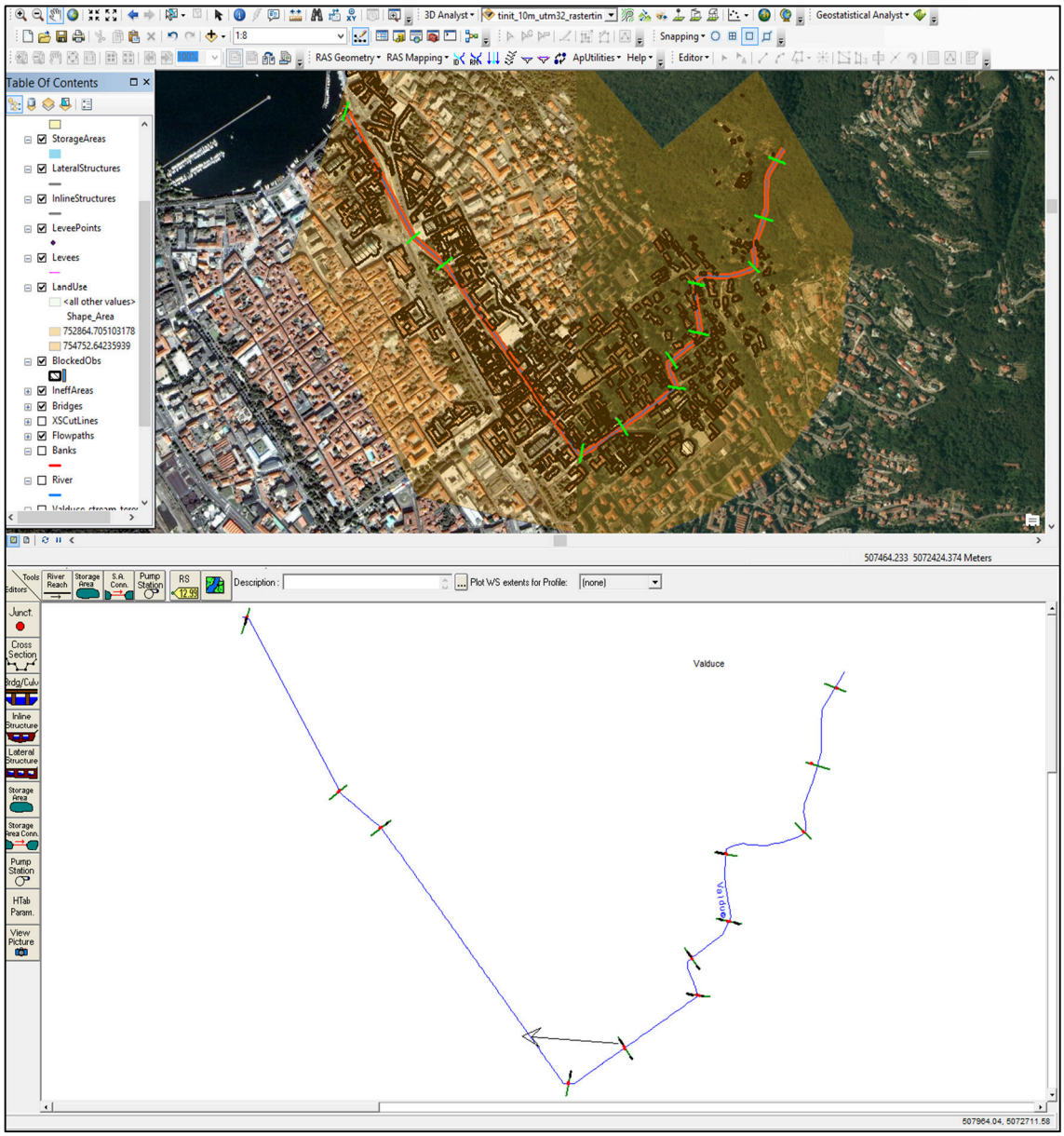

Figure 46: Valduce Torrent HEC-geoRAS layer dataset (up) and exported geometric model in HEC-RAS (down).

4.6.2 Hydraulic simulation with HEC-RAS

The geometric models exported from HEC-geoRAS were modified to introduce the properties of the buried channels that cannot be identified through the DTM analysis, as is shown in Figure 47c. These are underground and even field observations were difficult to retrieve. Moreover, Cosia and

Aperto torrents flow in artificial channels in their medium-low course. These channels could not be recognized from the DTM because of their dimensions, which are often smaller than the DTM cell (Figure 47b). The mountain course of the torrents instead flows into little narrow valleys that could be described through the DTM analysis (Figure 47a).

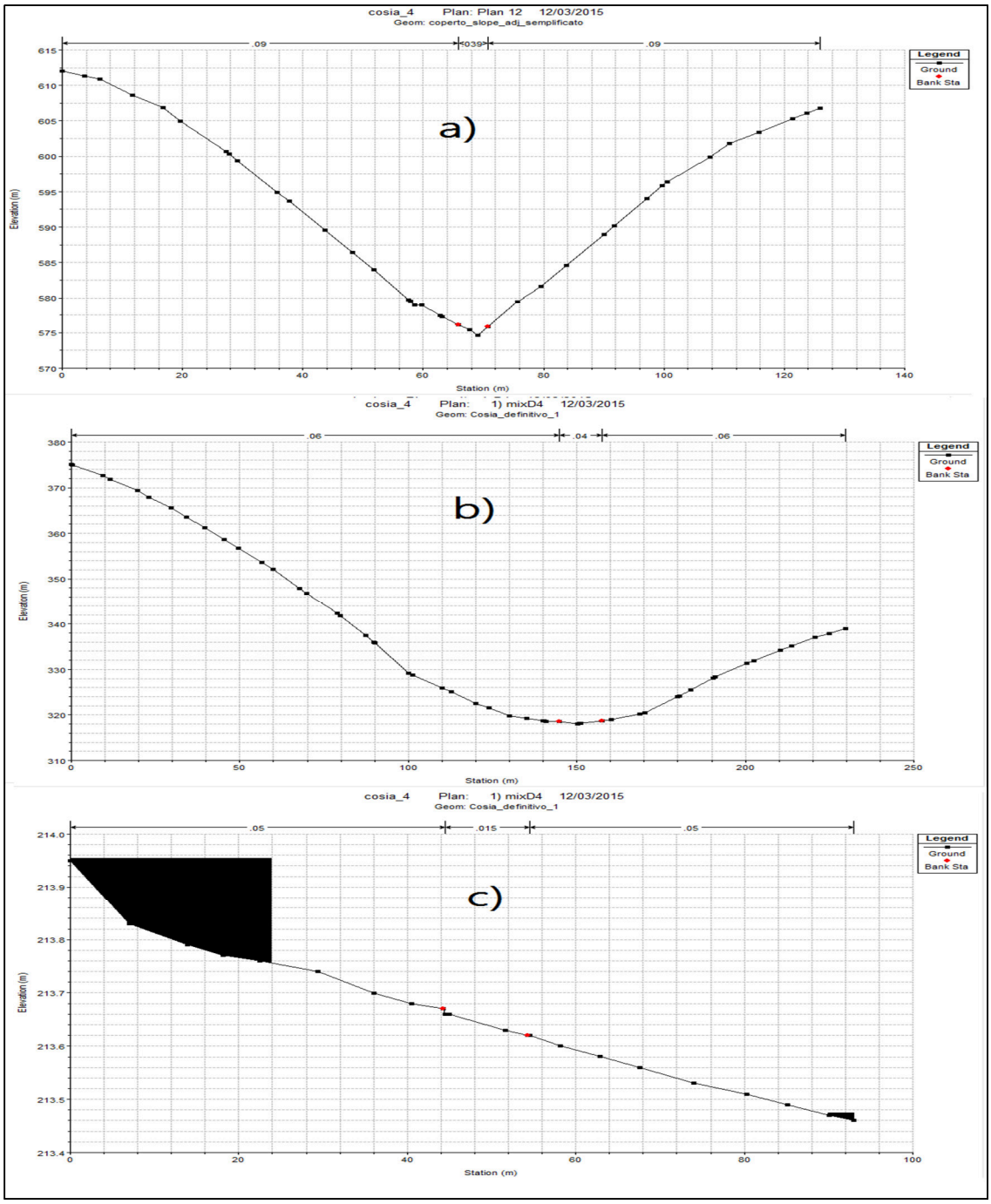

Figure 47: Examples of Cosia cross-section profiles obtained with HEC-geoRAS; a) Mountain course b) Medium-low course c) Buried path.

The information about the typical cross-section geometry along the medium-low course of Cosia and Aperto torrents were collected by means of field surveys with Geopaparazzi. These typical cross-sections were introduced by modifying the cross-section profiles obtained with HEC-geoRAS, as is shown in Figure 48.

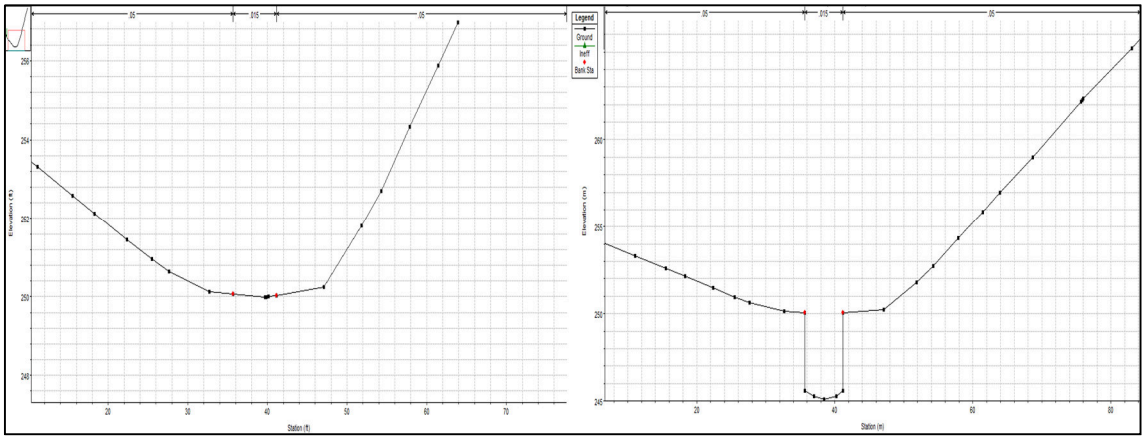

Figure 48: Example of modified cross-section profile for medium-low path of Aperto Torrent. Before (left) and after the modification (right).

The same procedure was used to input the geometry for the buried reach of Cosia, Valduce and Aperto torrents. The information about the buried channel geometry of Cosia Torrent was retrieved from a former hydraulic study (Cappelletti 2004), courtesy of Eng. Turconi from COMODEPUR s.p.a (Figure 49).

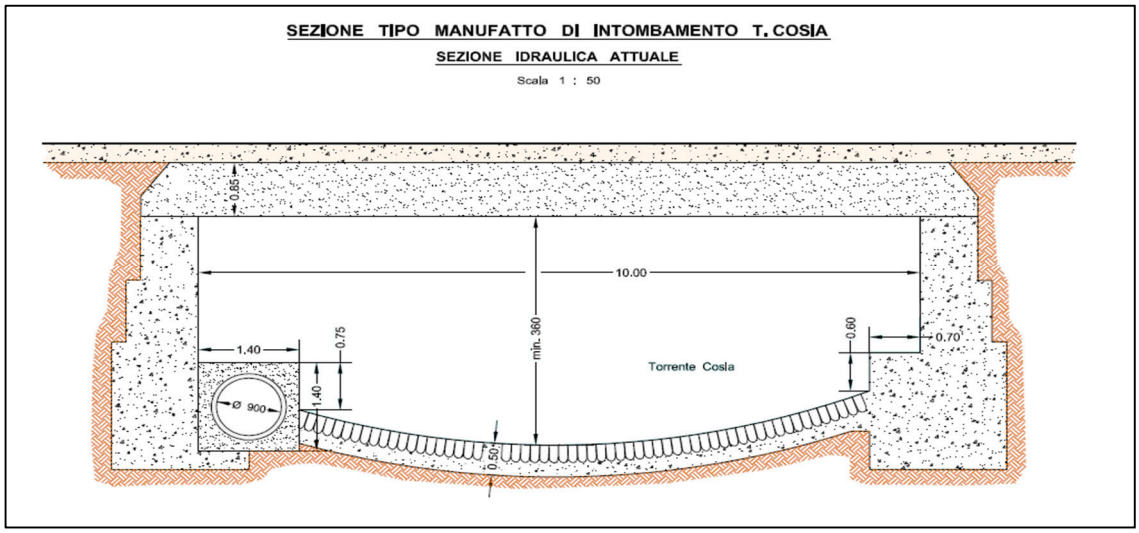

Figure 49: Cosia buried channel cross-section (Cappelletti 2004).

For what it concerns Valduce and Aperto buried channel geometry, these were retrieved from the Municipality Archive of Como City (Figure 50). Again, the shape of the channels was introduced by means of manual editing.

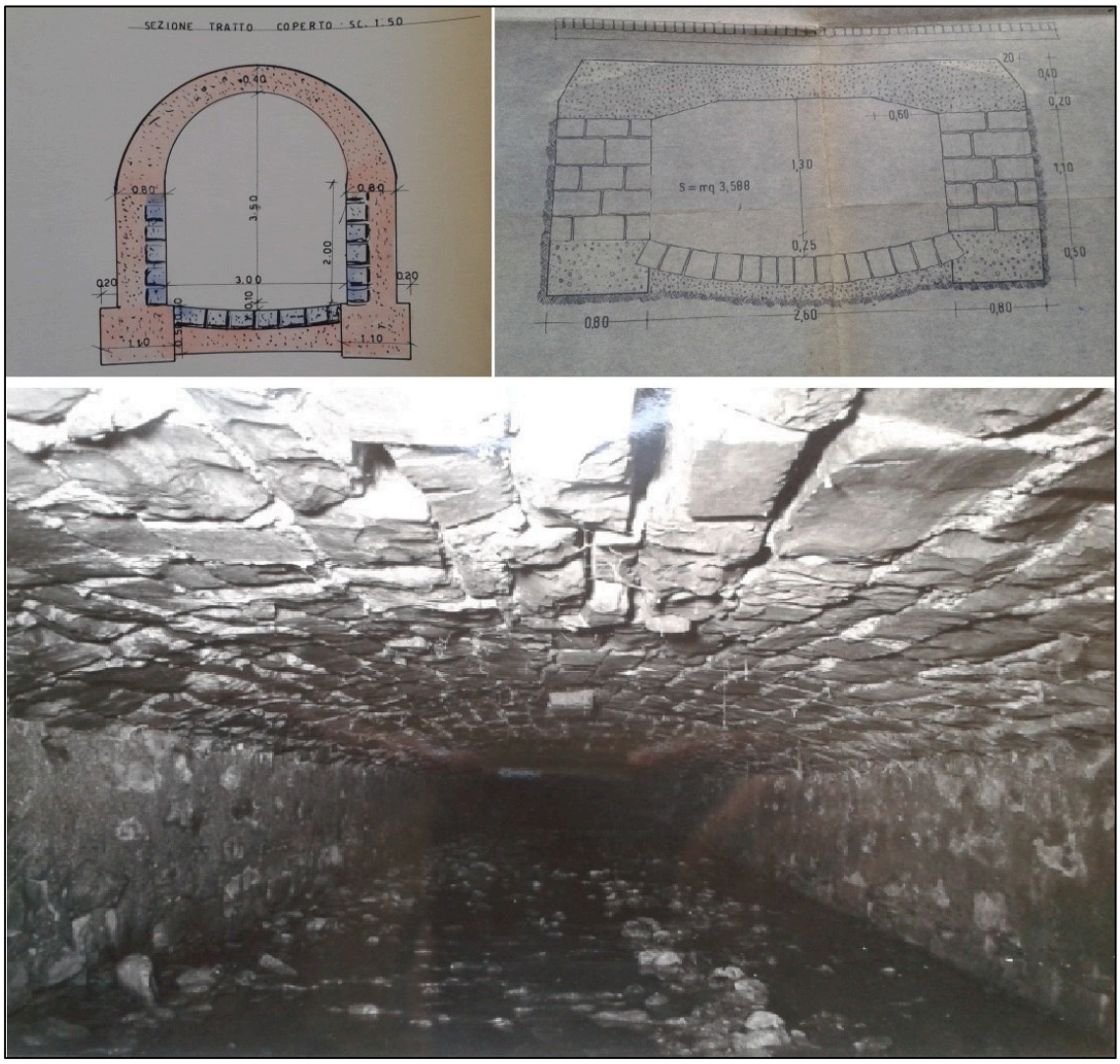

Figure 50: Valduce buried channel cross-sections (Como Municipality Archive).

In order to model the burial of the torrents, HEC-RAS *Bridge/Culvert editor* was used. Actually, this software allows modelling bridges and culverts bounded by an upstream and a downstream cross-section; thus, intermediate cross-sections could not be introduced for a single bridge deck. In order to overcome this limitation, series of bridge decks were used for any buried reach, to describe also the sinuosity of the buried paths. The hydraulic confluence between Aperto and Cosia torrents is buried and it was not possible to model it with a bridge

deck because HEC-RAS modelling capabilities did not allow this operation (Figure 51).

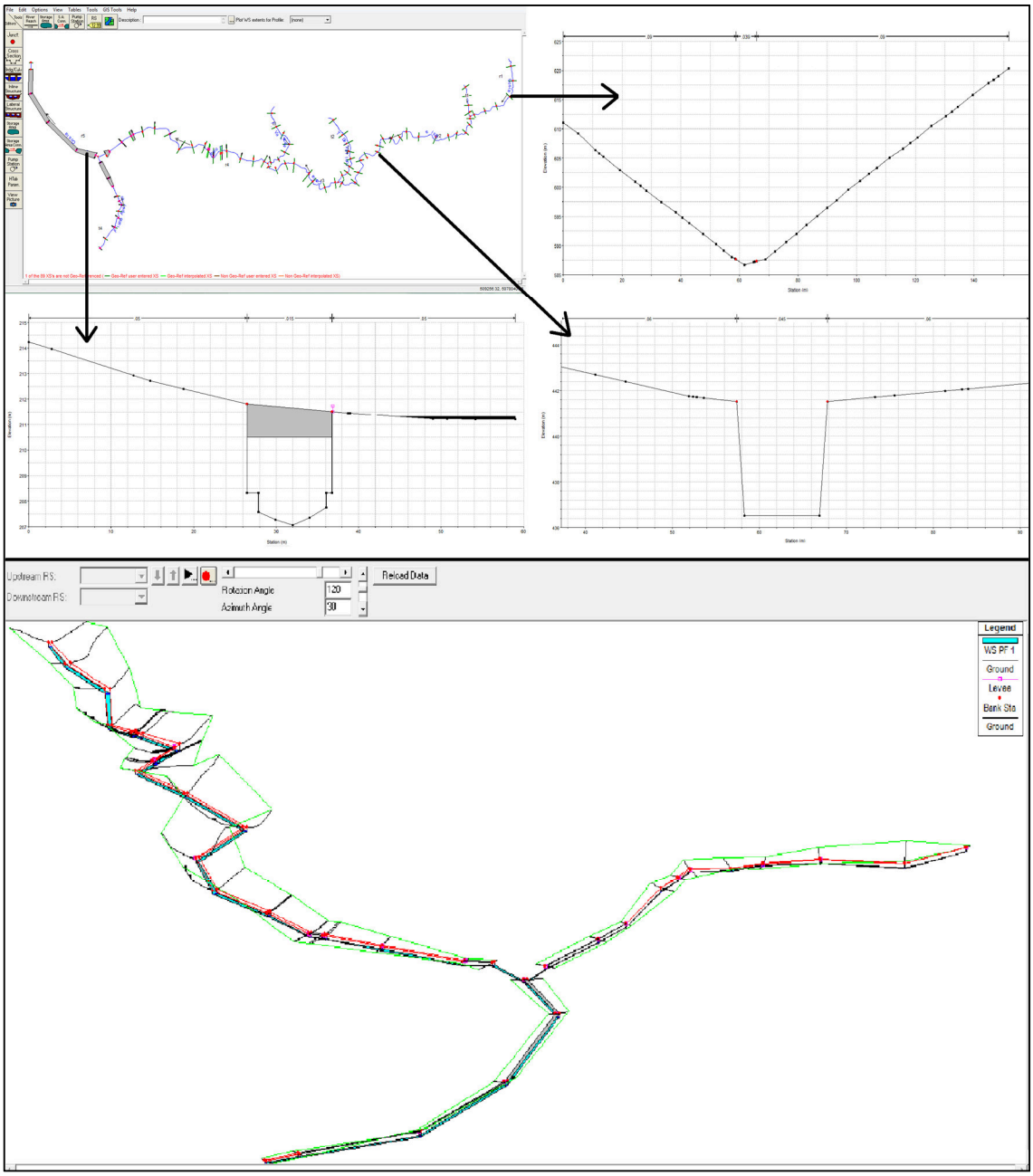

Figure 51: Cosia Torrent HEC-RAS geometric model.

The same procedure was applied to model the Valduce Torrent, as is shown in Figure 52.

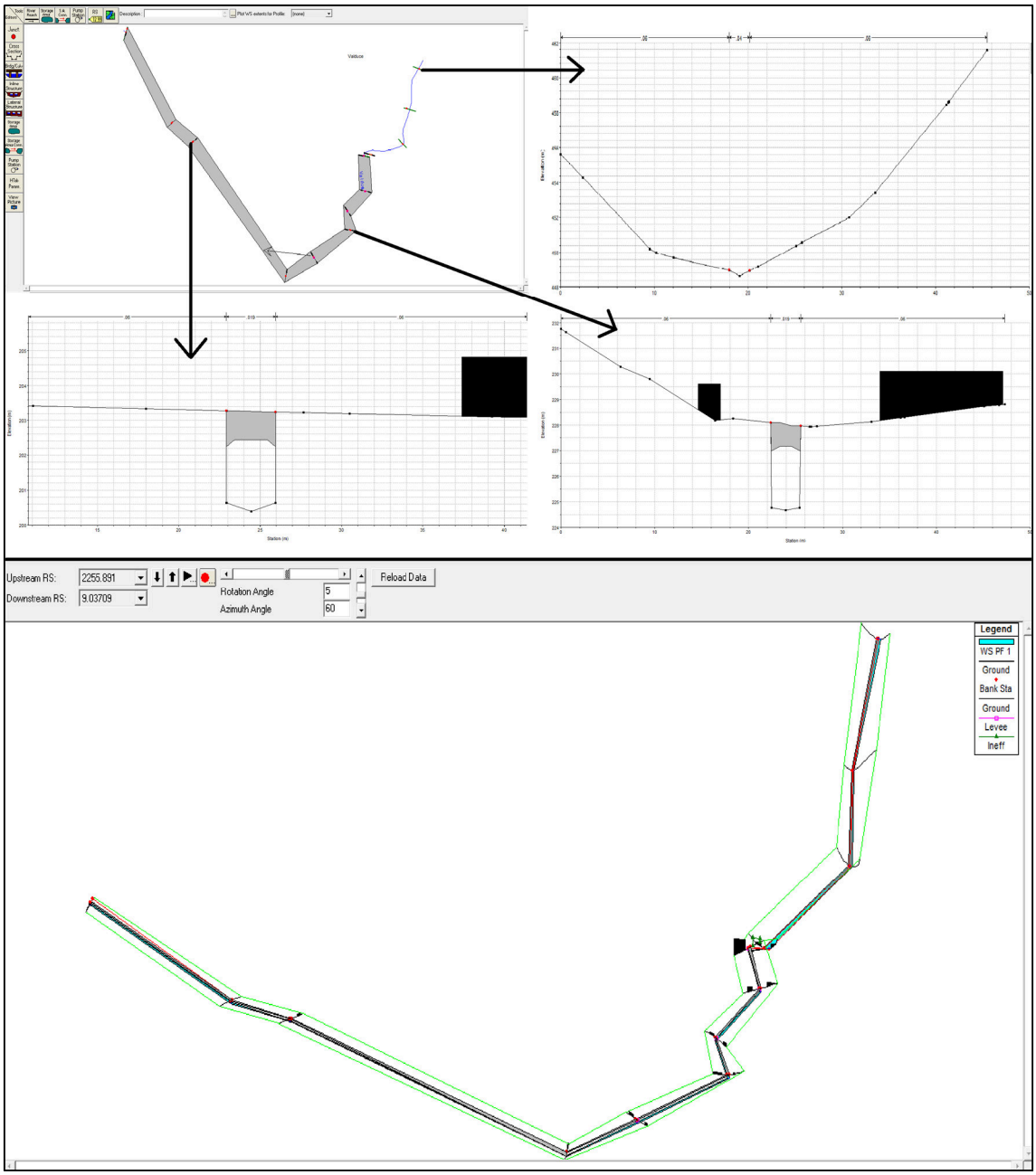

Figure 52: Valduce Torrent HEC-RAS geometric model.

The HEC-RAS is a one dimensional open flow model; thus, the presence of little gaps between two consecutive decks, which let the flow be always in contact with the atmosphere, do not allow to the buried channels to operate as pressure conduits (Figure 53). Even if it was not possible to simulate pressure flows along the buried channels, this simplification was considered suitable for the case study because the open flow was the working operation for which the

buried channels were designed. Therefore, when pressure flows eventually occur during the model simulation, they are shown as overflow phenomena.

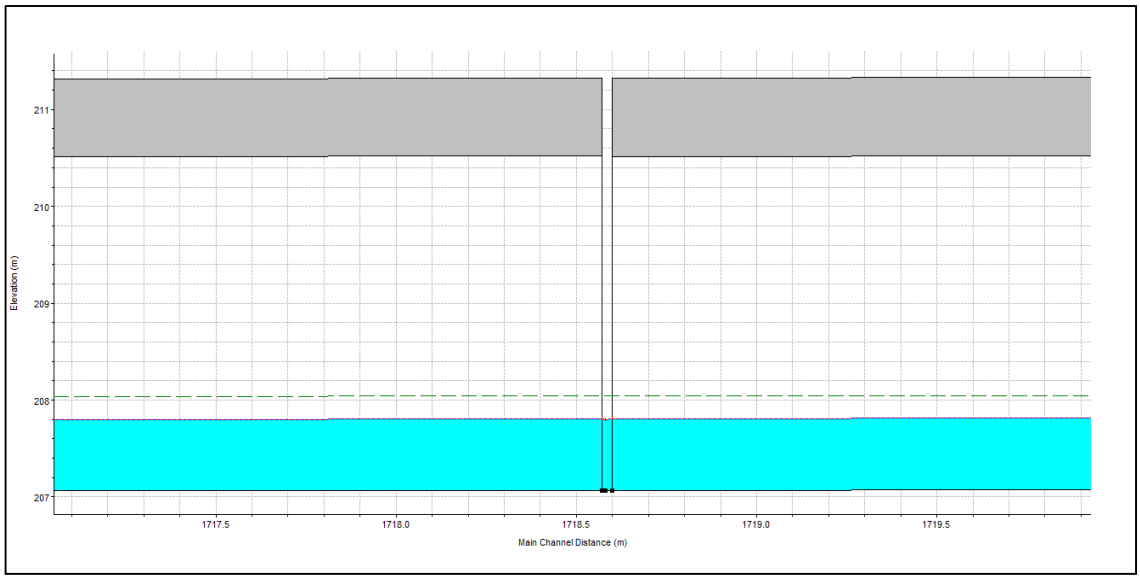

Figure 53: Buried channel profile showing a crawlspace between two consecutive bridge decks.

As explained before, important simplification for the torrents were introduced. Moreover, hydraulic structures such as weirs, sediment ponds etc., which are scattered along the watercourses, where not considered. This was mainly due to the lack of information about their geometries and positions. The buried riverbed slopes were set as uniform, in order to take into account the slope stabilization works that were done along Cosia, Valduce and Aperto riverbeds. The open channel slopes were assumed equal to the one retrieved from the DTM. Knowing both bottom and side materials, the hydraulic roughness were assigned by means of Manning's coefficient tables (e.g. Chow 1959).

The computation of the water profiles was performed by using the *Steady Flow Analysis tool* of HEC-RAS. This tool is capable of performing one-dimensional surface water profile calculation, for steady gradually varied flow in natural or constructed channels. Subcritical, supercritical, and mixed flow regime water surface profiles can be calculated. Water surface profiles were computed from one cross-section to the next by solving the flow energy balance equation (Equation 20) with an iterative procedure called Standard Step method (U.S. Army Corps of Engineers 2010). The software integrates along the paths the Energy equation (Figure 54), starting from the boundary conditions and the

geometric properties of any cross-section. A detailed explanation for the computational procedure and parameters is included in the software hydraulic reference manual (available at: http://www.hec.usace.army.mil/software/hec-ras/documentation/HEC-RAS_4.1_Reference_Manual.pdf).

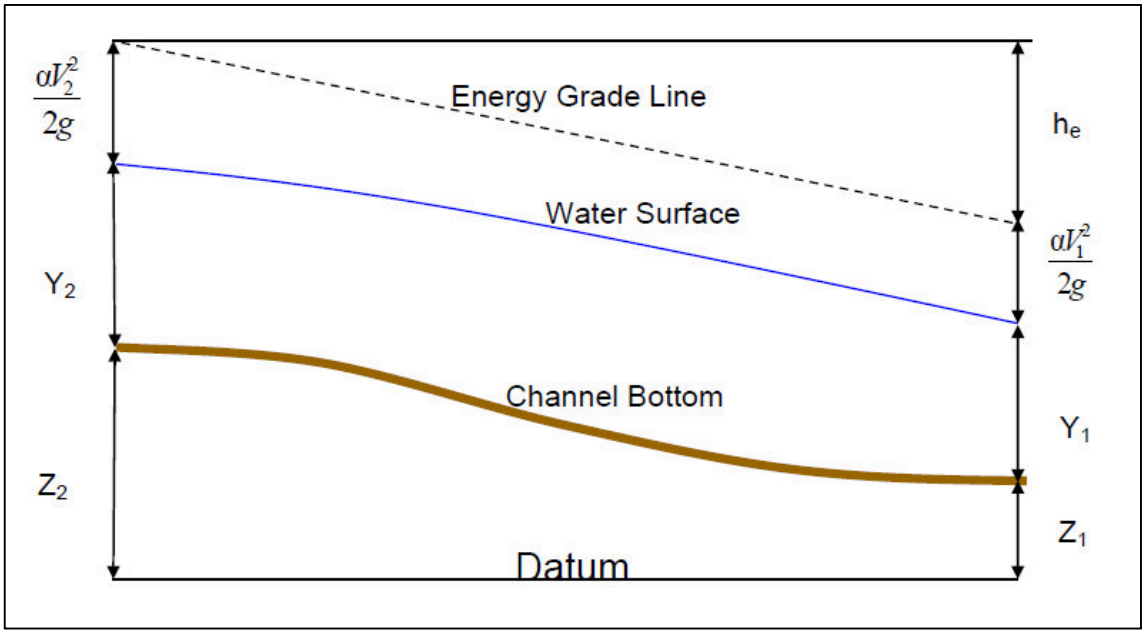

Figure 54:Flow Energy balance equation parameters (U.S. Army Corps of Engineers *2010*).

$$Z_2 + Y_2 + \frac{a_2 {V_2}^2}{2g} = Z_1 + Y_1 + \frac{a_1 {V_1}^2}{2g} + h_e$$

Equation 20: Flow energy balance equation.

Steady flow simulation required to set up specific upstream and downstream boundary conditions (BCs). The upstream BCs were set by imposing the initial stage equal to the Critical Depth. The downstream BCs were set at the watersheds outlets as a Known Water Level, set equal to 198 m a.s.l, which corresponds to the Lake Como surface level. Junction BCs were adopted at the hydraulic junctions between torrent branches.

Water profile computations were run by specifying the project discharges, which have been computed and selected in section 4.5. 1 m^3/s was added to Cosia outlet peak discharges in order to take into account for the wastewater treatment plant, which discharges into Cosia buried channel. This was done for 1999 and 2012 scenario. In 1955, the plant had not yet been built. Thus, it was possible to identify the water levels in both buried and open drainage network (Figure 55) as well as to identify possible overflow phenomena. The rating curves of each buried cross-section is among the software outputs. These are graphical representation of the relationship between discharge and a pertinent hydraulic property, such as depth of flow in the case of channels. Disclosures about peak discharge effects on the channel water profiles are discussed by analysing these particular graphs, in the following section.

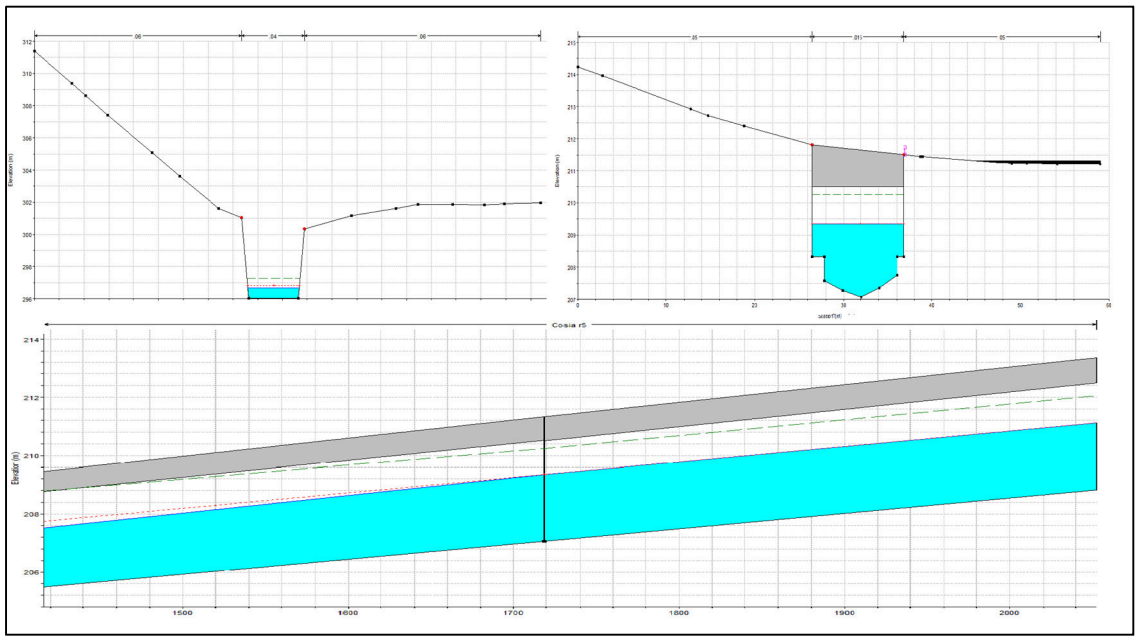

Figure 55: Example of simulated water profiles (light blue) with HEC-RAS. Cross-section view (up) and longitudinal profile view (down).

4.6.3 Results

The water surface profiles, obtained for the 2-year return period storm peak discharges, seem to give no particular problems for all of the land use scenarios and sub-scenarios considered. The buried channels proved to be able to convey these flowrates. This condition changes if higher return period storms are considered.

Regarding the Cosia Torrent, even the 200-year return period storm gives safely results along the buried the channel, for all land use scenarios considered. The observed differences between scenarios, on the water profile elevation, are significant; however, particular problematics could not be correlated to the land use alteration. The results obtained from 2012 and 1995 land use scenario are described, exploiting a rating curve, in Graph 10.

These two scenarios, related to the CN_max sub-scenario, were selected for comparison purpose. In fact, these described the extreme situations on land use alteration within the watersheds in the considered period. The discharge associated to a 200-years storm, yields to 20% residual conveyance reduction as it is shown in Graph 10.

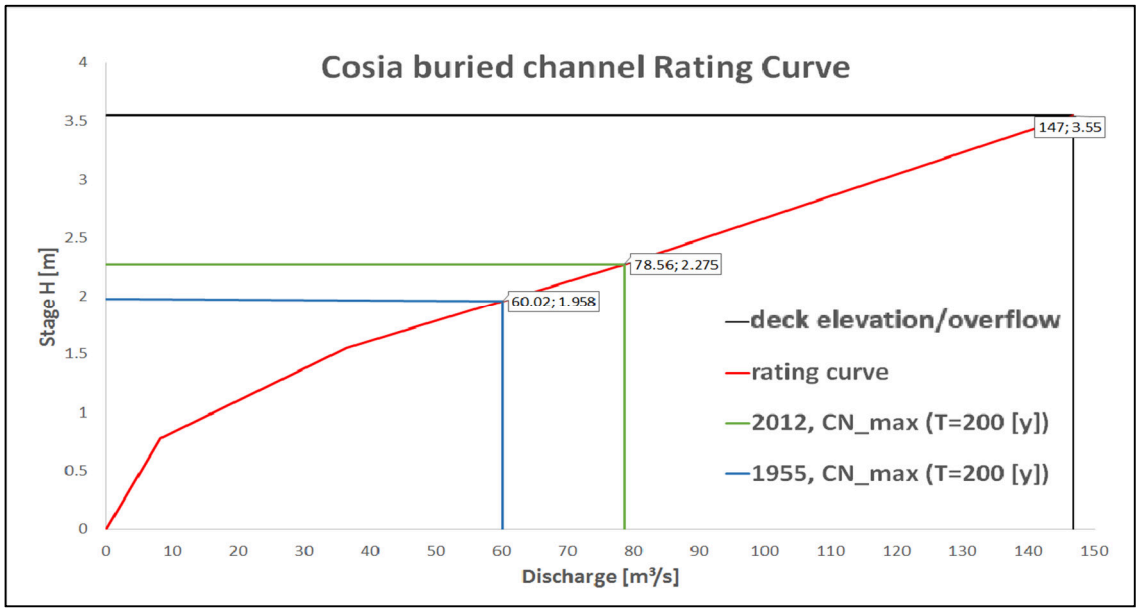

Graph 10: Rating Curve representative for Cosia buried channel.

A worst situation was obtained for the Aperto Torrent, mainly at the confluence with the Cosia Torrent. Comparing the 2012 and 1955 land use scenarios, the peak discharges increased drastically in the last sixty years and the estimated increase of the water surface elevation indicates a significant reduction of the residual conveyance up to 45% (more than double of the Cosia Torrent conveyance reduction). This is shown in Graph 11.

However, the efficiency of Aperto buried channel seems to be still adequate for these increased peak flowrates.

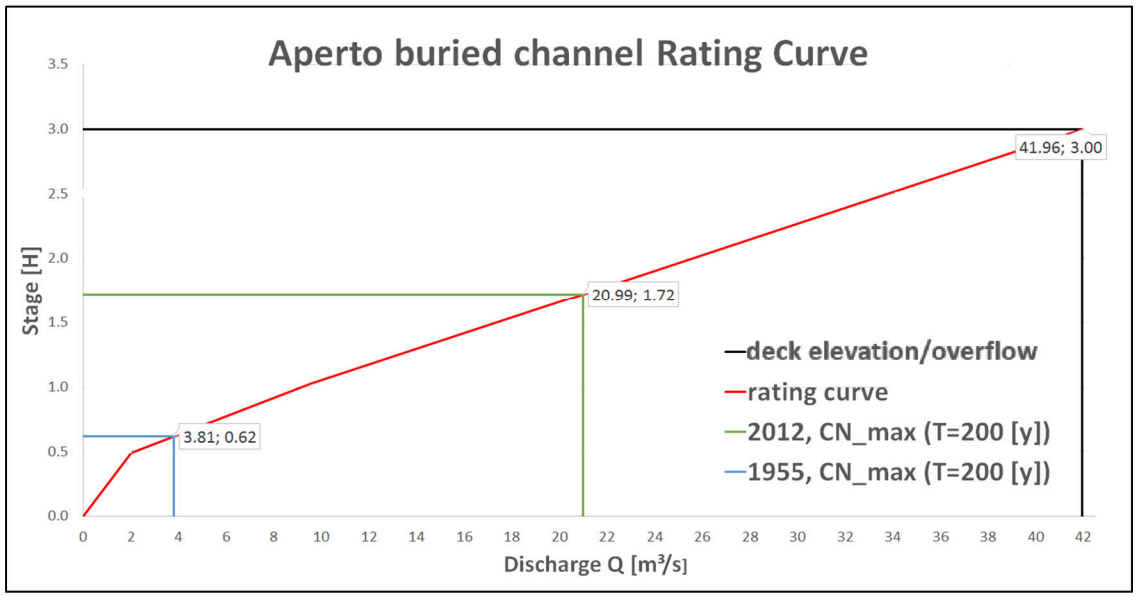

Graph 11: Rating Curve representative for Aperto buried channel.

Valduce Torrent presents different problems than the Aperto and Cosia torrents in fact; results show that overflow may occur even for peak discharges associated to 20-years return period storms. These flowrates, as shown in Graph 12, cannot be conveyed by the channel as open flow.

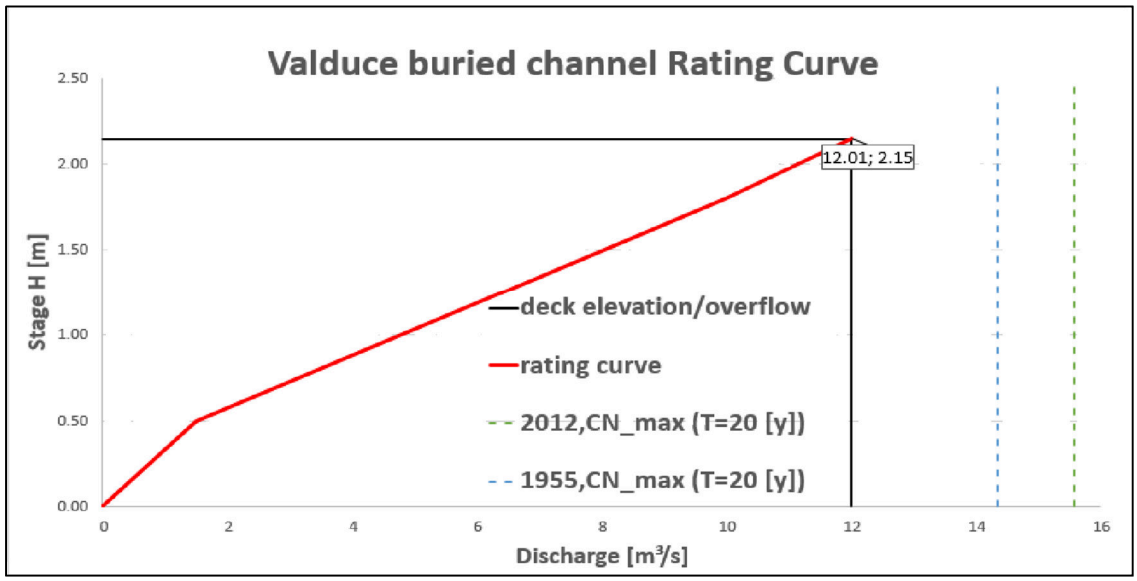

Graph 12: Rating Curve representative for Valduce buried channel.

These obtained results describe quite well the actual situation of the Valduce Torrent. Since the beginning of the channel burial, on the late XIX century, overflow problems have often occurred. Master plans and technical studies of that period report frequently uplift of manhole devices during Valduce Torrent floods. This phenomenon could be observed also in the recent past, as shows in Figure 56.

Figure 56: 11/10/2014, Valduce uplift manhole after intense rainfalls (QuiComo).

For what it concerns the Cosia Torrent, no recent floods are reported. However, when intense rainfalls happen in Como City, the torrent is often appointed in the local news. The last important flood was recalled in a local newspaper article, published on 17/11/2013 (Tajana 2013). This happened in 1951 during a huge flood event, which affected the entire north of Italy. Several landslides occurred in the neighbourhoods of Cosia riverbed (Figure 57) and 16 deaths were registered.

Figure 57: Landslide on Cosia Torrent, 1951 (Archivio Storico Istituto LUCE).

The obtained results can be considered reliable; nevertheless, the awareness on hydrological and hydraulic conditions of both watersheds and watercourses must kept high, in order to avoid unpleasant consequences along the territory.

5. WEBGIS

The knowledge of the territory is a necessary requirement for any person who wants to operate within it, e.g. an urban planner or simply a dweller interested in his/her life-space. This perception cannot subsist without knowing the physical and environmental features as well as their historical and cultural value (Turri 2002). GIS technologies are capable of including these different information in a single tool. Besides the geospatial analysis, which was carried out in the previous chapters, GIS were exploited also in order to spread the achieved results, in a very intuitive way. A specific WebGIS was developed in order to allow the access to the most meaningful outcomes of this work, which could be of interest for any of citizen and city user.

Distributing geospatial information via the Web is an enforcing factor for information providers. Internet allows all levels of society to access geospatial information. The usage of the Web as a platform, for distributing geospatial data, has been favored by a set of typical advantages. In particoular, a wide and distibuted public can be reach as well as the costs are very limited compared to those for printing/updating maps. Moreover, data can easly and quikcly updated and they are potentially independent from the platform used.

A WebGIS allows an interactive and dynamic data presentation as well as querying for data information. Geospatial data cannot be downloaded directly from this tool. Therefore, a WebGIS represented a suitable solution in order to allow the access the copyright maps, which were exploited in this study, otherwise accessible only under fee.

The WebGIS implementation based on a Server/Client software architecture (Figure 59). The Server Side was composed of GeoServer and Apache Web Server (http://httpd.apache.org). GeoServer allowed styling and publishing the geospatial data on the Web, by means of OGC standards. The list of the published data was included in the APPENDIX. The latter can be displayed by accessing the GeoServer URL http://geomobile.como.polimi.it:8080/geoserver, as shown in Figure 58. Alternatively, the layers can be imported as WMS layers in QGIS or in whatever WMS viewer. External servers were included in order to retrieve basemaps. These are: OpenStreeMap (http://www.openstreetmap.org), Bing (http://www.bing.com/maps), MapQuest (http://www.mapquest.com) and Stamen (http://maps.stamen.com).

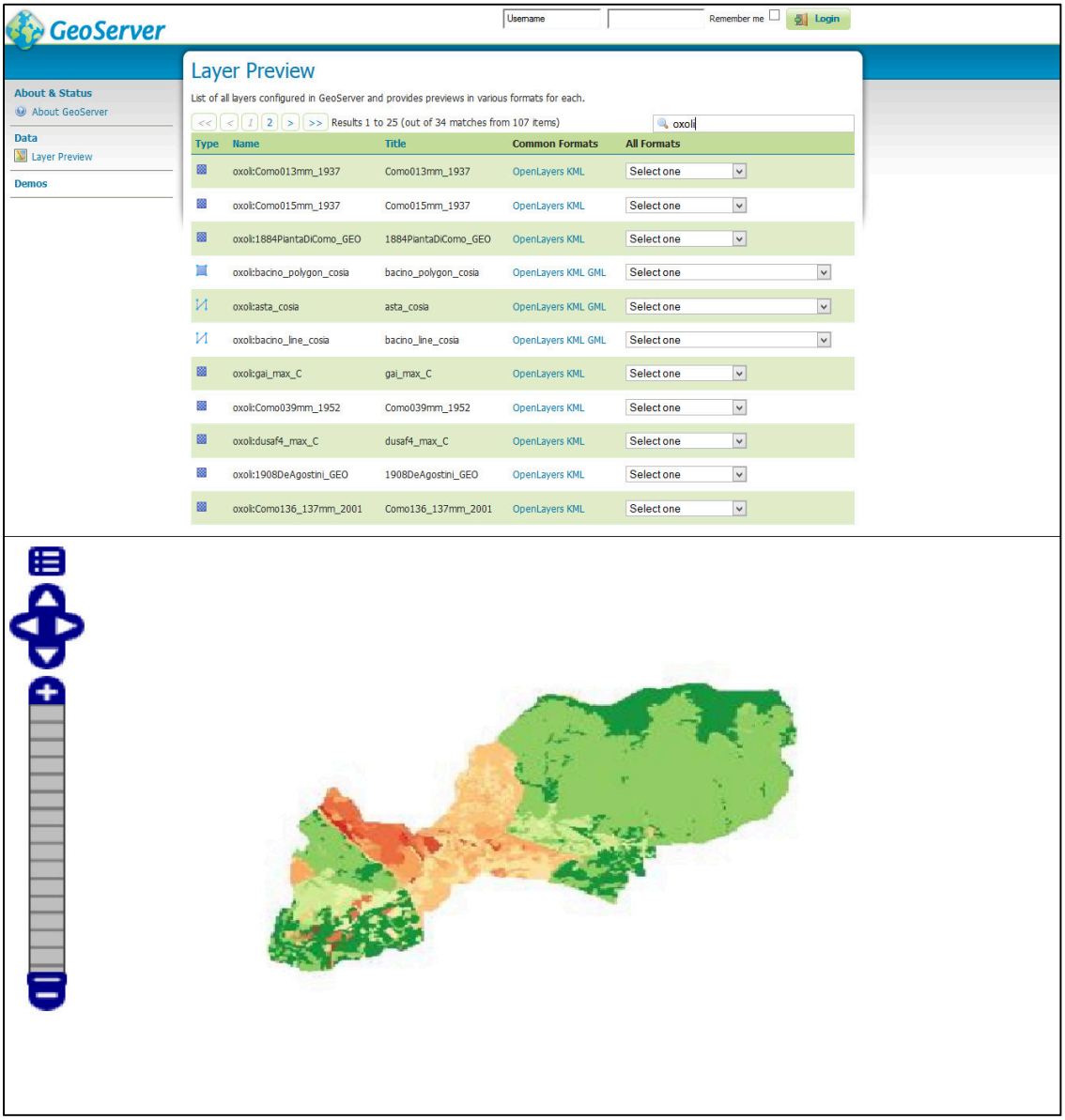

Figure 58: Layers preview with GeoServer.

The Client Side was developed by using Leaflet JavaScript library. This library allowed creating the map panel, adding basemaps and overlay layers. The last ones were included in the WebGIS as WMS or GeoJSON layers (http://geojason.info). The WMS layers were called directly from GeoServer, while GeoJSON layers were stored on the Client, enabling the query of their attributes. The query results are displayed in specific popups. An auxiliary library was involved in order to create a layer panel (Figure 60), containing all the available layers (https://github.com/stefanocudini/leaflet-panel-layers).

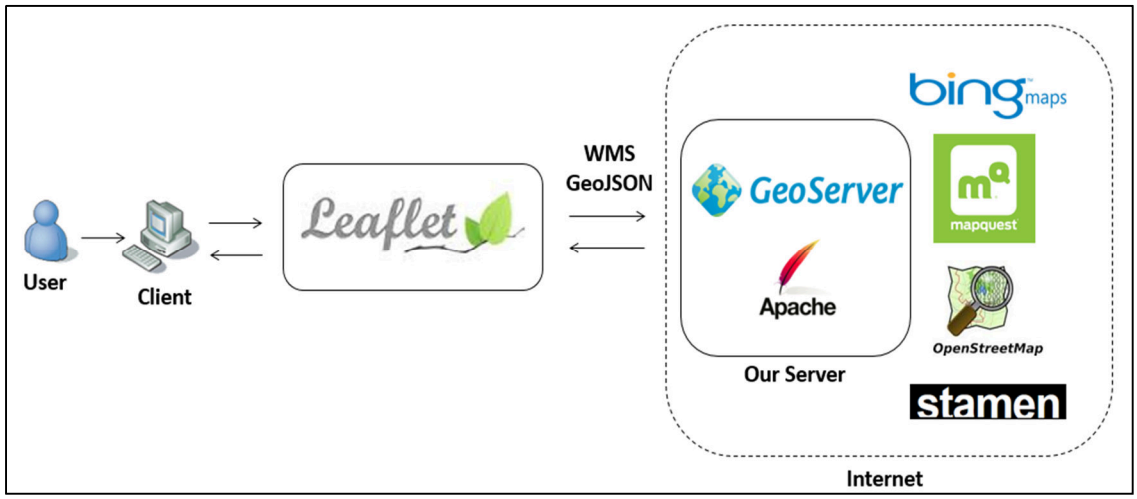

Figure 59: WebGIS software architecture.

The layers, which were included in the WebGIS, represent the historical maps, watershed and main watercourse features as well as soil runoff capacity maps (i.e. CN maps) and buried channel paths. Moreover, different basemaps were included, allowing the user to customize the WebGIS background. Both main watercourses and buried channels layers can be queried, simply clicking on them, retrieving the name of their specific elements by means of popups. The historical maps as well as the soil runoff capacity maps were listed inside the layer panel, by following their chronological order. The year, to which these data refer to, was included in the layer name. Other layers, describing basic features such as roads, railways and buildings were also included. The geospatial data can be explored by browsing the map with the mouse. All the layers can be turned on/off by using the layer panel. A specific legend for the soil runoff capacity map is displayed when these kind of layers are turned on. The zoom level can be also changed using the mouse scroll or double-clicking the map over the selected location as well as using the zoom button (Figure 60).

The WebGIS is visible at: http://geomobile.como.polimi.it/buriedtorrents.

The availability and accessibility of environmental information is of primary importance for local governments, as support in land planning, as well as for citizens in order to develop an increased environmental awareness. Thus, the diffusion of information, related to geospatial phenomena, through WebGISs, can be considered as the best practice to adopt. Information about the buried torrents paths (Figure 61), the changes in the urban setting (Figure 62) as well

as the alteration of soil runoff capacity (Figure 63) were made available to anyone, through simple maps. Moreover, the use of FOSS solution, which were involved in this study, allowed customizing the WebGIS, minimizing development time and costs.

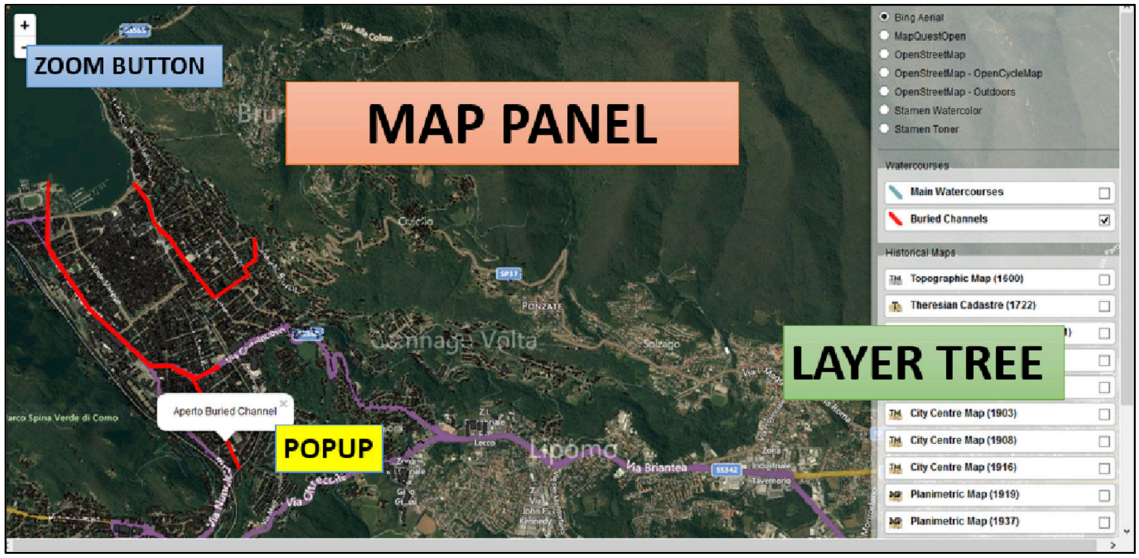

Figure 60: WebGIS features.

Figure 61: WebGIS displaying the buried channel paths.

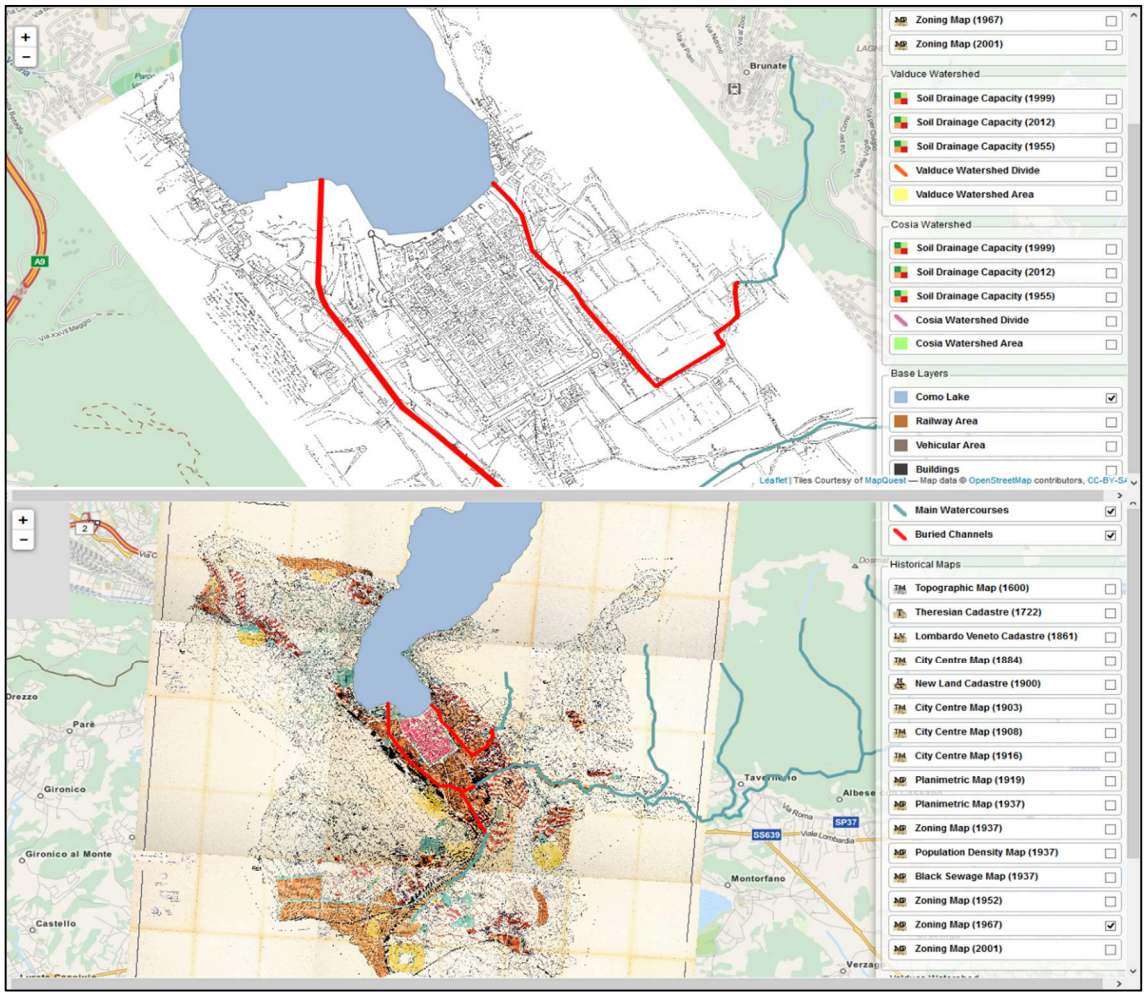

Figure 62: WebGIS displaying different historical maps.

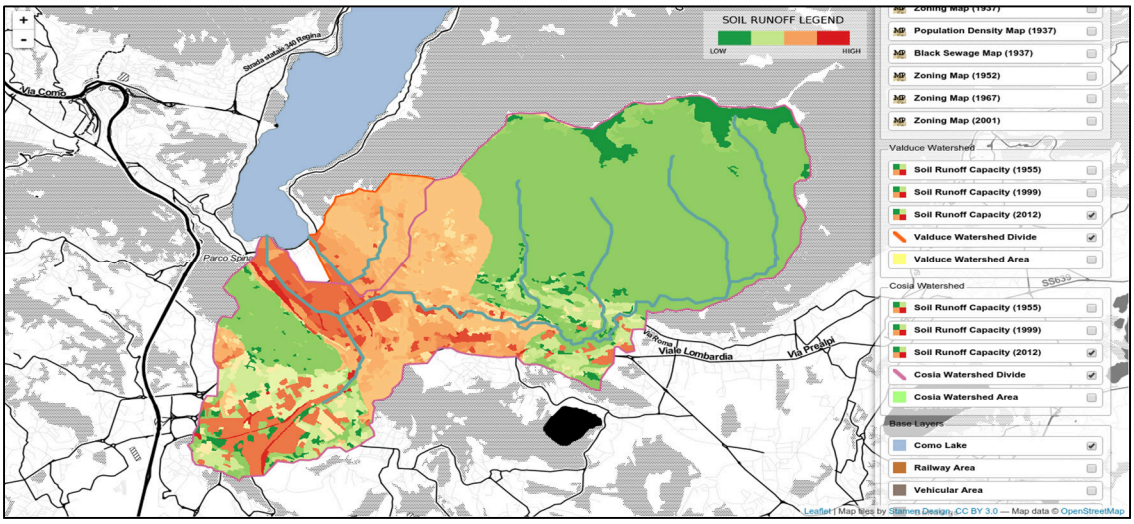

Figure 63: WebGIS displaying soil runoff capacity maps.

CONCLUSIONS AND FURTHER IMPROVEMENTS

Evolution of the urban settings, changes in land use as well as in peak flood discharges for the studied watercourses were clearly underlined. The available geospatial data, which were processed with the different GIS software, demonstrated to be effective in carrying out this analysis for the urbanization effects. On the other hand, additional historical information for the study area (e.g. master plans, historical books etc.) were needed in order to retrieve details, which were not detectable only through the map analysis.

From hydrological and hydraulic modelling results, no particular problems associated to the urbanization processes were identified for what it concerns the Cosia Watershed. The Cosia and Aperto buried channels demonstrate to still have an adequate conveyance even for discharges associated with high return period storms (i.e. 200 years). However, monitoring and maintenance of both channels and watersheds must be performed in order to maintain this safety situation. The Valduce buried channel conveyance instead, demonstrate to be insufficient even for discharges associated with medium return period storms (i.e. 20 years). In this last case, structural interventions should be designed in order to increase the discharge capacity, to avoid overflow phenomena.

For what it concerns the hydrological models, it should be noticed that to validate the results it is necessary to assess their accuracy by comparing them with the real situation. This operation requires flow measurements, which are strongly recommended in order to reduce the uncertainties affecting the model parameters and the related outcomes. The hydraulic model can be also improved by means of extensive field surveys to take into account important features, such as the riverbed stabilization works and all the inline structures present along the path, as well as to get a better description of the cross-section characteristics.

An intuitive access to the meaningful geospatial data has been provided through the WebGIS. However, this represents just a first prototype. The graphical interface as well as the capabilities of the system will be improved as described in the following. To provide users with not only a spatial but also a temporal

perception, the inclusion of a time slidebar is planned, which will allow to filter the visualization of layers according to the historical period they refer to. The inclusion of a transparency slidebar is also planned, which will allow to select the layer opacity, enabling the comparison between different overlay layers.

REFERENCES

Adrien, N.G. & Nicolas, G., 2004. *Computational Hydraulics and Hydrology: An Illustrated Dictionary*, Boca Raton, Florida: CRC Press.

Aymond et al., 2005. The urban stream syndrome: current knowledge and the search for a cure. , 24(3), pp.706–723.

C. Muñoz & S. Altaf, 2010. *Como in the XVIII Century: Evolution of Como During The Centuries*, Available at: http://webgis.como.polimi.it/GIScourse10/como_hist_utente08/html/en_Intro.html.

Cameron, T. & Ackerman, P., 2012. HEC-GeoRAS GIS Tools for Support of HEC-RAS using ArcGIS 10. , p.242.

Cappelletti, A., 2004. Rlazione Idrologica - Idraulica: Documentazione tecnica a corredo della domanda di concession scarico acque reflue depurate nel Torrente Cosia.

Chow, V. Te, 1959. *Open-channel hydraulics*, McGraw-Hill.

Chow, V. Te, Maidment, D.R. & Mays, L.W., 1988. *Applied Hydrology*,

Conzen, M., 2010. A cartographic Analysis of Como's urban Morphology. In *Cartografia di Paesaggi, Paesaggi nella Cartografia (Cerreti C., Federzoni L., Salgaro S.)*. Bologna: Pàtron Editore, p. 423.

DeMichele, C., Rosso, R. & Rulli, M.C.., 2005. *Il Regime delle Precipitazioni Intense sulla Lombardia: Modello di Previsione Statistica delle Precipitazioni di Forte Intensità e Breve Durata*,

Dixey, F., 1975. *Engineering Hydrology*, Oxford University Press.

Đurić, A., 2014. *A simple WebGIS for viewing the evolution of the city of Como.* Politecnico di Milano. Available at: https://www.politesi.polimi.it/handle/10589/93415.

Environmental Agency, 2011. B3: Review of EU policy Drivers for River Restoration. , p.66.

Fasolini, D. et al., 2010. *DUSAF*, Available at: http://www.ersaf.lombardia.it.

Ferro, V., 2006. *La Sistemazione Dei Bacini Fluviali* 2nd Editio. Mc-Graw Hill, ed.,

G. Rumi et al., 1995. *Como e il suo territorio*, Milano: Cariplo.

Gianoncelli, M., 1975. *Como e la Sua Convalle: Indagine Storica sull'Origine ed Evoluzione Urbanistica Dei Borghi e Dei Corpi Santi Di Como*, Como: New Press.

Giussani & Catelli, 1919. *Progetto piano regolatore e di ampliamento della città di Como*, Como. Available at: http://www.rapu.it/ricerca/pdf/como_txt007.pdf.

Grimaldi, S. et al., 2010. *Analisi Critca Dei Metodi Di Stima Del Tempo Di Corrivazione*. In XXXII Convegno Nazionale di Idraulica e Costruzioni Idrauliche Palermo, 14-17 settembre 2010, pp. 14–17.

Hawkins, R.H. et al., 2009. *Curve Number Hydrology: State of the Practice.*,

Heisse et al., 2009. *The London Rivers Action Plan*, Available at: www.therrc.co.uk.

Howard B. C., N.G., 2013. 11 Rivers Forced Underground. Available at: http://environment.nationalgeographic.com/environment/photos/underground-rivers/.

Jorio, S., 2006. Vie di transito e attestazioni materiali di Como romana: alcuni esempi. *Produzioni e Commerci in Transpadana in Età Romana*. Available at: http://www.archeologicacomo.it/conferenza_nov2006/pages/jorio.htm.

Marrazzi et al., 1967. *Piano regolatore urbanistico generale*, Como. Available at: http://www.rapu.it/ricerca/pdf/como_txt015.pdfdf.

Minghini, M., 2010. *Trasformazioni Cartografiche, Geocatalogo e Servizio Web di Visualizzazione dei Catasti Storici di Como*. Politecnico di Milano. Available at: https://www.politesi.polimi.it/handle/10589/5883.

Mishra, S.K. & Singh, V.P., 2003. *Soil Conservation Service Curve Number (SCS-CN) Methodology*, Dordrecht: Springer Netherlands.

Musy, A. & Higy, C., 2011. *Hydrology: A Science of Nature* Science Publishers, ed., CNC Press.

Nakamura, K., Tockner, K. & Amano, K., 2006. River and Wetland Restoration : Lessons from Japan. , 56(5).

Rota et al., 2001. *Piano regolatore urbanistico generale*, Como. Available at: http://www.rapu.it/ricerca/pdf/como_txt035.pdf.

Sivapalan, M., Savenije, H.H.G. & Blöschl, G., 2012. Socio-hydrology: A new science of people and water. *Hydrological Processes*, 26(8), pp.1270–1276. Available at: http://doi.wiley.com/10.1002/hyp.8426 [Accessed October 28, 2014].

Società Archeologica Comense, 2012. Capitolo 1 – Cenni storici sulle mura di Como. In Como, pp. 1–13. Available at: http://www.archeologicacomo.it/admin/gruppo/immagini/Capitolo_1.pdf.

Tajana, C., 2013. Quei Fiumi Sotto Como E' l'Ora di Scoprirli. *La Provincia*.

Tarboton, D; Bras, R.L; Iturbe, R., 1991. On the Extraction of Channel Networks from Digital Elevation Data. *Hydrologic Processes*, pp.81–100.

Tarquini, S. et al., 2012. Release of a 10-m-resolution DEM for the Italian territory: Comparison with global-coverage DEMs and anaglyph-mode exploration via the web. *Computers & Geosciences*, 38(1), pp.168–170. Available at: http://linkinghub.elsevier.com/retrieve/pii/S0098300411001609 [Accessed November 18, 2014].

Tewolde, M. & Smithers, J., 2007. Flood Routing In Ungauged Catchments Using Muskingum Methods. *Water SA*, 32(3), pp.379–388.

Turri, E., 2002. *La conoscenza del territorio. Metodologia per un'analisi storico-geografica*, Venezia: Marsilio Editori.

U.S. Army Corps of Engineers, 2010. HEC-RAS River Analysis System: Hydraulic Reference Manual. , p.417.

U. S. Department of Agriculture, 2004. Part 630: Hydrology National Engineering Handbook. In *National Engineering Handbook*. Available at: http://www.nrcs.usda.gov/wps/portal/nrcs/detailfull/national/water/?cid=stelprdb1043063.

U. S. Department of Agriculture, 2009. Small Watershed Hydrology: WinTR-55 User Guide. , p.142. Available at: http://www.nrcs.usda.gov/wps/portal/nrcs/detailfull/national/water/?cid=stelprdb1042901.

Ufficio Urbanistica Comune di Como, 1937. *Progetto piano regolatore e di ampliamento della città di Como*, Como. Available at: http://www.rapu.it/ricerca/pdf/como_txt014.pdf.

Wagener, T., Wheater, H.S. & Gupta, H. V., 2004. *Rainfall-Runoff Modelling in Gauged and Ungauged Catchments*, London: Imperial College Press.

Zlinszky, a. & Timár, G., 2013. Historic Maps As a Data Source for Socio-Hydrology: a case study of the Lake Balaton wetland system, Hungary. *Hydrology and Earth System Sciences*, 17(11), pp.4589–4606. Available at: http://www.hydrol-earth-syst-sci.net/17/4589/2013/ [Accessed December 15, 2014].

WEBLIOGRAPHY

ArcGIS, http://www.arcgis.com ArcGIS

Archivio RAPu, http://www.rapu.it

Archivio di Stato di Como, http://www.ascomo.beniculturali.it

Bing Maps, http://www.bing.com/maps

ESRI, http://www.esri.com

Geopaparazzi, http://geopaparazzi.github.io/geopaparazzi

GeoServer, http://geoserver.org

GNU website, http://www.gnu.org

Google Earth, http://earth.google.com

HEC-RAS, http://www.hec.usace.army.mil/software/hec-ras

Heli-DEM, http://helidem.eu

HydroloGIS, https://sites.google.com/a/hydrologis.com

Leaflet, http://leafletjs.com

MapQuest,http://www.mapquest.com

OpenStreetMap, http://www.openstreetmap.org

OSGeo, http://www.osgeo.org

QGIS, http://qgis.org

Società Archologica Comense, http://www.archeologicacomo.it

Stamen, http://maps.stamen.com

USDA, http://www.usda.gov

Web C.A.R.T.E, http://webcarte.como.polimi.it

APPENDIX

ORIGINAL FORMAT	NAME (in the GeoServer)	SOURCE, YEAR, DESCRIPTION
Raster	Como013mm_1937	Master plan, 1937, average population density map
Raster	Como015mm_1937	Master plan, 1937, Urban Centre Planimetry
Raster	1884PiantaDiComo_GEO	1884, city centre map
Shapefile	bacino_polygon_cosia	Cosia Watershed area
Shapefile	asta_cosia	Cosia Torrent path
Shapefile	bacino_line_cosia	Cosia Watershed divide
Raster	gai_max_C	1955, Cosia Watershed, soil runoff capacity map
Raster	Como039mm_1952	Master plan, 1952, zoning map
Raster	dusaf4_max_C	2012, Cosia Watershed soil runoff capacity map
Raster	1908DeAgostini_GEO	1908, city centre map
Raster	Como136_137mm_2001	Master plan, 2001, zoning map
Raster	geoTopo_1600	XVI century, Topographic map of Como
Raster	Como042_050mm_1967	Master plan, 1967, zoning map
Raster	dusaf4_max_V	2012, Valduce Watershed soil runoff capacity map
Raster	dusaf1_max_C	1999, Cosia Watershed soil runoff capacity
Raster	Como009mm_1937	Master plan 1937, zoning map
Raster	gai_max_V	1955, Valduce Watershed soil runoff capacity map
Raster	Como025mm_1937	Master plan, 1937, black sewage schema

Raster	dusaf1_max_V	1999, Valduce Watershed soil runoff capacity map
Raster	geo1861	Lombardo –Veneto Cadastre, 1861, suburbs map
Raster	1903Catelli_GEO	1903, city centre map
Shapefile	asta_valduce	Valduce Torrent path
Shapefile	bacino_line_valduce	Cosia Watershed divide
Shapefile	bacino_polygon_valduce	Cosia Watershed area
Raster	Como001mm_1919	Master plan, 1919, Urban Centre Planimetry
Raster	geoTeresian_1722	Theresian Cadastre, 1722, suburbs map
Raster	1916TouringClub_GEO	1916, city centre map
Raster	geo_1900	New Land Cadastre, 1861, suburbs map
Shapefile	reticolo_principale_wgs	Main drainage network
Shapefile	fiumi_coperti	Buried channel paths
Shapefile	lago	Lake Como
Shapefile	area_edificio	Buildings of Como
Shapefile	area_ferroviaria	Railways of Como
Shapefile	area_stradale	Roads of Como

Appendix Table 1: Selected layers for the WebGIS, available as WMS layers at: http://geomobile.como.polimi.it:8080/geoserver

ACKNOWLEDGMENTS

First, I would like to express my gratitude to my supervisors, Prof.ssa Maria Antonia Brovelli and Eng. Priscila Escobar Rojo, for helping me during my thesis work as well as for the patience demonstrated in supporting me during this year. Special thanks go also to the Geomatic Laboratory staff, especially to Marco and Eylul without whom this work would not be completed.

Now comes the end of my studies, and I will not forget my mates with whom I shared the best (but also the worst) moments of my student carrier. In particular, I wish to thank Walter, I am sure that an important part of my successes is owed to you. Special thanks go to Ksenija, Nadya, Giacomo, Andrea, Martino and Davide whom supported me and let me to enjoy these unforgettable years. I want to thank also Politecnico di Milano and mainly Como Campus for allowing me to have this amazing studying experience.

Finally, I would like to thank my family and all my friends. This all would not be happened without the infinite support they have given me.